MODERN DEVELOPMENTS IN SCINTILLATORS

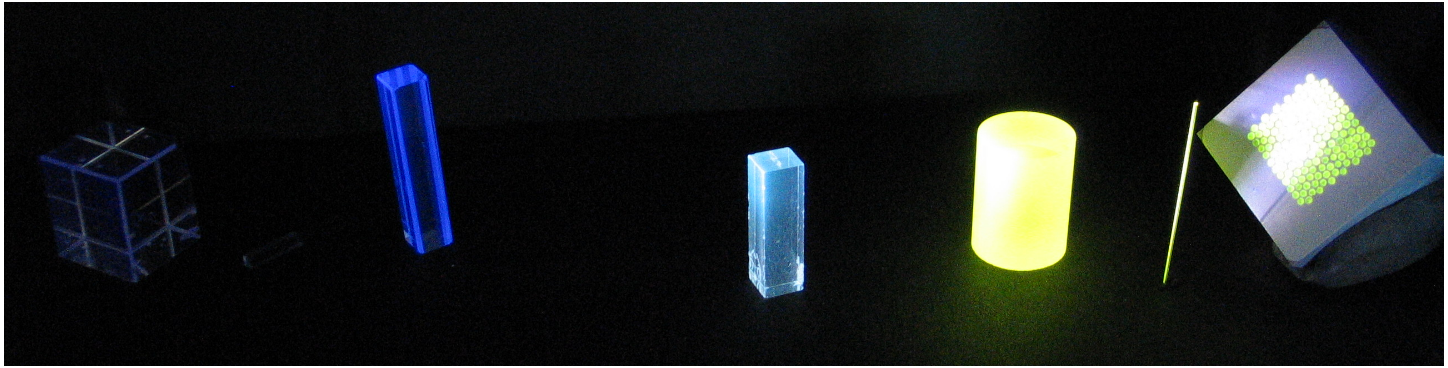

E. Auffray, *CERN, EP-CMX*
HighRR Lecture Week 2021

Principle of scintillation

When energy of incident particle is converted in light by the material

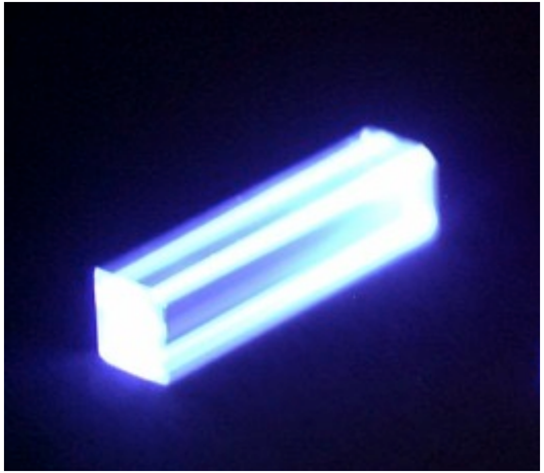

Scintillator

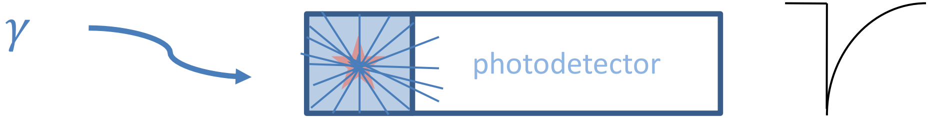

Principle of scintillation

Light production

γ

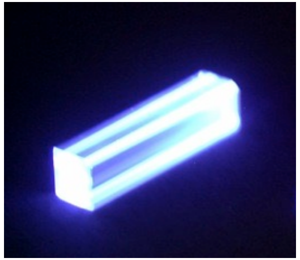

Particle deposits energy in scintillator, scintillator produces photons in UV-visible range

$$N_{prod.Photon} = \eta_{conv} E_{\gamma}$$

Light detection

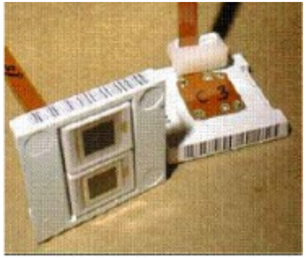

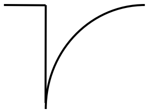

The produced photons are collected by photodetector
Photodetector produces photelectron

$$N_{pe} = \eta_{coll}.\, QE.\, N_{prod.Photon}$$

Different types of scintillators

Organic scintillators

Crystal, liquid, plastic

- Low density: <2g/cm^3
- Low Z
- Light Yield <10000ph/MeV
- Decay times few ns
- Moderate rad hardness

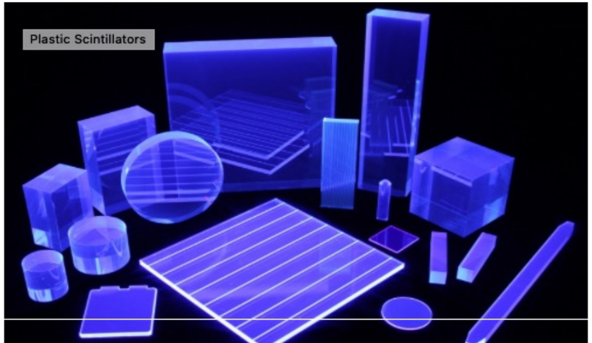

https://scionix.nl/frame/

Inorganic scintillators

Liquid noble gas

- LAr, LKr, LXe
- Cryogenic temperature
- Moderate density 1.4-3g/cm^3
- Moderate Z
- Light Yield 50000ph/MeV

Crystals

- high density: up to 9g/cm^3
- High Z
- Light Yield: up to 70000ph/MeV
- Decay time: ns to msec
- Good radiation hardness

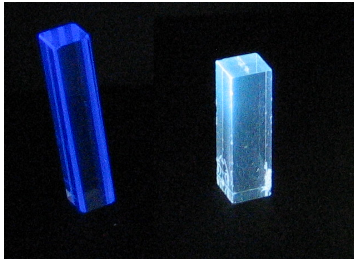

Choice of scintillator depends on the requirements of the application

- Density
- Light yield
- Decay time
- Radiation hardness (for some applications HEP, Astronomy)
- Feasibility to be manufactured, reproducibility
- Feasibility of large size, easy handling and "machinable
- Cost

Many Applications used scintillators

- Astronomy and dark matter searches
- High Energy Physics
- Medical Imaging
- X ray and gamma spectroscopy
- Monitoring in nuclear plants
- Neutron detection
- Oil well drilling

ORGANIC SCINTILLATORS

Organic scintillators

Aromatic hydrocarbon compounds with benzene ring
The emission mechanism:
Transitions between energy levels of a single molecule

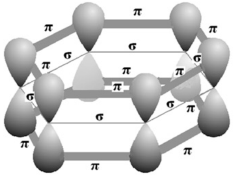

The π molecular orbital in benzene

$\Rightarrow$ can be observed independently of the physical state:

- Pure organic crystals: eg. Anthracene, Stilbene,
- Liquid organic solutions: dissolved in a solvent
- Plastic scintillators: dissolved & polymerized

J. B. Birks Fig 3.7
(G. Knoll Fig 8.1)

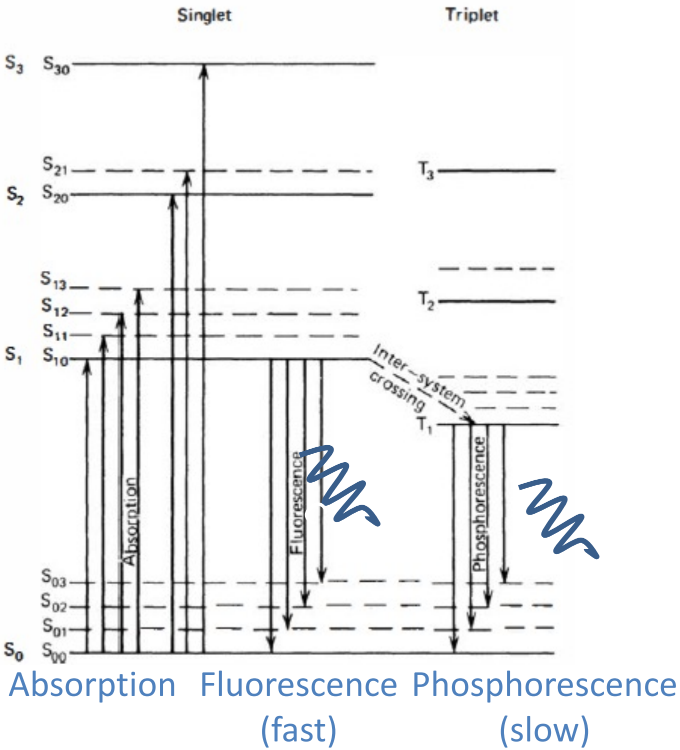

Electronic levels of organic molecule with π-electron system

Organic Crystal scintillator

One component material

Crystal	Chemical formula	Density	n	Decay time	emission (nm)
Anthracene	$C_{14}H_{10}$	1,25	1,62	30ns	447
Stilbene	$C_{14}H_{12}$	1,16	1,62	4.5	390

- Usually fast (a few ns)
- different emission wavelengths
- used for pulse shape discrimination neutron/gamma
- Anthracene has a very good light yield: 20000ph/MeV

G. Hull et al,
IEEE TNS Vol 56,N3,2009,899--903

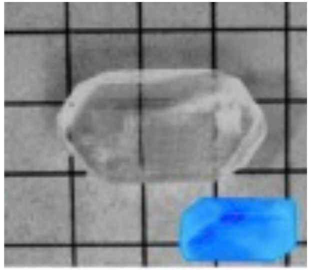

Anthracene

https://www.inradoptics.com/products/scintillation-crystals

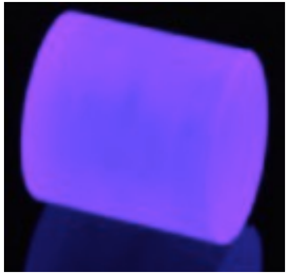

stilbene

Emission of some organic crystal scintillators

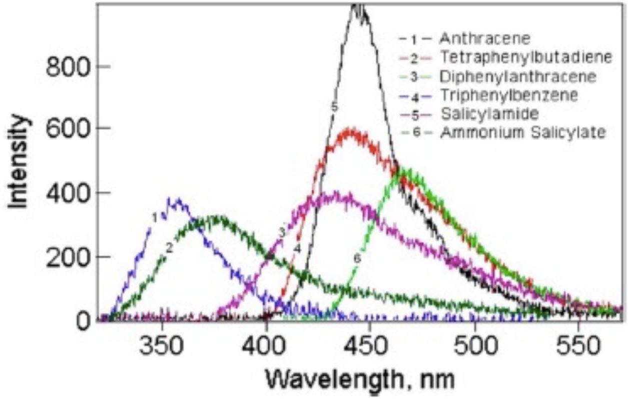

G. Hull et al, IEEE TNS Vol 56,N3,2009,899--903

Liquid/Plastic scintillators

Composed of 2-3 components: Base + fluors

1. Primary ionization => excitation of molecules in the base polymer
2. De-excitation of the base polymer
   =>produces scintillation photons (~ 300 nm) absorbed by primary fluor,
   => Energy transfer directly to the fluor in a very short distance.
3. Primary fluor emits at a longer wavelength (~ 340 nm),
4. absorbed by a secondary fluor
5. Secondary fluor emits in the visible (~ 400 nm)
6. Detect by photodetector

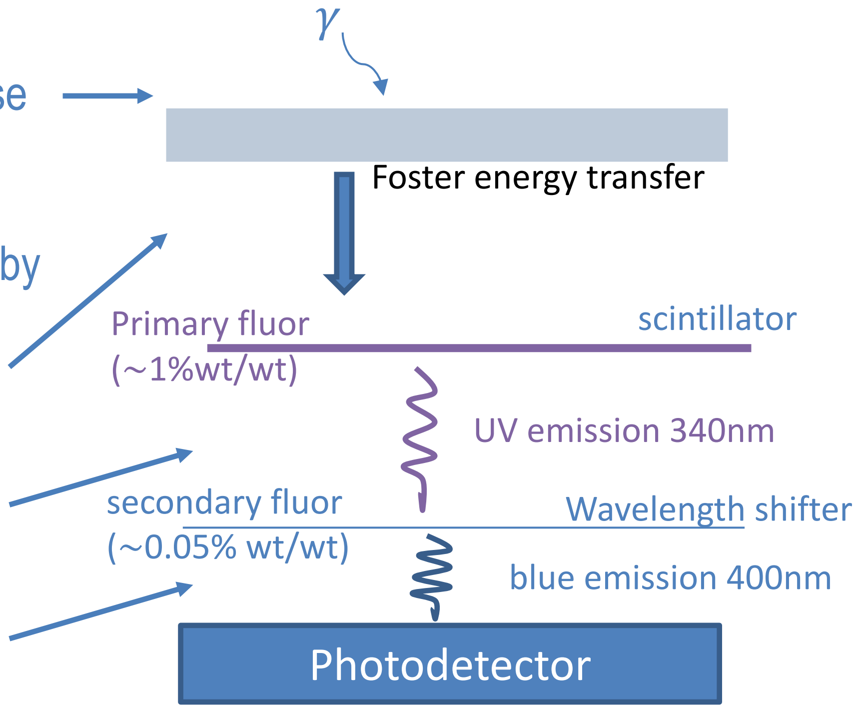

Liquid/Plastic scintillators

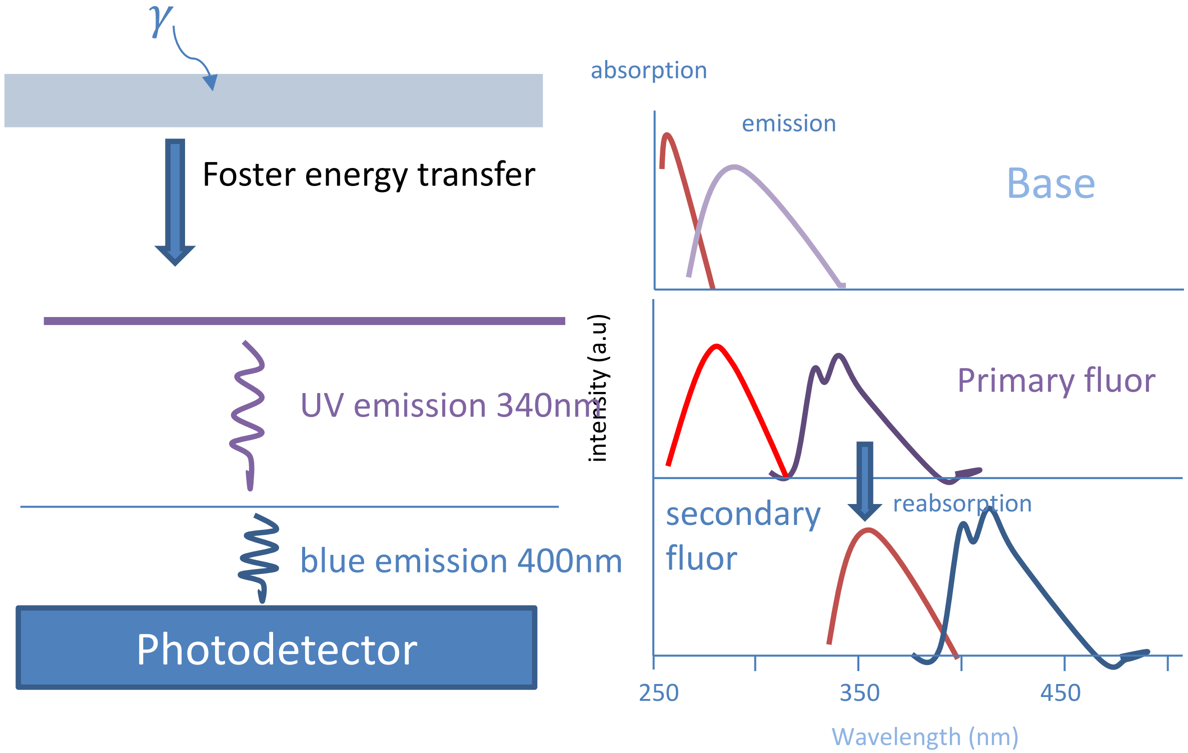

Liquid	Plastic
Benzene, Toluène, Xylène	polyphénilbenzène, polystyrène polyvinyletoluène,
p-Terphénil, PBD, PPO, POPOP, 3g/l	
POPOP, BBQ	

Shift of the emission to higher wavelength

Liquid scintillators

Table 8.1 Properties of Some Commercially Available Organic Scintillators

G. Knoll, Radiation detection and measurements, P226

NE	Eljen	St. Gobain	Light Output % Anthracene*	Wavelength of Max Emission (nm)	Decay Constant (ns)	Attenuation Length (cm)	Refractive Index	H/C Ratio	Density	Loading Element % by weight or dist. feature	Softening or Flash Point (°C)	Uses
	Liquid											
NE-213	EJ-301	BC-501 A	78	425	3.2		1.51	1.212	0.874	Pulse shape discrim.	26	γ > 100 keV, fast n spectroscopy
NE-224	EJ-305	BC-505	80	425	2.5		1.50	1.331	0.877	High light output	47	γ, fast n, large volume
	EJ-309		75	425	3.5		1.57	1.25	0.964	High flash point	144	pulse shape discrimination
NE-226	EJ-313	BC-509	20	425	3.1		1.38	0.0035	1.61	F	10	γ, fast n
	EJ-321H	BC-517H	52	425	2.0			1.89	0.86	Mineral oil-based	81	γ, fast n, cosmic, charged particles
		BC-517P	28	425	2.2			2.05	0.85	Mineral oil-based	115	γ, fast n, cosmic, charged particles
NE-235C	EJ-325	BC-519	60	425	4.0			1.73	0.875	Pulse shape discrim.	74	γ, fast n, n-γ discrimination
NE-323	EJ-331	BC-521	60	425	4.0			1.31	0.89	Gd (to 1%)	44	Neutron spectroscopy, neutrino research
NE-321A	EJ-339	BC-523A	65	425	3.7			1.67	0.93	Enriched ^{10}B	1	Total absorption neutron spectrometry
	EJ-335	BC-525	56	425	3.8			1.57	0.88	Gd (to 1%)	64	Neutron spectrometry, neutrino research
		BC-533	51	425	3.0			1.96	0.8	Low temp operation	65	γ, fast n, cosmic
NE-230		BC-537	61	425	2.8		1.50	.99 (D:C)	0.954	^{2}H	-11	Fast n, pulse shape discrimination
NE-314A		BC-551	40	425	2.2			1.31	0.902	Pb (5% w/w)	44	γ, X-rays < 200 keV
		BC-553	34	425	3.8			1.47	0.951	Sn (10% w/w)	42	γ, X-rays

=> Very fast 2- 4ns

See: St Gobain web page https://www.crystals.saint-gobain.com/products/organic-scintillation-materials

Eljen web page https://eljentechnology.com/products/plastic-scintillators

Plastic scintillators

Table 8.1 Properties of Some Commercially Available Organic Scintillators

G. Knoll, Radiationdetection and measurements, P226

NE	Eljen	St. Gobain	Light Output % Anthracene*	Wavelength of Max Emission (nm)	Decay Constant (ns)	Attenuation Length (cm)	Refractive Index	H/C Ratio	Density	Loading Element % by weight or dist. feature	Softening or Flash Point (°C)	Uses
	Plastic											
NE-102A	EJ-212	BC-400	65	423	2.4	250	1.581	1.103	1.032		70	General purpose
NE-104	EJ-204	BC-404	68	408	1.8	160	1.58	1.107	1.032	1.8 ns time constant	70	Fast counting
Pilot F	EJ-200	BC-408	64	425	2.1	380	1.58	1.104	1.032		70	TOF counters, large area
NE-110	EJ-208	BC-412	60	434	3.3	400	1.58	1.104	1.032	Longest attn. length	70	General purpose, large area, long strips
		BC-420	64	391	1.5	110	1.58	1.100	1.032	1.5 ns time constant	70	Ultrafast timing, sheet areas
NE-111A	EJ-232	BC-422	55	370	1.4	8	1.58	1.102	1.032	1.4 ns time constant	70	Very fast timing, small sizes
		BC-422Q	11	370	0.7	<8	1.58	1.102	1.032	Benzephenone, 1%	70	Ultrafast timing, ultrafast counting
NE-103	EJ-260	BC-428	36	480	12.5	150	1.58	1.103	1.032	Green emitter	70	Photodiodes and CCDs; phoswich detectors
NE-108		BC-430	45	580	16.8	NA	1.58	1.108	1.032	Red emitter	70	Silicon photodiodes and red-enhanced PMTs
		BC-436	52	425	2.2	NA	1.61	0.960D:C	1.130	Deuterium, 13.8%	90	Thin disks
NE-115	EJ-240	BC-444	41	428	285	180	1.58	1.109	1.032		70	Phoswich detectors for *dE/dx* studies
NE-142	EJ-256	BC-452	32	424	2.1	150	1.58	1.134	1.080	Lead, 5%	60	X-ray dosimetry (<100 keV)
		BC-454	48	425	2.2	120	1.58	1.169	1.026	Boron, 5%	60	Neutron spectrometry, thermal neutrons
NE-105	EJ-252	BC-470	46	423	2.4	200	1.58	1.098	1.037	Air equivalent	65	Dosimetry
		BC-490	55	425	2.3		1.58	1.107	1.030	Casting resin	70	General purpose
		BC-498	65	423	2.4		1.58	1.103	1.032	Applied like paint	70	β, γ detection

=> Very fast 2- 4ns

See: St Gobain web page https://www.crystals.saint-gobain.com/products/organic-scintillation-materials

Eljen web page https://eljentechnology.com/products/plastic-scintillators

Plastic scintillators

Possibility to have various shapes

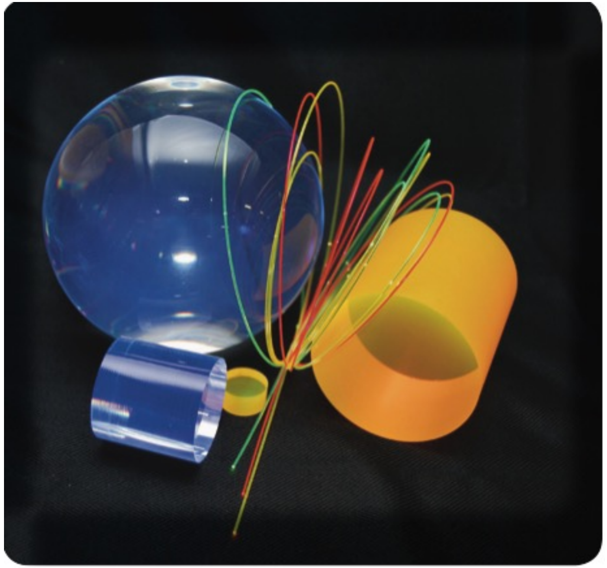

https://www.crystals.saint-gobain.com/sites/imdf.crystals.com/files/documents/organics-plastic-scintillators.pdf

Large size

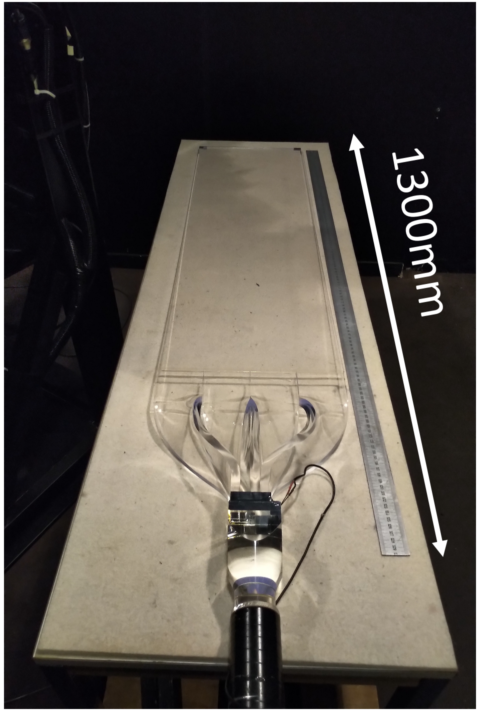

Wavelength shifter used as light guide

Bar

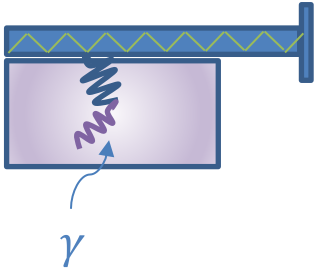

Fibers

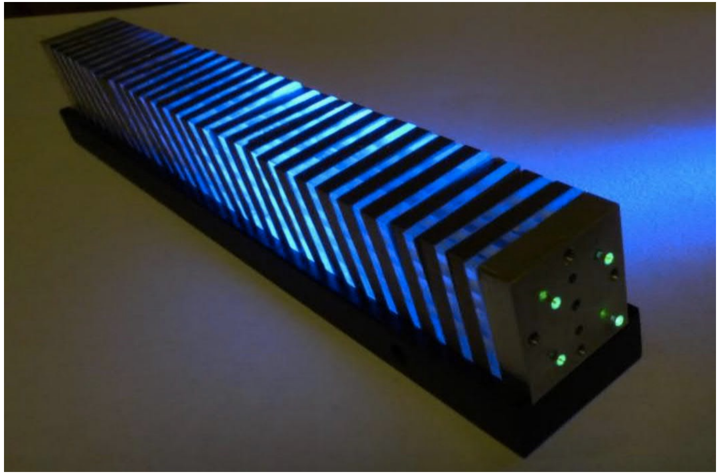

INORGANIC SCINTILLATORS

LIQUID NOBLE GAS

Liquid noble gas scintillators

The fluorescence mechanism is an atomic process

From: http://darkmatter.ethz.ch

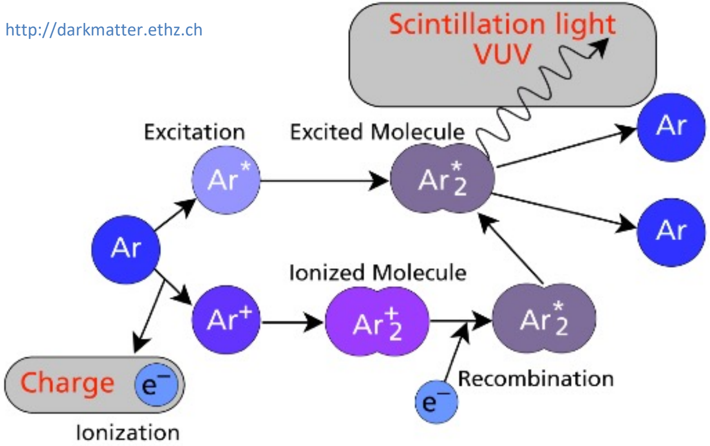

Fast emission < 10 ns but in VUV 130 < λ < 180 nm
Ionisation:≈20eV/pair
Hight light Yield
Required cryogeny
used in experiments searching for dark matter

	LAr	L Xe
Atonimic number	18	54
Density (g/cm3)	1.4	2.95
Boiling Point (°/1 atm)	87.3	165
Radiation length Xo (cm)	14	2.4
Moliere radius (cm)	8	4.2
Interaction Length (cm)	84	57
Emission (nm)	128	174
Light yield (ph/MeV)	40000	42000
Decay time (ns) fast /slow	6.5/ 1590	2.2/ 27

https://courses.lumenlearning.com/introchem/chapter/the-noble-gases-group-18/
T. Doke et al., NIMA A291 (1990) 617-620

INORGANIC CRYSTAL SCINTILLATORS

120 years of inorganic scintillators

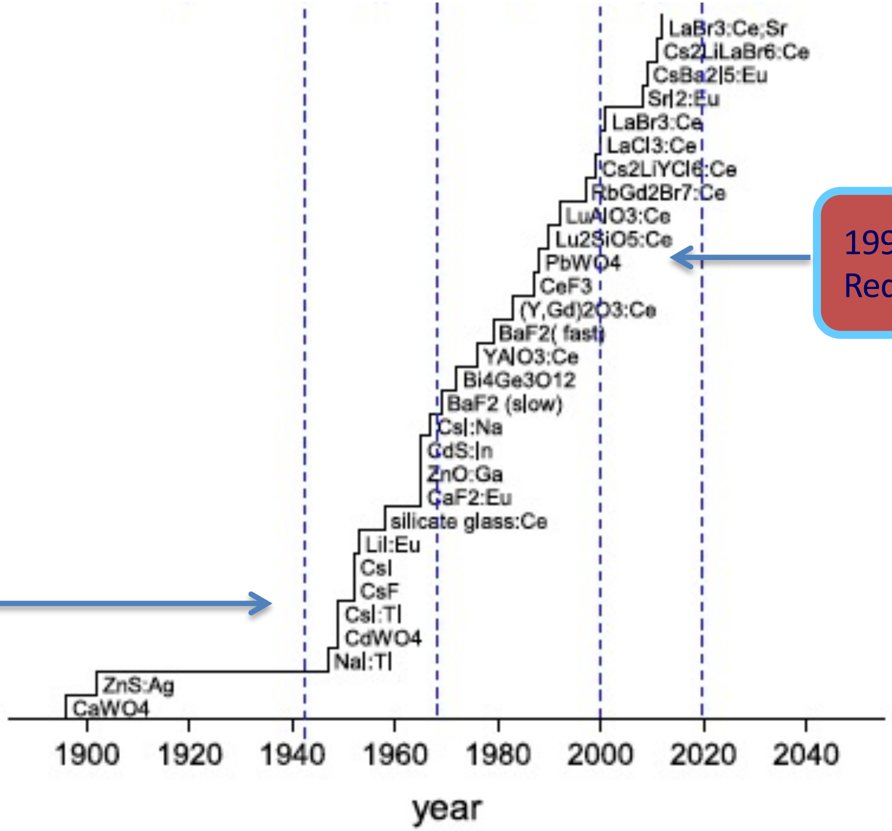

1940:
Invention of the photomultiplier tube

1990:
Request for scintillators for LHC

P. Dorenbos, Optical Materials: X 1 (2019) 100021, https://doi.org/10.1016/j.omx.2019.100021

Scintillation process in inorganic crystals

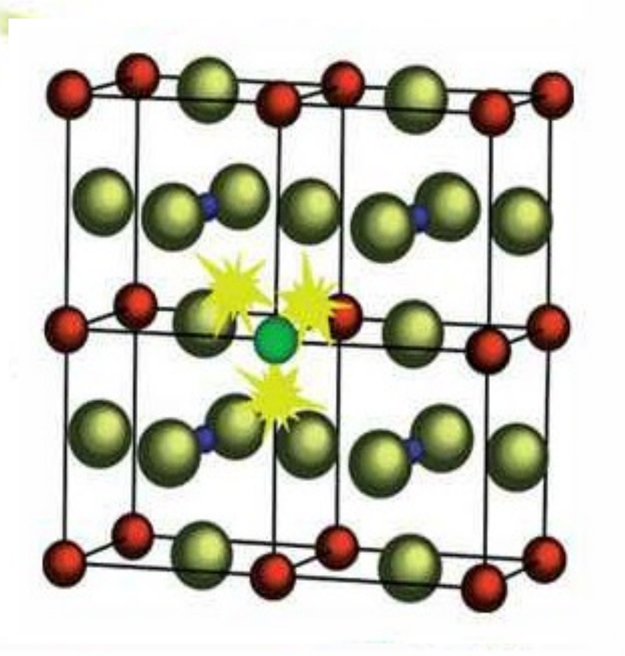

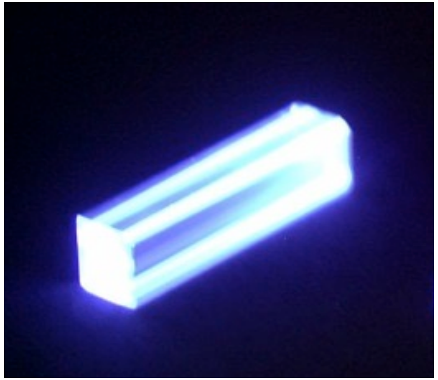

The scintillation process chain

From eh pair creation to light emission

A. Vasiliev, SCINT99 conference,

Band structure

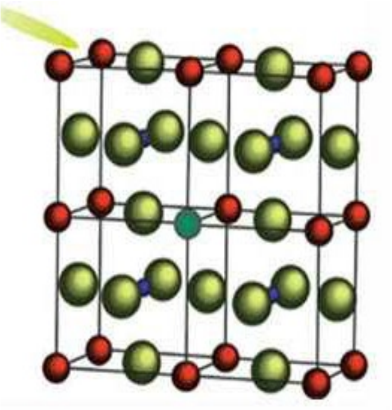

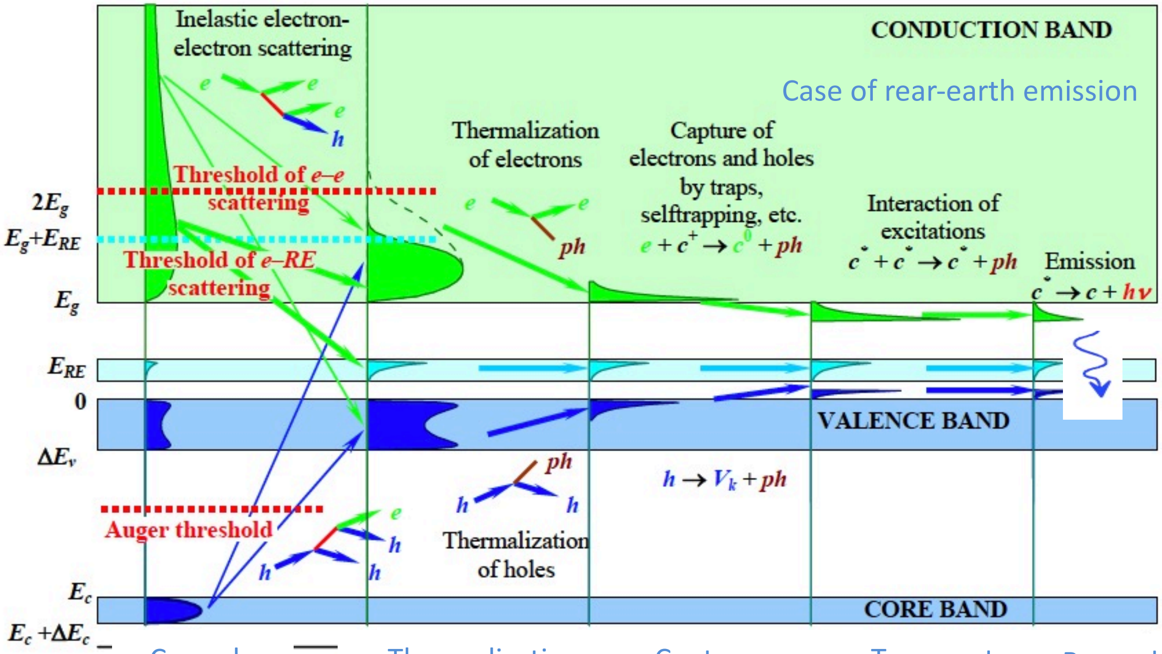

Cascade	Thermalization	Capture	Transport	Recombination
1fs	<1ps	150 fs- 50 ps	0-10 ns	≳0 .5 ns

Scintillation Yield $N_{eh} = \dfrac{E_\gamma}{\beta E_g}$ S Q

Scintillation Yield

$$LY = \frac{E_\gamma}{\beta E_g} SQ \;\; with\ \beta \text{ between 2-3}$$

Strong dependence with band gap energy

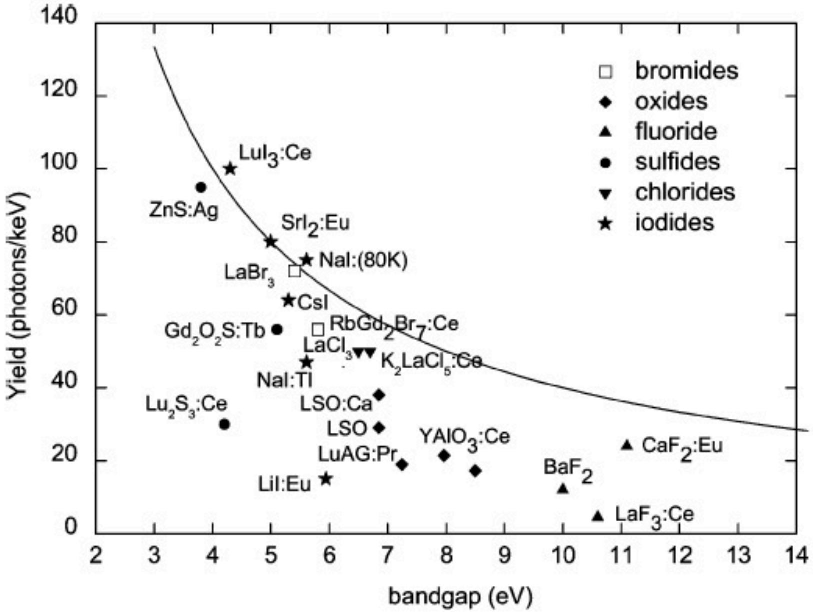

Fig. 5. Scintillation yield as function of the bandgap of compounds. The solid curve represents the maximum attainable scintillation yield assuming a β value of 2.5. Data points represent observed yields for fluoride, chloride, bromide, iodide, oxide, and sulfide compounds.

P. Dorenbos, IEEE TNS 57, 3 (2010) 1162-1167

Emission spectra

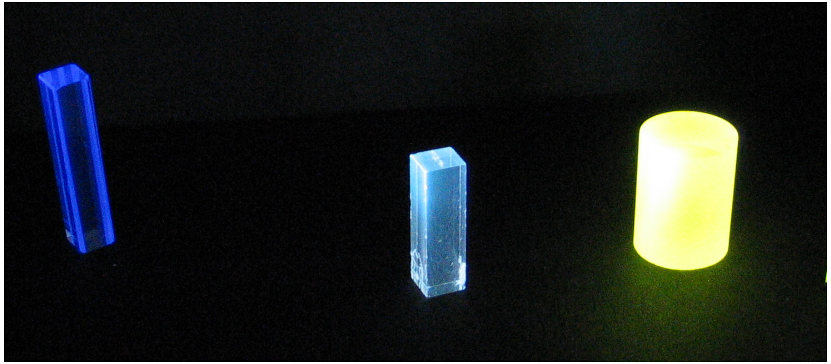

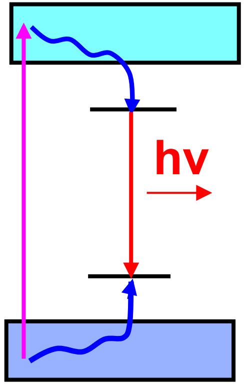

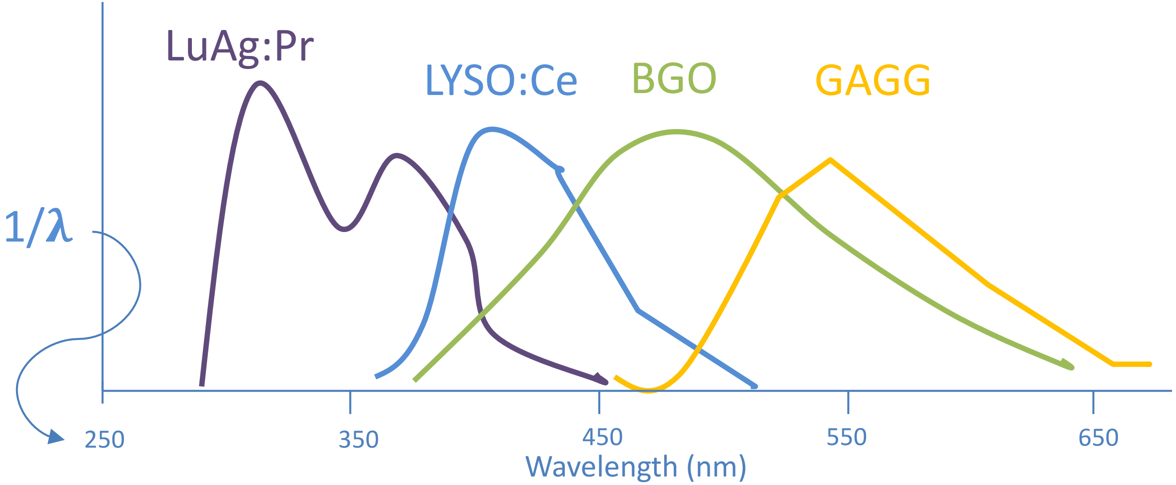

Emission spectra

LuAG:Pr

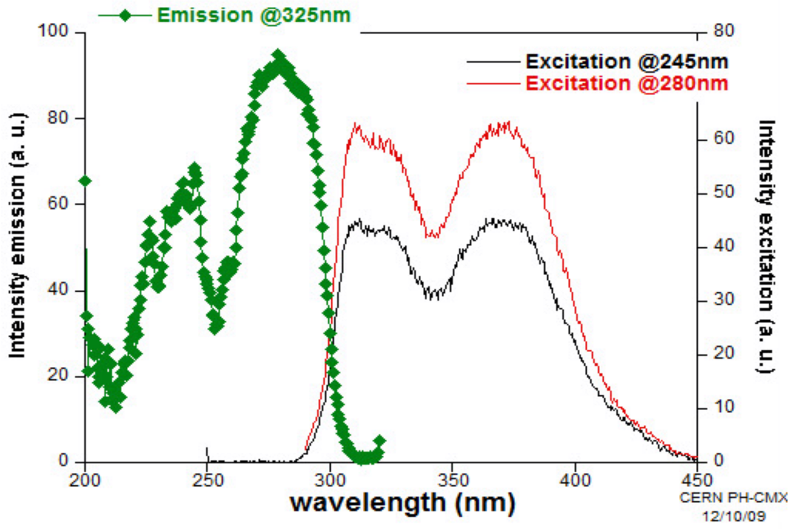

320nm, 370nm

LuAG:Ce

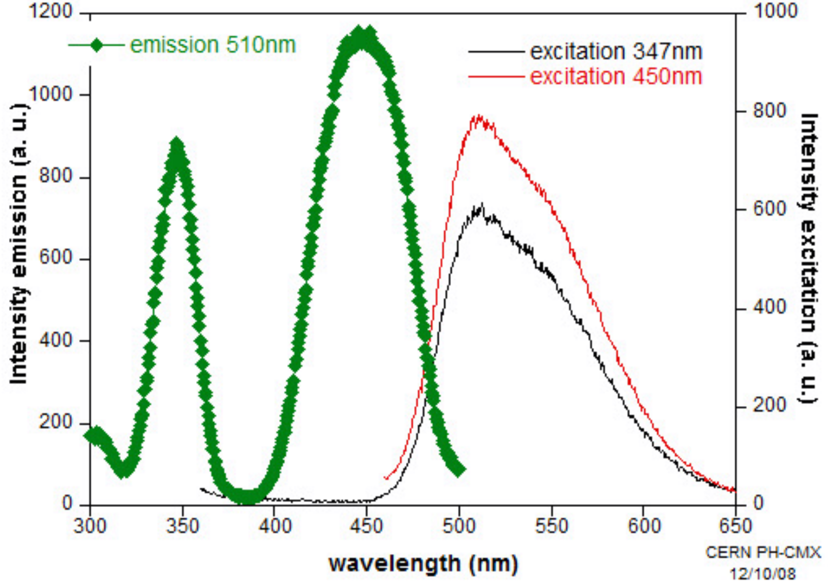

520nm

Same host materials but different dopant => different emission wavelengths

Scintillation pulse spectra

Rise time τ_r

Population
of luminescence center

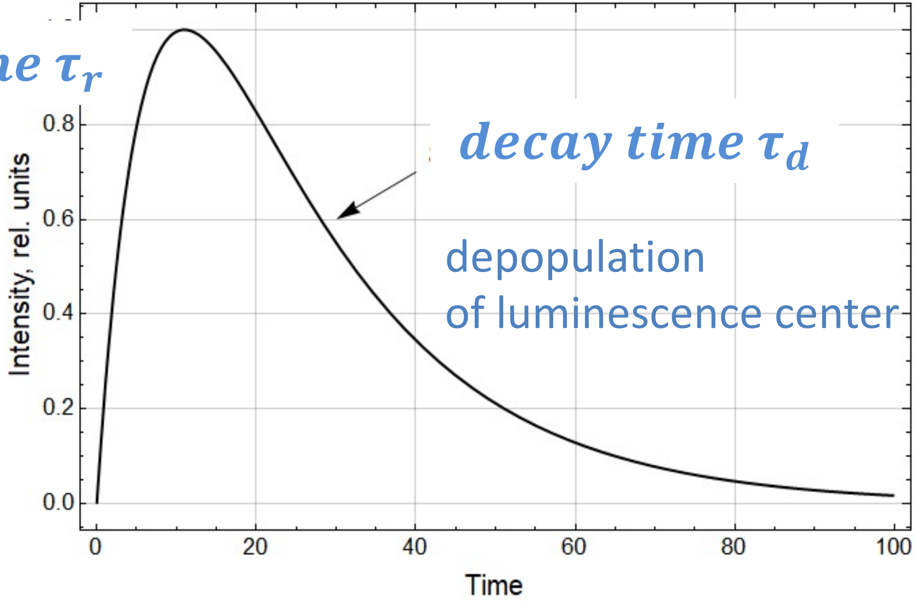

decay time τ_d

depopulation
of luminescence center

$$S(t) = Io(1 - e^{-t/\tau_r})e^{-t/\tau_d}$$

Scintillation pulse spectra

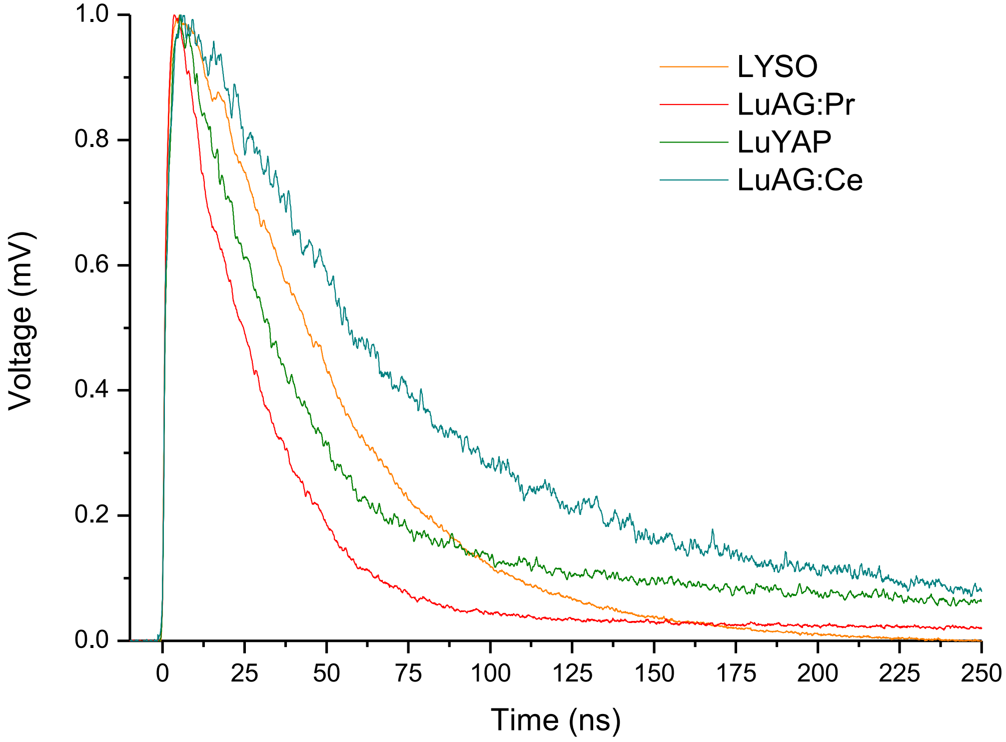

Variation of decay constant with type of material

Main parameters influencing the time resolution of scintillating materials

Rise time(τ_r)

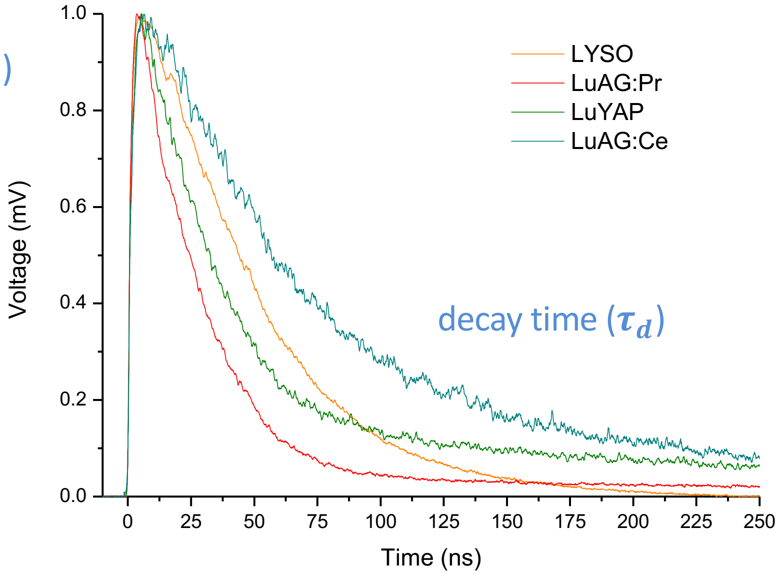

decay time (τ_d)

$$I(t) = \frac{N_{pe\infty}}{\tau_d^2}(\tau_r + \tau_d)(1 - e^{-t/\tau_r})e^{-t/\tau_d}$$

Number of photoelectrons detected

$$N(t) = \frac{N_{pe\infty}}{\tau_d} * \frac{t^2}{2\tau_r}$$

The coincidence time resolution CTR [FWHM]

$$CTR\ \alpha \sqrt{\frac{\tau_d \tau_r}{N_{pe\infty}}}$$

Y. Shao, Phys. Med. Biol., vol. 52, pp. 1103–1117, 2007.

CTR @511 keV for several scintillators

Typical crystal size 2x2x3mm³

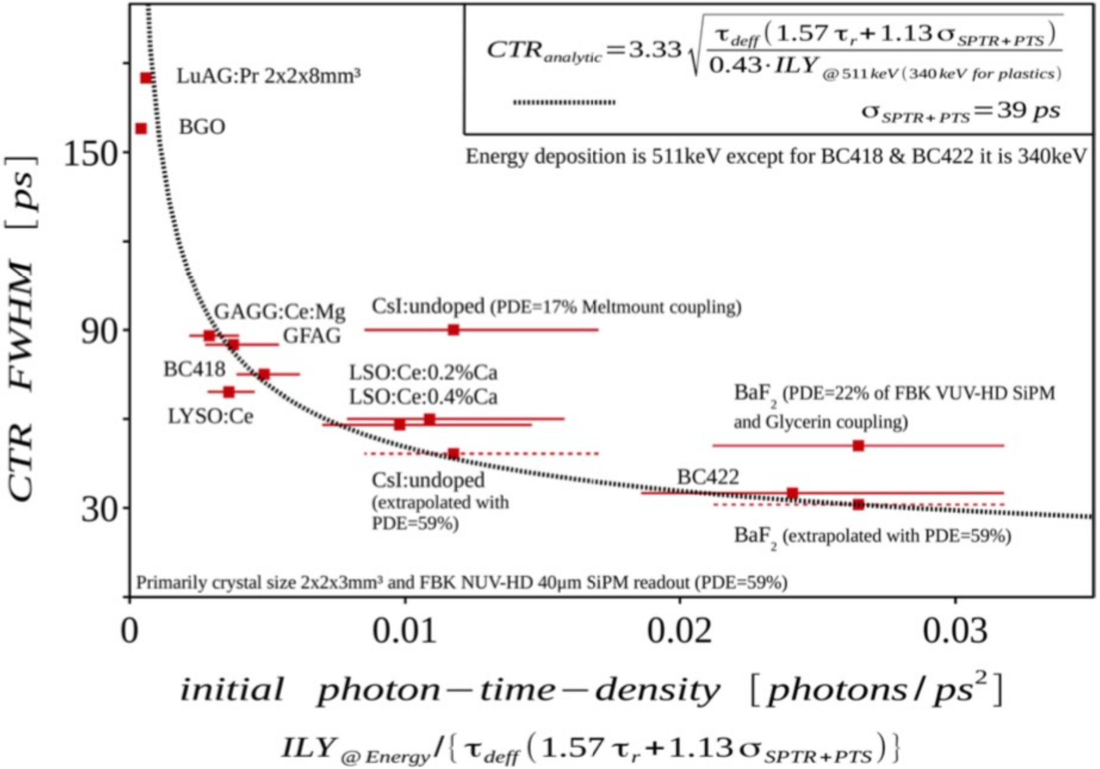

Analytic CTR expression
S. Vinogradov,
NIMA 912 (2018) 149-153

S. Gundacker et al. Phys. Med. Biol. 65 (2020) 025001

Characteristics of some inorganic crystals

	Na(Tl)	CsI	CsI(Tl)	BGO	PWO	CeF_3	BaF_2	LSO	$LaBr_3$ (Ce)	LuAP Pr/Ce	LuAG: Pr/Ce	GAGG:Ce
ϱ (g/cm^3)	3.67	4.51	4.51	7.13	8.3	6.16	4.89	7.4	5.29	8.34	6.73	6.63
X_o (cm)	2.59	1.86	1.86	1.12	0.89	1.66	2.03	1.14	1.88	1.08	1.41	1.56
Rm (cm)	4.13	3.57	3.57	2.23	2	2.41	3.1	2.07	2.85		2.33	2.1
n	1.85	1.79	1.95	2.15	2.2	1.8	1.5	1.82	1.9	1.97	1.84	1.9
λ (nm)	415	310/420	550	480	420	310	195-220/310	420	356	310/365	290,350/535	520
τ (ns)	230	6/35	10.5	300	10/30	5/30	0.8/630	40	20	20/18	20/70	50-90
LY (ph/MeV)	38000	2000	54000	8000	200	2000	1500/10000	33000	63000	15000/11400	>15000/>25000	>35000

Classification of scintillators

- Density
- Light Yield
- Energy Resolution
- Decay Time

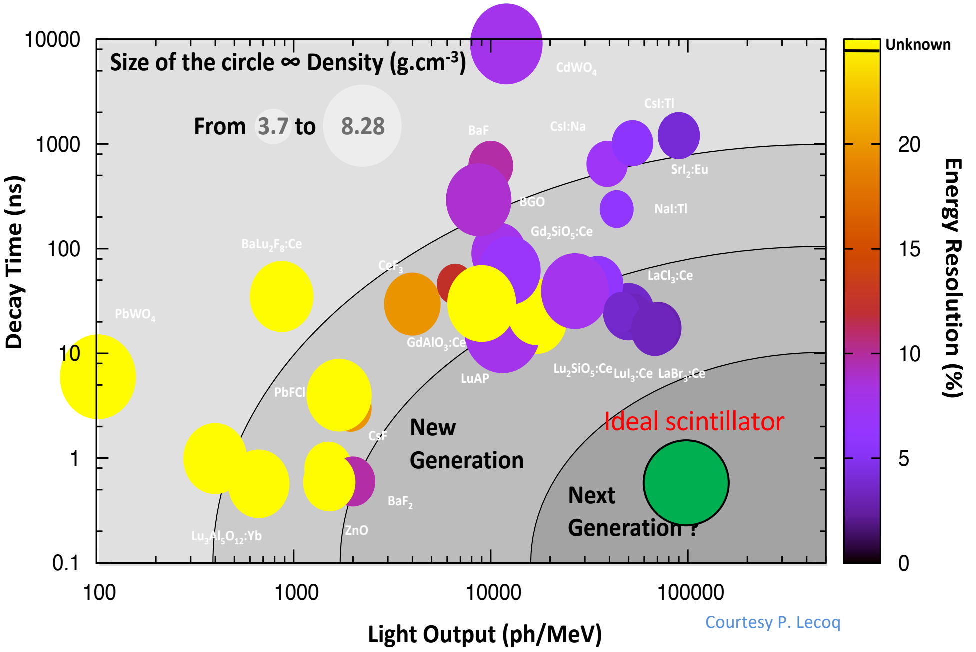

Courtesy P. Lecoq

Important parameters for scintillators

- Transmission
- Radiation damage
- Light Yield, energy resolution
- Decay time

Optical Transmission

Ratio between the intensity of light entering (I_0) and exiting (I) the crystal

$$T = \frac{I}{I_0}$$

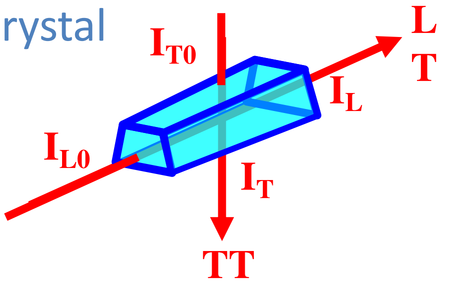

- detect presence of defects and/or dopants in the crystal
- detect presence of diffusion centres
- control the transparency in the spectral region of luminescence emission
- control the uniformity of the optical properties along the crystal length

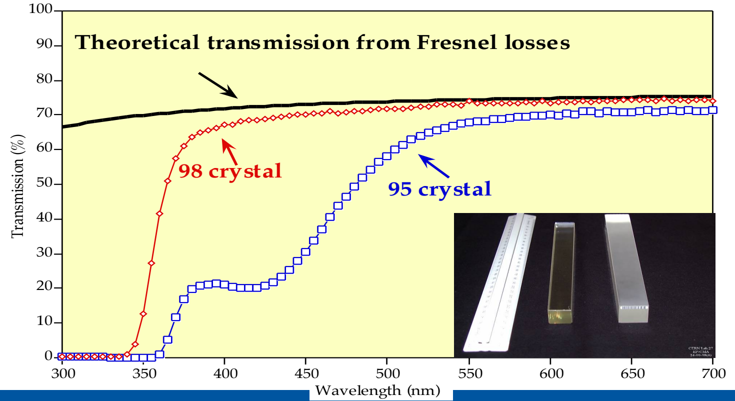

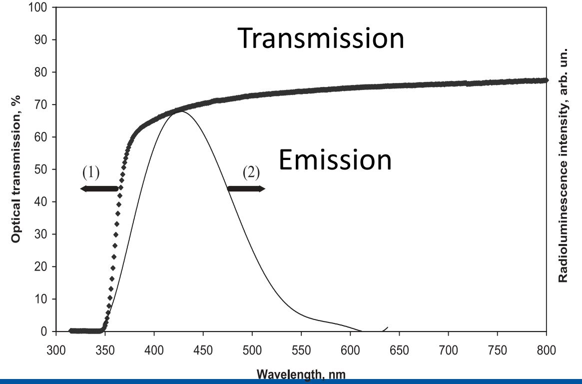

The importance of radiation hardness

→ Reduction of light collection on photodetector
→ Degradation of energy resolution

With irradiation :
creation of color centers which absorb light
=> Degradation of transparency

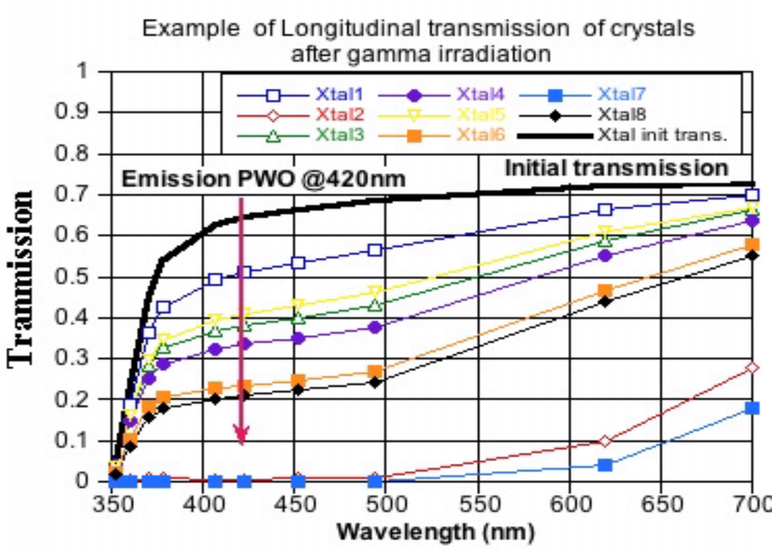

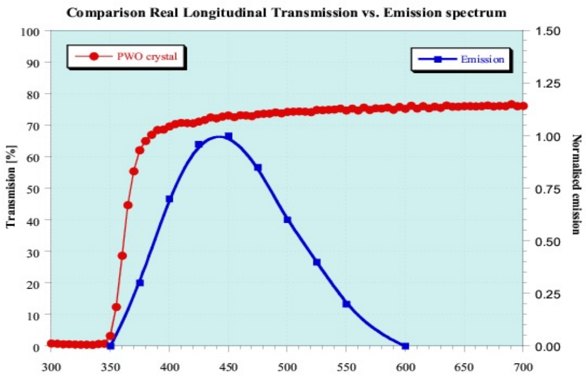

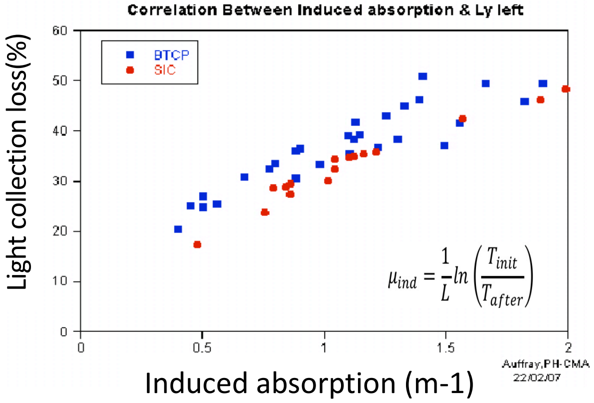

Light output

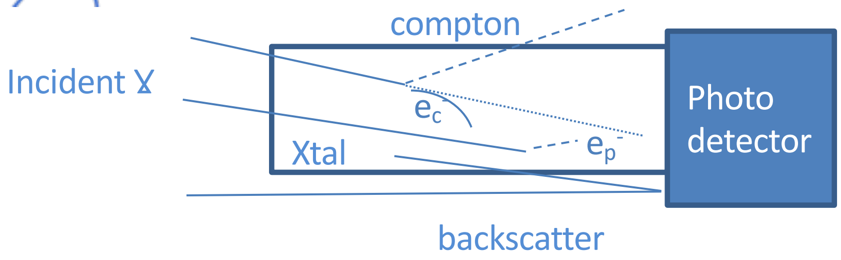

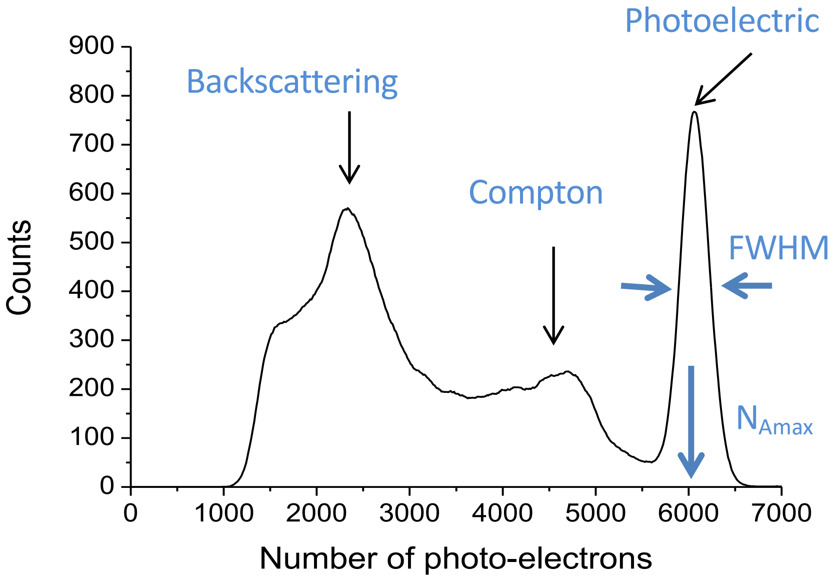

Light output:

Number of photons emitted by the scintillator and collected on the front face of the photocathode per unit of energy deposited by an incident particle, usually *photons/MeV*

$$LY(pe/MeV) = \frac{N_{A\max} - Ped}{Peak_{se} - Ped} \, x \, \frac{1}{E_{inc}}$$

Energy resolution:

ratio between the full width at half maximum and the position of the photopeak

$$\left(\frac{\Delta E}{E}\right)_{FWHM} = \frac{FWHM}{N_{A_{\max}}} x100$$

FWHM – Full Width at Half Maximum,
N_{Amax} position of the peak maximum

Light output

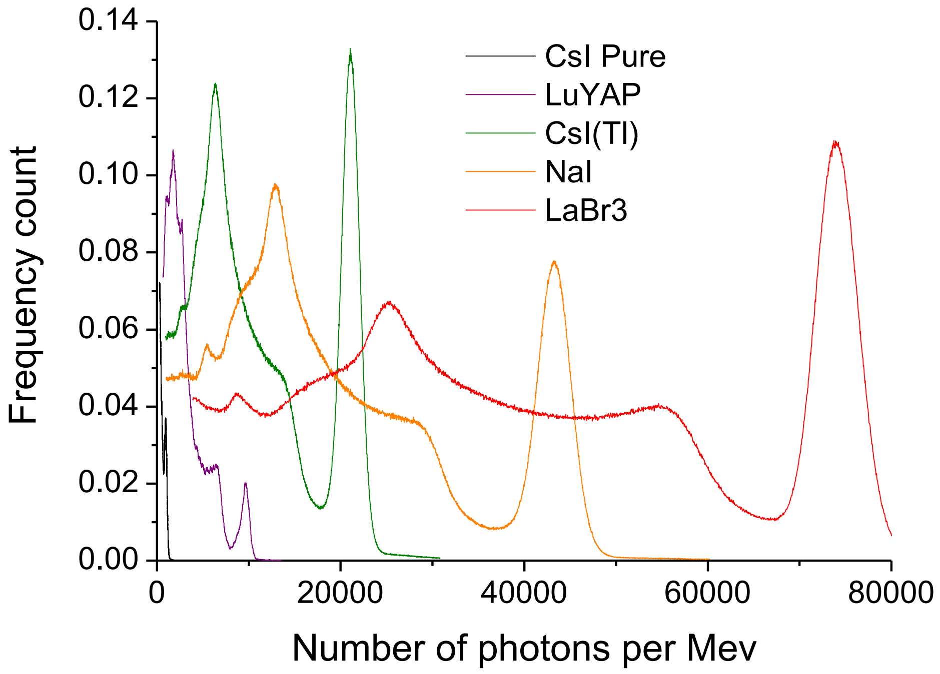

LY varies with crystal types

Energy resolution

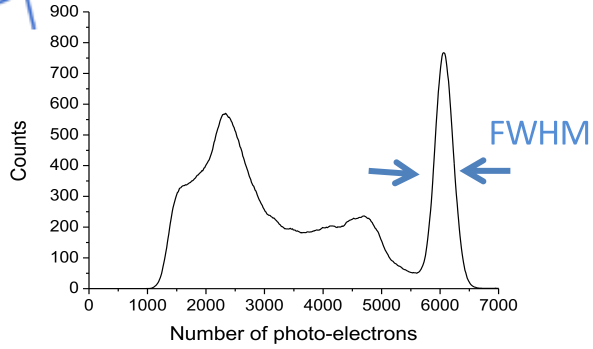

$$E_r^{\,2} = \left(\frac{\Delta E}{E}\right)^2 = (\delta_{sc})^2 + \left(\frac{\Delta N}{N}\right)^2$$

Photostatistic contribution $\frac{\Delta N}{N} = 2.36 * \sqrt{\frac{1+\varepsilon}{N_{pe}}}$

Intrinsic crystal contribution $(\delta_{sc})^2$

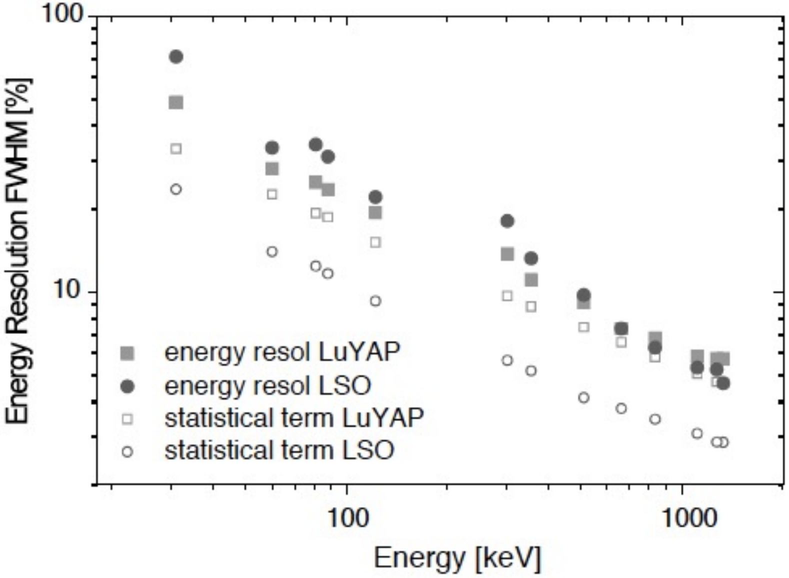

C. Kuntner et al., NIM A 493 (2002) 131–136

Non linearity of light output

Non proportionality : $\sigma_{np} = \sqrt{\frac{1}{N}\sum_{i=1}^{N}\left(\frac{Y(E_i)}{Y(662)} - 1\right)^2}$

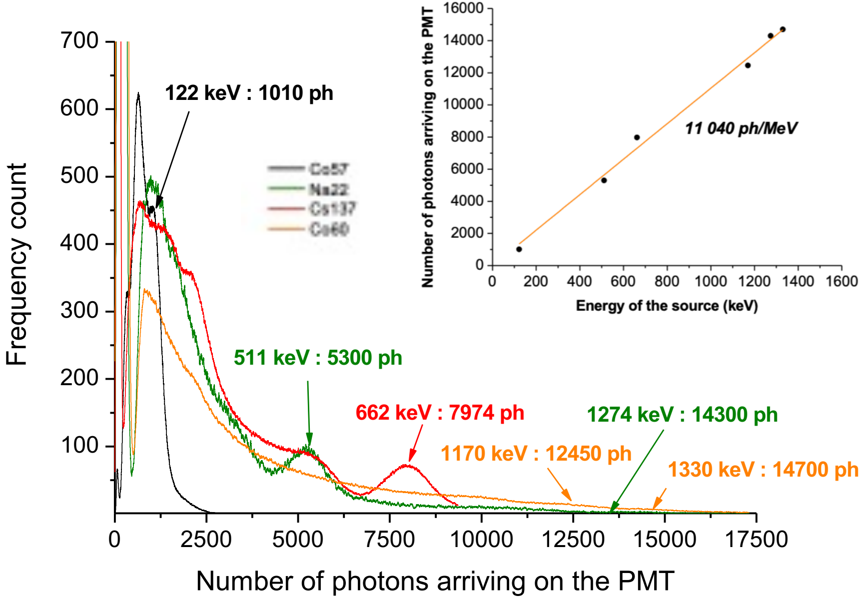

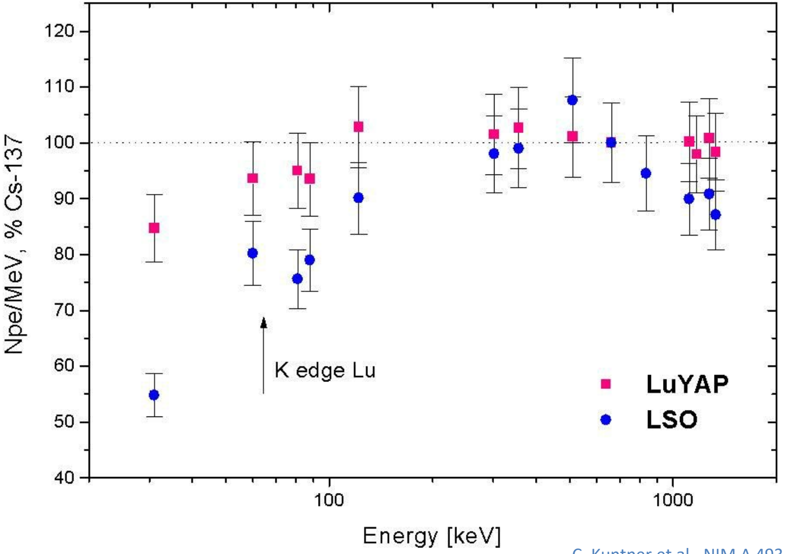

C. Kuntner et al., NIM A 493 (2002) 131–136

Non proportionality varies with crystal

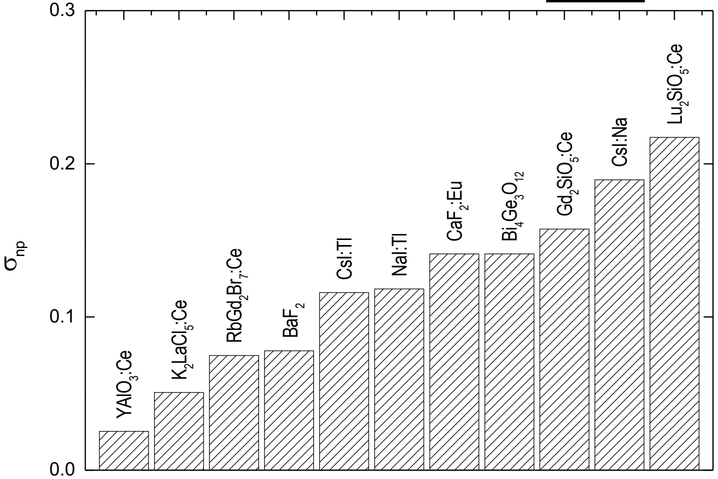

$$\sigma_{np} = \sqrt{\frac{1}{N}\sum_{i=1}^{N}\left(\frac{Y(E_i)}{Y(662)} - 1\right)^2}$$

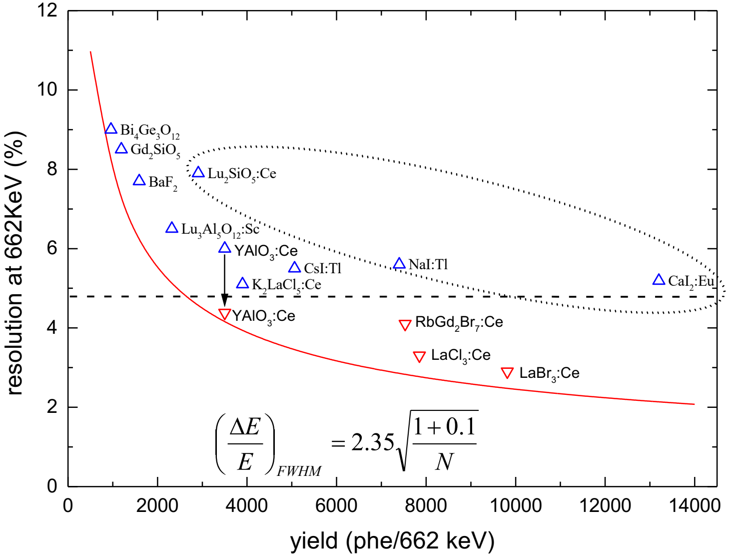

P. Dorenbos, SCINT2001 conference

Time coincidence resolution measurements

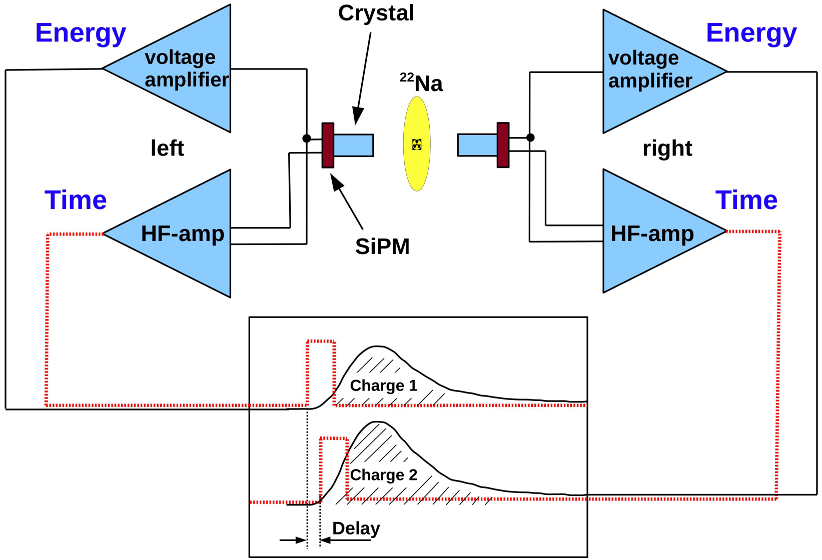

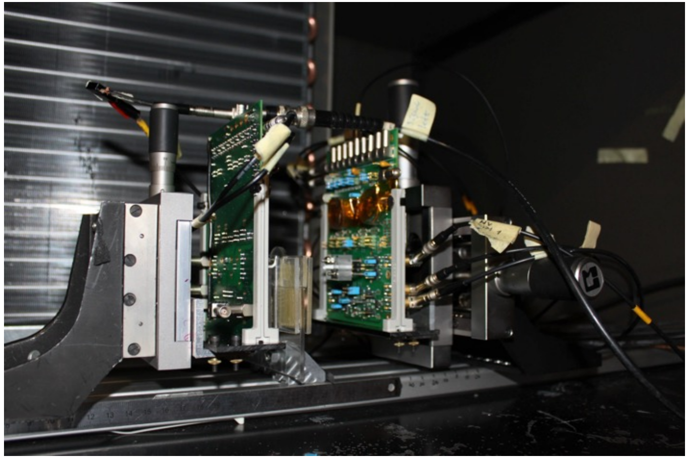

Time coincidence resolution set-up developped in lab 27 by S. Gundacker

Data acquisition:
LeCroy Oscilloscope DDA 735Zi with 3.5GHz Bandwdith and 40Gs/s
High frequency readout

S. Gundacker, PhD thesis
S. Gundacker et al, JINST 8 P07014 2013
J. Gates et al, PMB Phys. Med. Biol. (2018) 63 185022
S. Gundacker et al., Phys. Med. Biol. (2019) 64 055012

Time coincidence resolution measurements

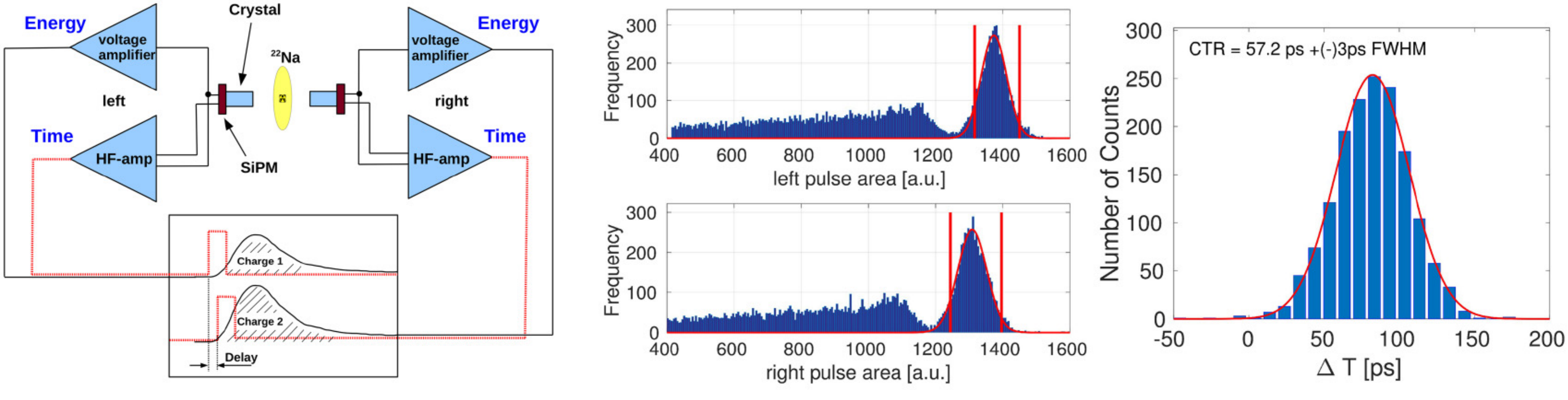

(a) (b)

Data acquisition:
LeCroy Oscilloscope DDA 735Zi with 3.5GHz Bandwdith and 40Gs/s
High frequency readout

S. Gundacker et al., Phys. Med. Biol. (2019) 64 055012

Production methods

Vertical Bridgman technique

Currently used methods based on the works of Bridgman (1925), Stober (1925) & Stockbarger (1936).

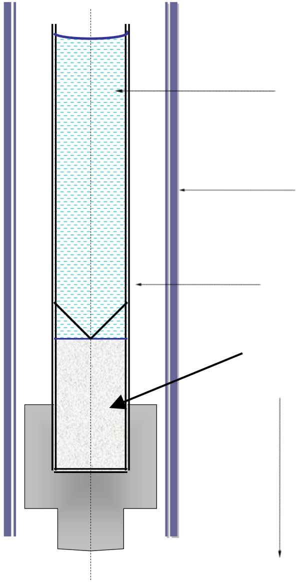

For high-melting materials, the melt contained in a crucible/ampoule is progressively frozen from one end by slow pulling down to the cold zone.

Courtesy A. Petrosyan

Czochralski technique

Developed by Czochralski (1918);

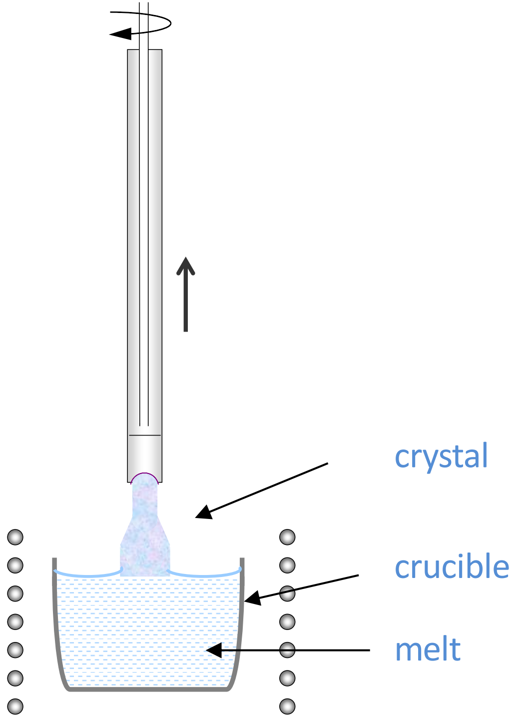

The melt is contained in a crucible made of Ir, Mo, Pt, Rh or Re, the crystal is grown at the free top surface of the melt; the rotating seed crystal is put into contact with the melt and pulled upwards at a given rate.

Courtesy A. Petrosyan

Example of crystal Ingots

PWO (BTCP)

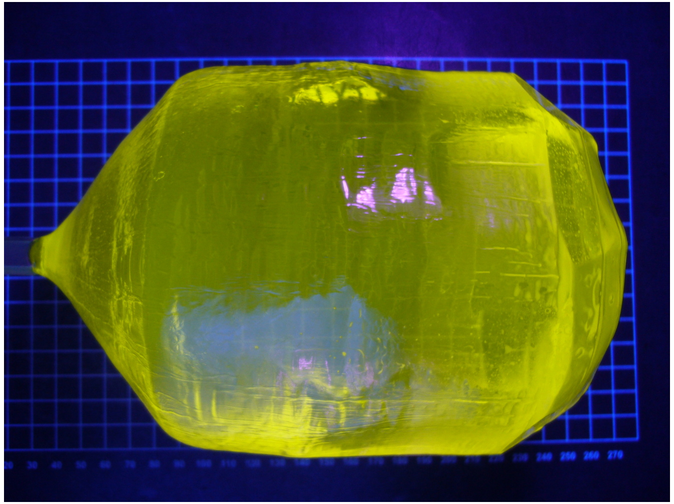

YAG (Crytur)

Micro-Pulling down technology for crystal fibre growth

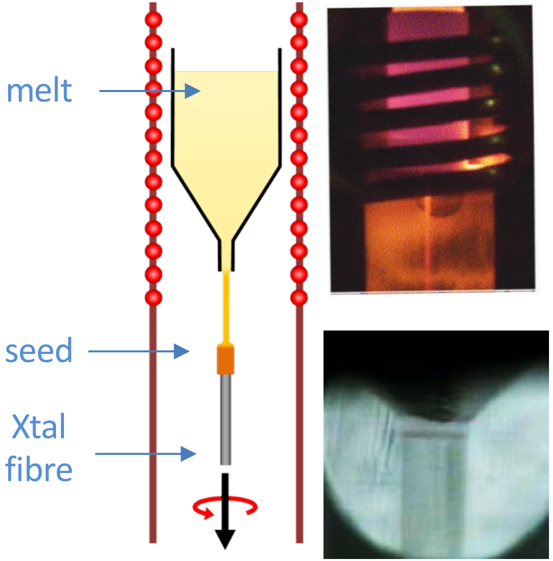

Courtesy Fibercryst

The melt is contained in a crucible with a capillary die at the centre bottom. the growth process starts after connection of the seed with a melt drop at capillary die. Then the seed is pulled down continuously to form the crystal fibre

Micro-Pulling down technology for crystal fibre growth

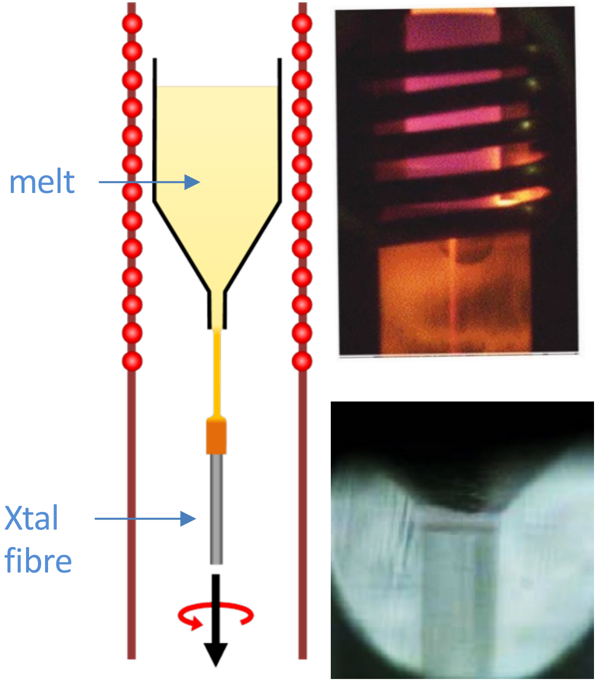

Courtesy Fibercryst

Micro-pulling down (µPD) : multiple advantages

- Wide range of diameters 300 µm – 3 mm
- Lengths up to 2 m
- Multiple geometries for capillary die ○□⬡
- Fast pulling rates
- Multi-fibres pulling possibilities (in parallel)

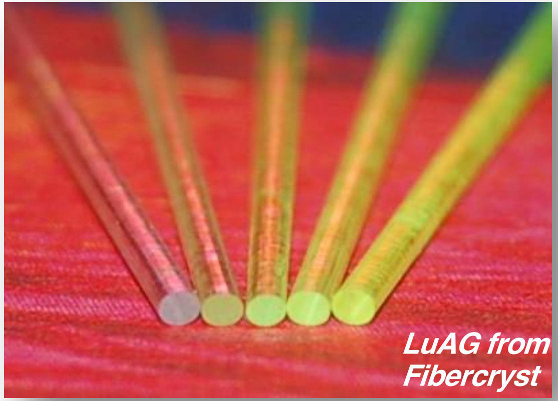

Edge-defined film-fed growth method (EFG)

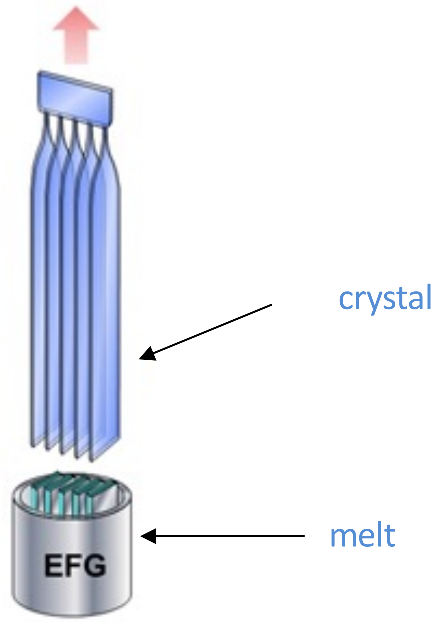

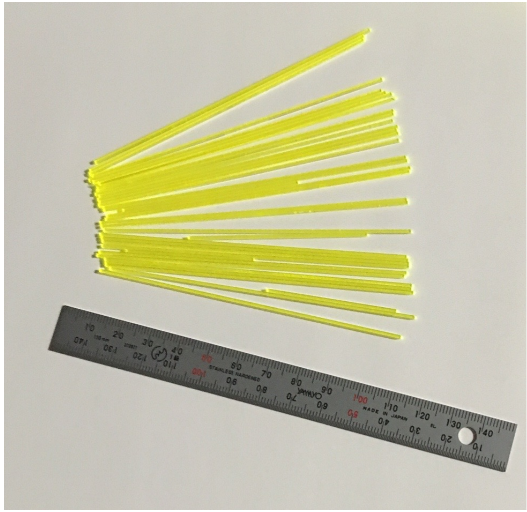

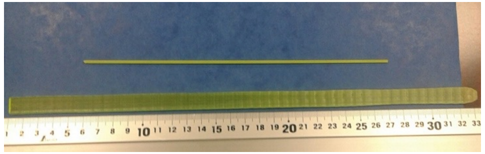

EFG-grown plate & fiber of LuAG:Ce
from Adamant Namiki Co , Japan

New production method: 3D printing

A way to design detector with unconventional shape

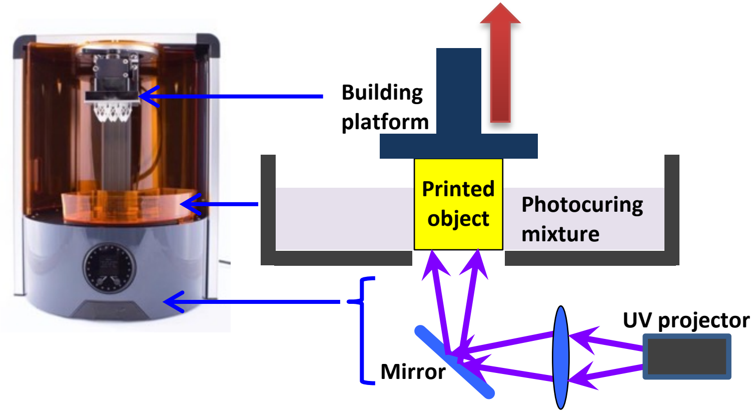

Printing is done layer-by-layer
Voxel size is ~50 x 50 x 10-50 µm

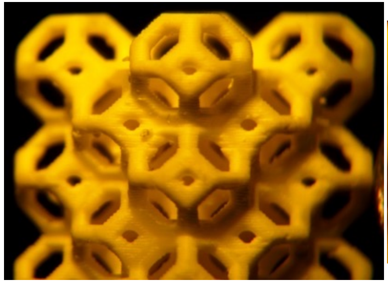

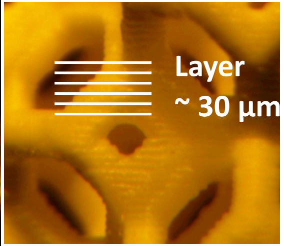

YAG

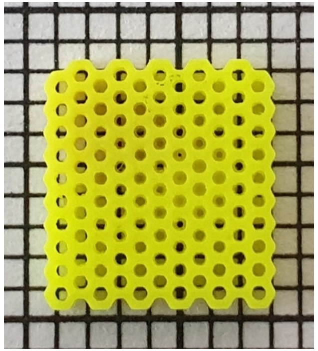

YAGG

Hole ⌀<400 µm

Courtesy of G. Dossovitky, Kurchatov Institute

PHOTODETECTORS

Photodetector

A photodetector converts light in electrical pulse

3 main steps:

1. Generation of a primary photoelectron or electron-hole (e-h) pair by an incident photon by the photoelectric or photoconductive effect,

2. Amplification of the p.e. signal to detectable levels by one or more multiplicative bombardment steps and/or an avalanche process (usually),

3. Collection of the secondary electrons to form the electrical signal

Photodetector main characteristics

- Quantum efficiency/photodetection efficiency (QE or PDE)
- Gain (G)
- Dark current or dark noise
- Energy resolution
- Dynamic range
- Time dependence of the response
- Rate capability

Various types of photodetectors

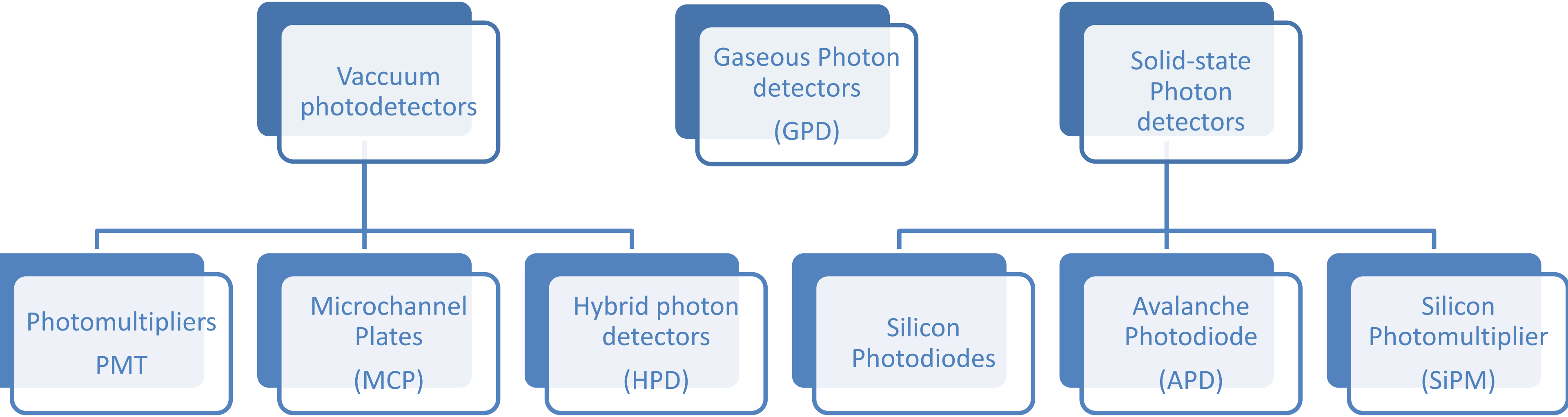

Main characteristics of photodetectors

Table 35.2: Representative characteristics of some photodetectors commonly used in particle physics. The time resolution of the devices listed here vary in the 10–2000 ps range.

Type	λ (nm)	$\epsilon_Q \epsilon_C$	Gain	Risetime (ns)	Area (mm^2)	1-p.e noise (Hz)	HV (V)	Price (USD)
PMT *	115–1700	0.15–0.25	10^3–10^7	0.7–10	10^2–10^5	10–10^4	500–3000	100–5000
MCP*	100–650	0.01–0.10	10^3–10^7	0.15–0.3	10^2–10^4	0.1–200	500–3500	10–6000
HPD*	115–850	0.1–0.3	10^3–10^4	7	10^2–10^5	10–10^3	$\sim 2 \times 10^4$	~600
GPM*	115–500	0.15–0.3	10^3–10^6	$O(0.1)$	$O(10)$	10–10^3	300–2000	$O(10)$
APD	300–1700	~0.7	10–10^8	$O(1)$	10–10^3	1–10^3	400–1400	$O(100)$
PPD	320–900	0.15–0.3	10^5–10^6	~ 1	1–10	$O(10^6)$	30–60	$O(100)$
VLPC	500–600	~0.9	$\sim 5 \times 10^4$	~ 10	1	$O(10^4)$	~7	~1

*These devices often come in multi-anode configurations. In such cases, area, noise, and price are to be considered on a "per readout-channel" basis.

P.A. Zyla *et al.* (Particle Data Group), Prog. Theor. Exp. Phys. **2020**, 083C01 (2020)
https://pdg.lbl.gov/2020/download/Prog.Theor.Exp.Phys.2020.083C01.pdf

Photomultiplier principle

Fig. 1 from P. Kirzan, S. Korpar, Annu. Rev. Nucl. Part. Sci. 2013. 63:329–49

1) Photo emission from photocathode
⇒ QE : 10% to 40%
Depends photocathode + wavelength

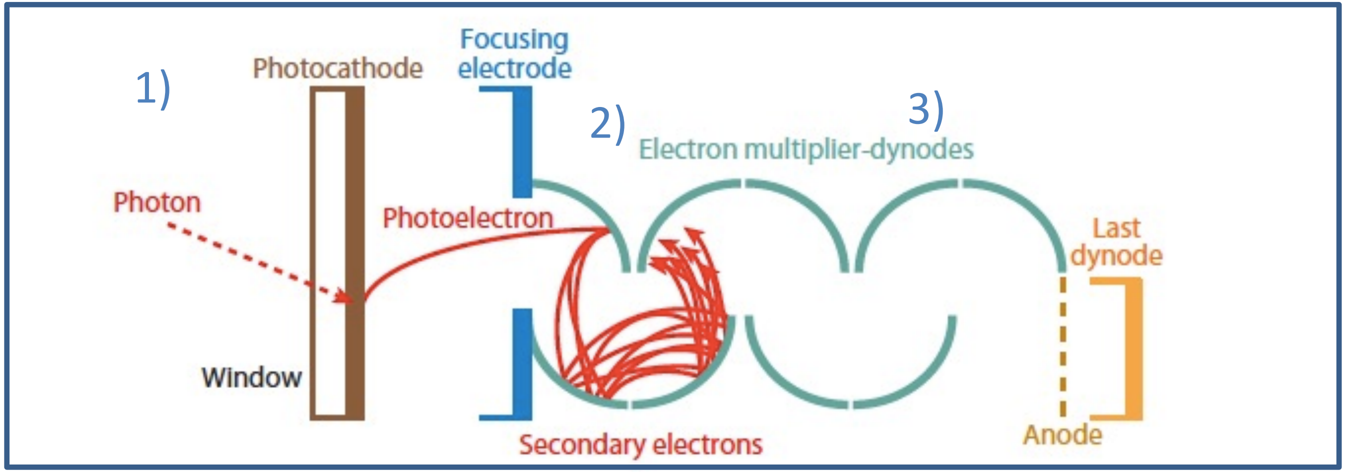

2) Collection pe 1st dynode

3) Mutiplication through dynodes
⇒ Gain : $\delta_1 * \delta_2 * \delta_3 .... * \delta_N$
G: 10^4 to 10^6

Main disadvantages : Sensitivity to Magnetic field, High HV bias

Variety of photomultipliers

A large variety of PMT

https://www.hamamatsu.com/resources/pdf/etd/PMT_handbook_v3aE.pdf

QE depends on photocathode types

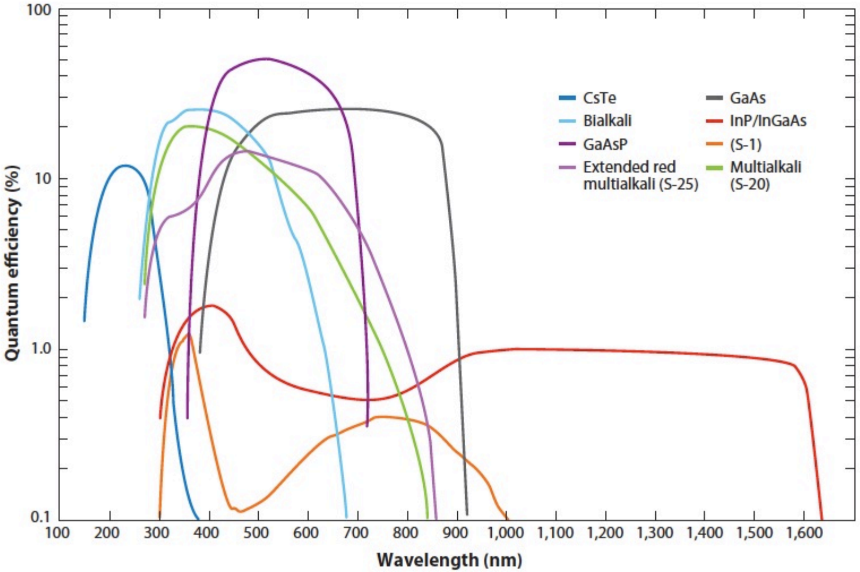

Fig. 2 From P. Kirzan, S. Korpar, Annu. Rev. Nucl. Part. Sci. 2013. 63:329–49

Variety of photomultipliers

A large variety of PMT

https://www.hamamatsu.com/resources/pdf/etd/PMT_handbook_v3aE.pdf

=> Choice of PMT depends on scintillator emission

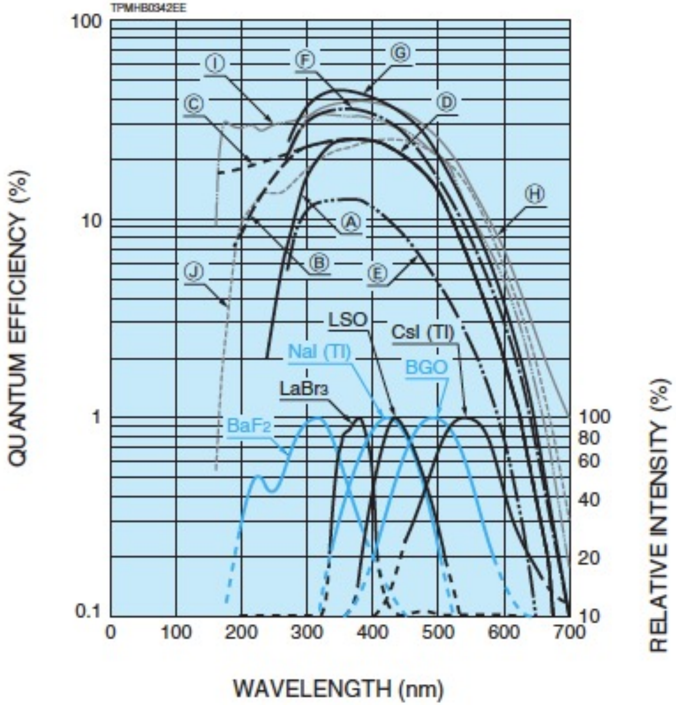

Fig 34: From Photomultiplier tubes and assemblie for scintillation vaunting &HEP Hamamatsu
https://www.hamamatsu.com/resources/pdf/etd/High_energy_PMT_TPMZ0003E.pdf

Silicon Photodetectors

Photodiode	Avalanche Photodiode	Geiger avalanche Photodiode

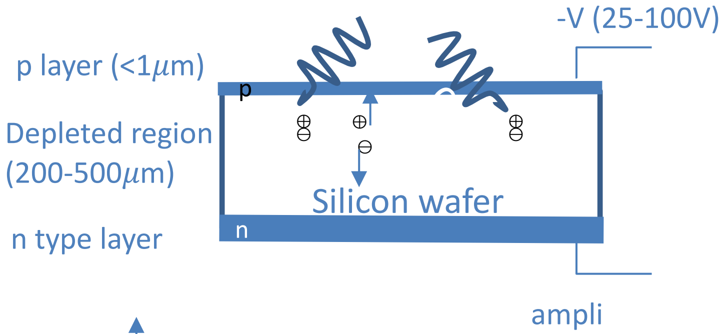

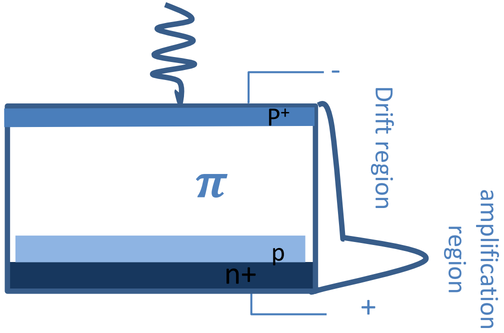

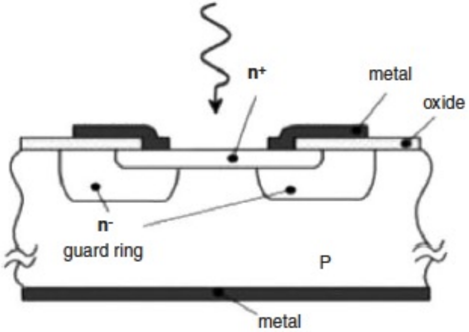

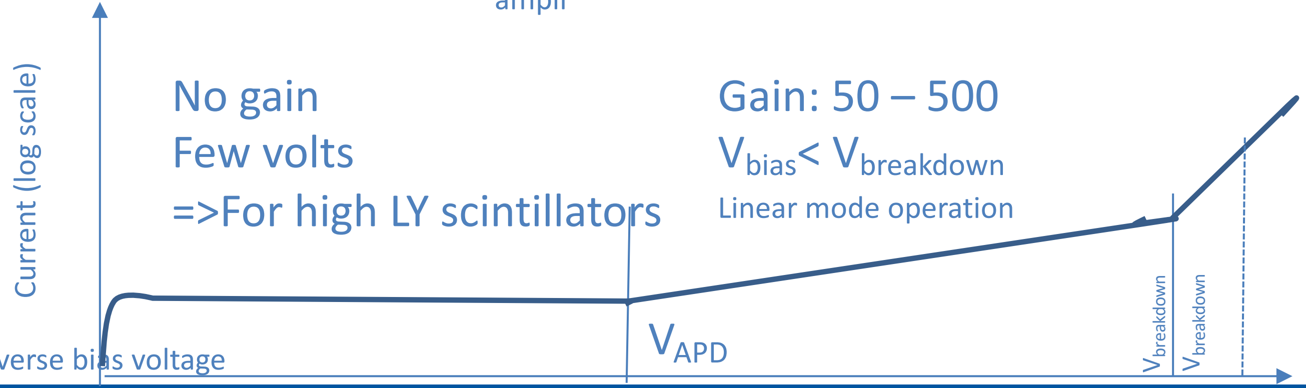

No gain
Few volts
=>For high LY scintillators

Gain: 50 – 500
$V_{bias} < V_{breakdown}$
Linear mode operation

Gain: very high
$V_{bias} > V_{breakdown}$
Geiger –mode operation

P. Kirzan, S. Korpar, Annu. Rev. Nucl. Part. Sci. 2013. 63:329–49

Silicon photomultiplier (SiPM)

Array of single SPADs on a common Si substrate,
all SPADs with quenching resistor are in parallel

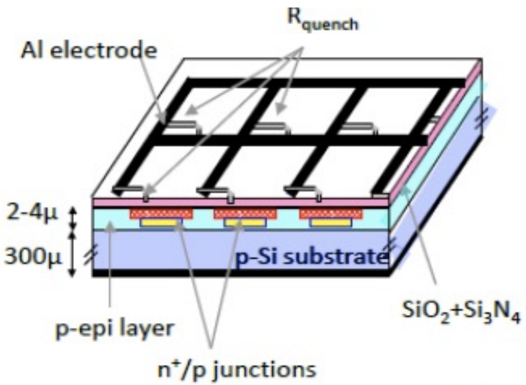

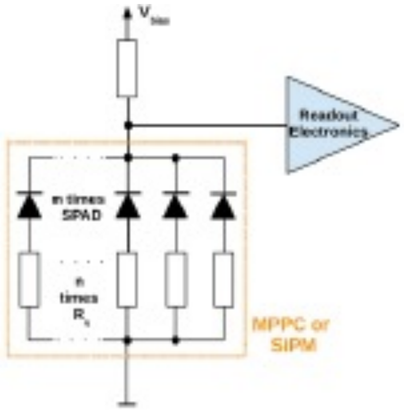

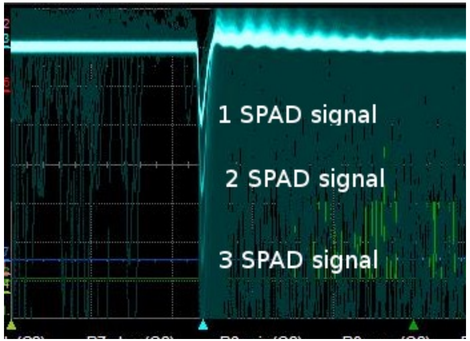

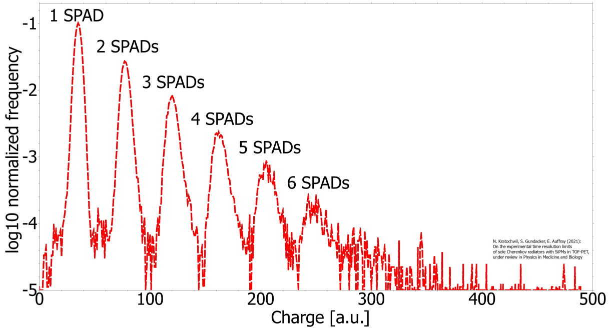

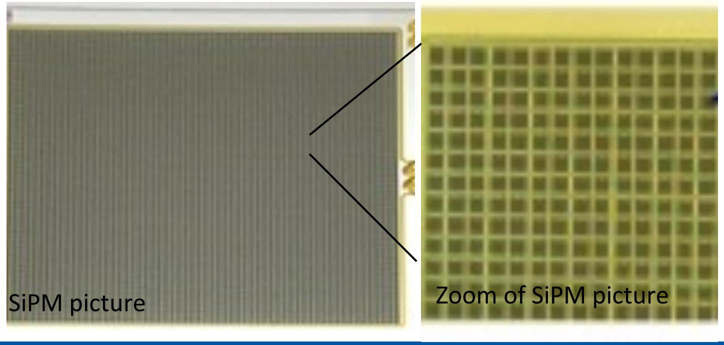

SiPM picture

Zoom of SiPM picture

N. Kratochwill et al. Phys. Med. Biol. 66 (2021) 195001

photon detection efficiency(PDE)

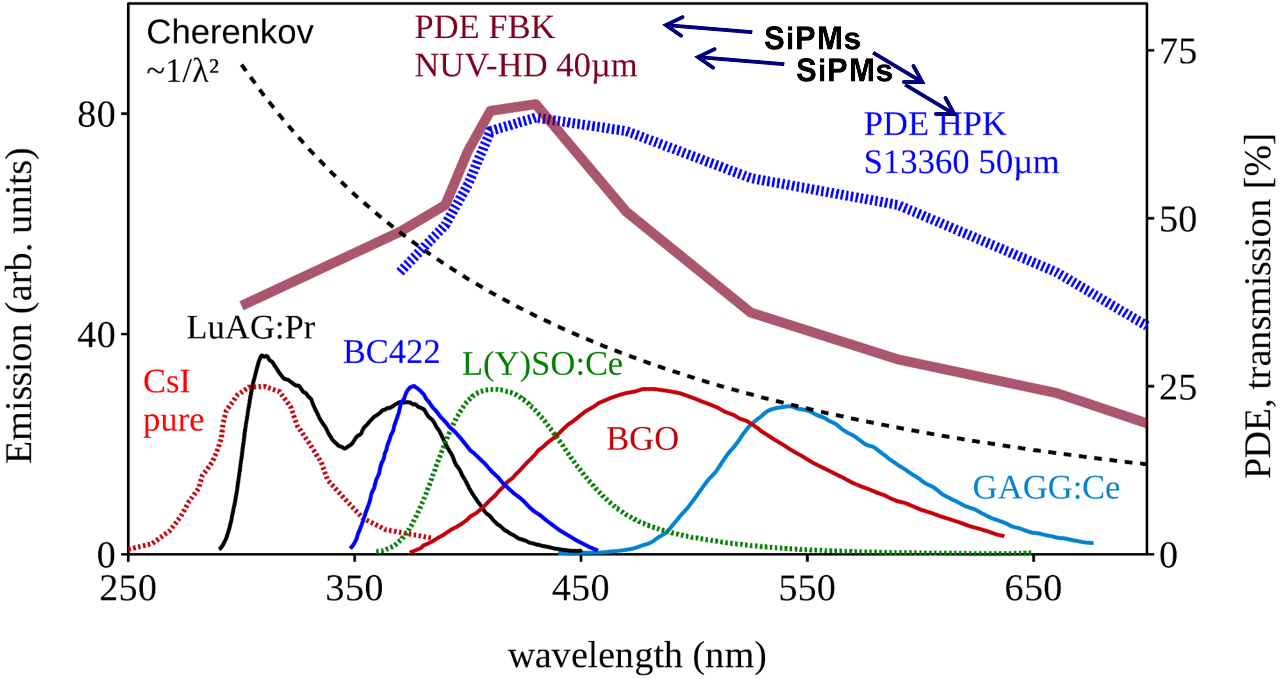

S. Gundacker et al. Phys. Med. Biol. 65 (2020) 025001

APPLICATIONS

Many Applications used scintillators

- Astronomy and dark matter searches
- High Energy Physics → Calorimetry
- Medical Imaging → PET
- X ray and gamma spectroscopy
- Monitoring in nuclear plants
- Neutrons detection
- Oil well drilling

Oil well logging

Detector concept

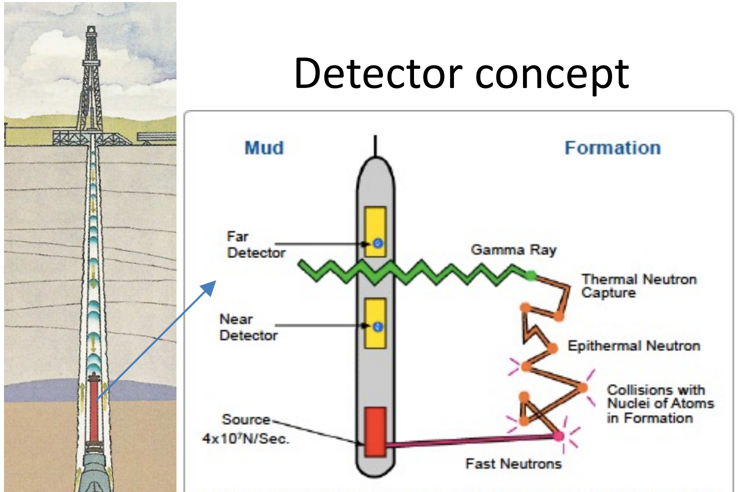

Figure 6: Generalized Neutron Logging Tool illustrates a typical neutron logging tool (Schlumberger, 2010).

A. Bu, Oil Gas Res 2016, 2:2
DOI: 10.4172/2472-0518.1000113

Requirements:

- High density, High Z
- Good energy resolution
- Coverage of energy from few 0 to 3 MeV
- Non hydroscopic
- Rugged
- Good high temperature performance 20 to 175^{o}C
- Used crystals NaI(Tl), BGO with some limitations

=> R&D for new scintillators: with higher density, faster, low temperature variation of LY: LuAP, YAP …

See also M. Vasilyev, V. Khabashesku, Engineering of Scintillation Materials and Radiation Technologies. Ed M. Korjik & A Gektin springer 303-324

Security

Vehicule inspection

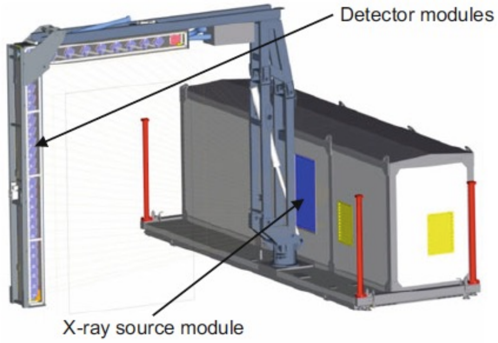

Personal Radiation detector

https://www.thermofisher.com/order/catalog/product/4250671#/4250671

Requirements:

- High light Yield
- High energy resolution
- Coverage of energy from few 10keV to 5 MeV
- Scintillating crystal/plastic scintillator depending size of the detector
- Usually used Na(Tl) or PVT(polyvinyltoluene)
- R&D on many other scintillators ongoing

V. Linev et al., Engineering of Scintillation Materials and Radiation Technologies. Ed M. Korjik & A Gektin springer 325-339

Gammay ray Space Telescope

Fermi Gamma Ray Space Telescope (FGST)-: Large area telescope (LAT)

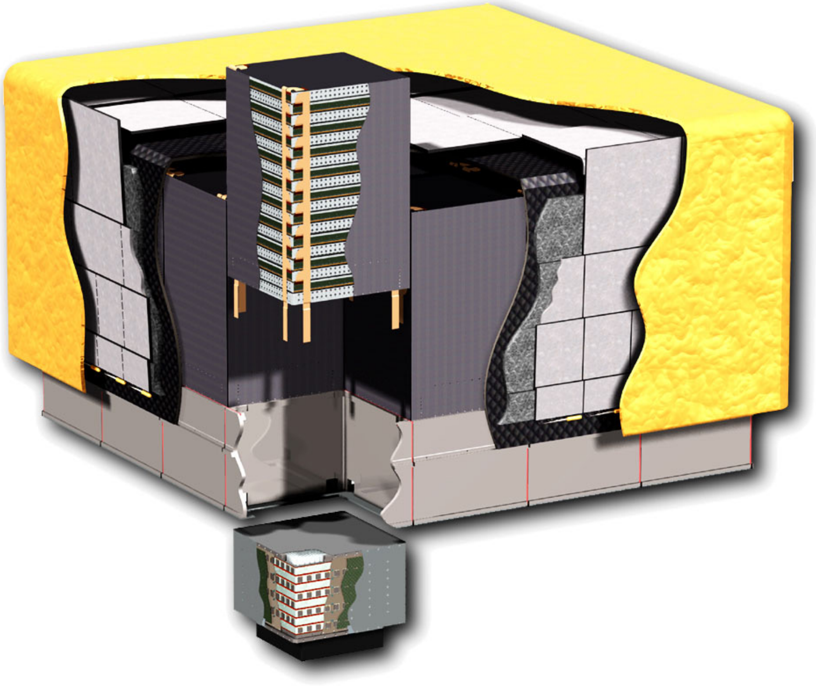

Aim: measure directions, energies & arrival time of γ rays with energy 20MeV to 300GeV:

- Tracking:
  silicon microstrip detector with tungsten sheets converted layer
- Crystal calorimeter:
  CsI Scintillator with photodiode readout (16*96 crystals of $2.7*2*32.6cm^3$) readout with photodiode

Handbook of particle detection and Imaging, C Gruppen, I Buvat, springer 2018

Search for dark matter

Weakly Interacting Massive Particles (WIMPs)

***C**ryogenic **R**are **E**vent **S**earch with **S**uperconducting* (CRESST) experiment:

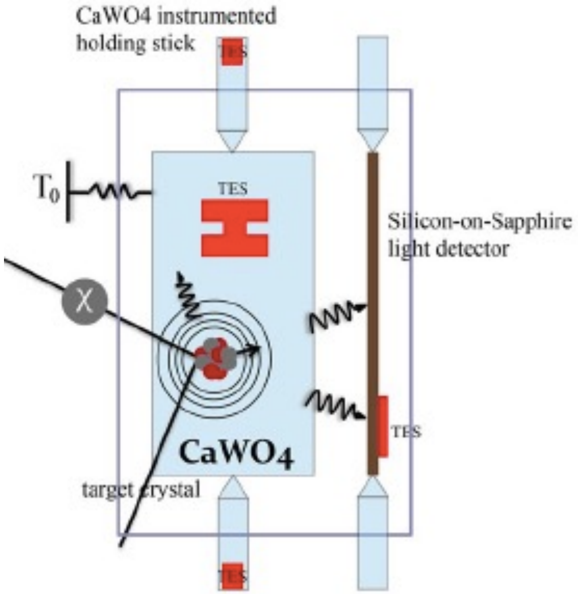

Direct detection - elastic scattering of nuclei

1. Low energy recoil: 20 keV
2. Expected event rate ≈ 1/kg year

⇒ Background rejection using simultaneous observation of the light signal and heat signal.

=> Temperature 15mK

M. Mancuso et al. Journal of Low Temperature Physics (2020) 199:547–555
https://doi.org/10.1007/s10909-020-02343-3

Search for dark matter

Weakly Interacting Massive Particles (WIMPs)

CRESST Detector

The CRESST Detector Modules are arranged in a support structure which can hold up to 33 crystals, corresponding to 10kg of detector material.

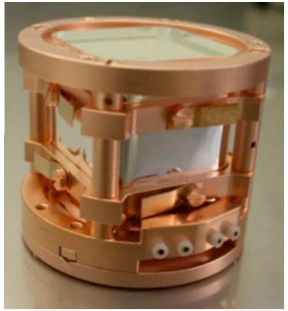

Requirements

- high light yield at low temperatures
- large atomic number A
- large light yield
- Radiopurity (ex Lu, Rb, K, U, Th)
- Suitable thermodynamics characteristics

$CaWO_4$ (τ=300µs; LY≈28'000ph/MeV) is used (⌀4*4cm)
=> large on-going effort to improve the purity of material

Possible other candidates

- under study $ZnWO_4$, $CaMoO_4$, $CdMoO_4$, $CdWO_4$

https://www.cresst.de/pictures.php

Search for dark matter

Xenon experiment:
3200T of liquid Xenon registered both scintillation and charge signal
=> Energy and position of interacting particle

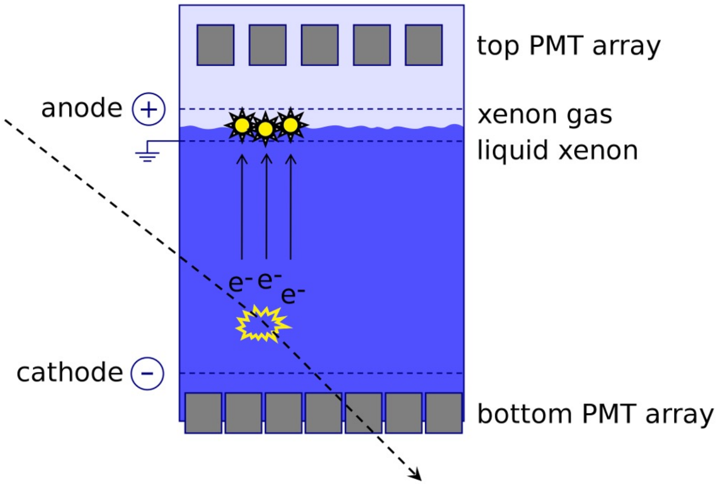

Pictures from http://www.xenon1t.org

Search for neutrinoless double beta decay

Enriched Xenon Observatory (EXO-200), nEXO experiment

Simultaneous readout of charge and scintillation in a large and homogeneous Liquid Xe TPC

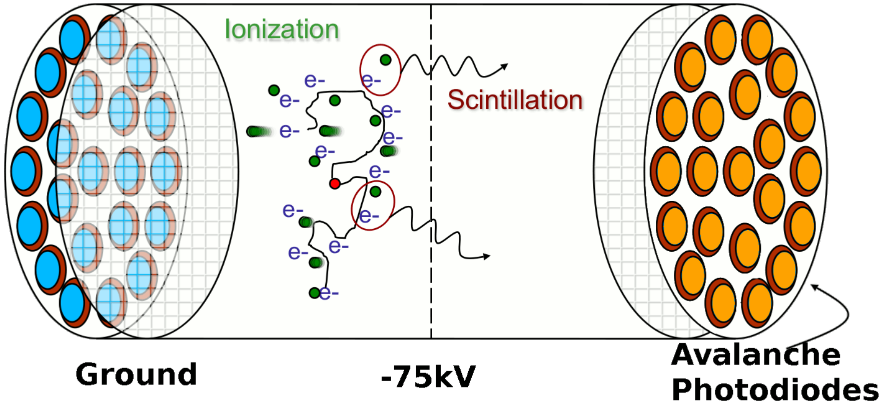

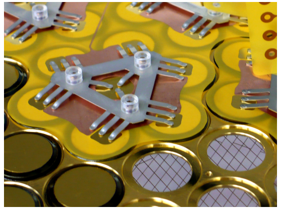

The EXO-200 experiment: 200kg of Xe liquid put a limit on the half- life of the process of > 1.1 x 10^{25} years,

Bigger detector nEXO on development:

⇒ 5 tonnes cryogenic, liquid xenon, enriched to 80% in the isotope ^{136}Xe

⇒ development of high speed VUV photodetector to detect 175nm UV emission of Xe

https://fiveyearplan.triumf.ca/teams-tools/nexo-next-enriched-xenon-observatory/

Calorimetry

Aim: Measure the total energy of high energy particle with best energy resolution for both electromagnetic ($e^{\pm}$, γ) and hadronic particles ($\pi^{\pm}$, $p^{\pm}$, $K^{\pm}$, n …)

Electromagnetic shower

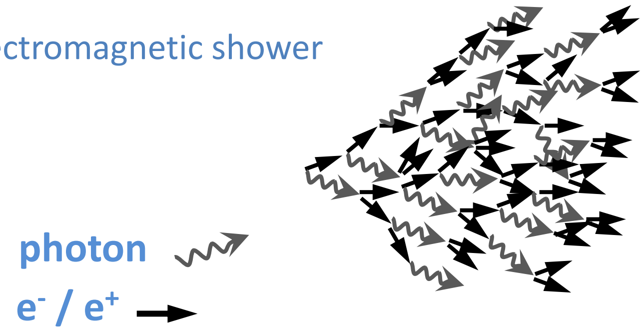

Hadronic shower

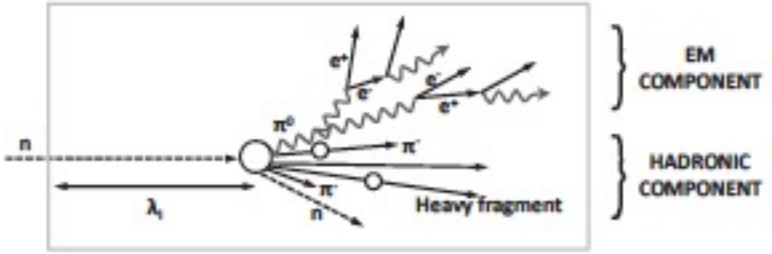

- Two types
  - Homogeneous: 1 material both absorber and active material
  - Sampling: 2 materials : absorber and active material

=> Homogenous better energy resolution

Development of an electromagnetic shower

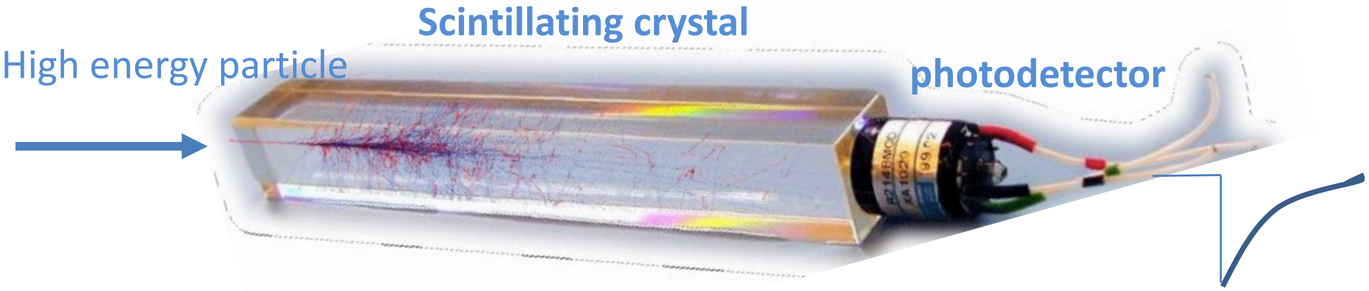

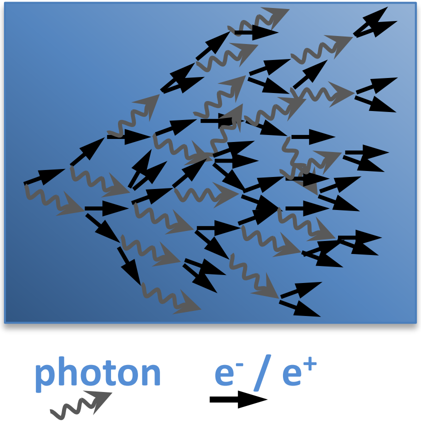

Characterized by:

- Radiation length X_o (g/cm^2): After 1 X_o : energy left is 1/e incident energy

$$X_0 = \frac{716.4A}{Z(1+Z)\ln\left(\frac{287}{\sqrt{Z}}\right)}$$

- Molière radius R_m(g/cm^2): Transverse size of shower: 95% in average of the shower's energy deposition is contained $R_m = 0.035 * X_o * (Z + 1.4)$

=> High Z material is preferable

Electromagnetic shower

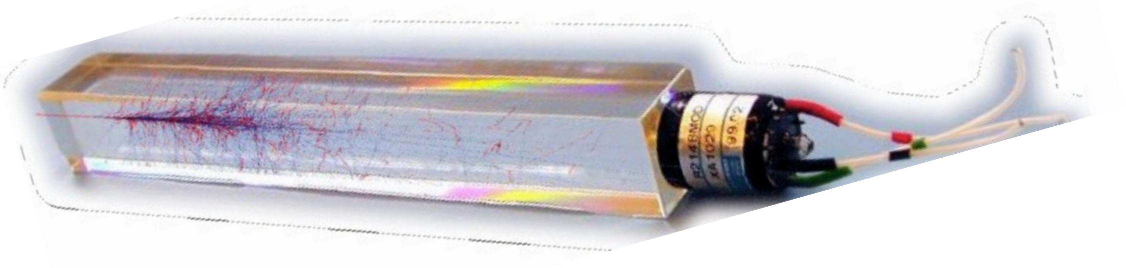

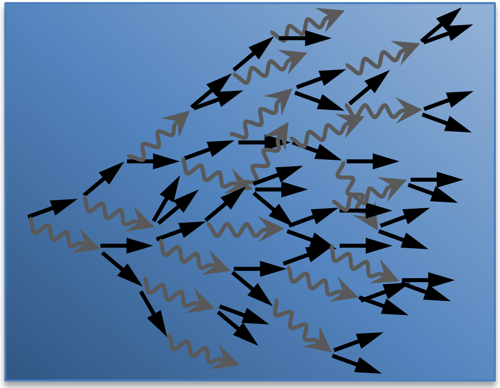

photon

e^- / e^+

Energy Resolution

$$\frac{\sigma_E}{E} = \frac{a}{\sqrt{E}} \oplus \frac{b}{E} \oplus c$$

a: statistical term: depends mainly on light yield => low for reasonable light Yield

b: noise term negligible

c: Constant term: depends on light uniformity, calibration

Light collection Uniformity

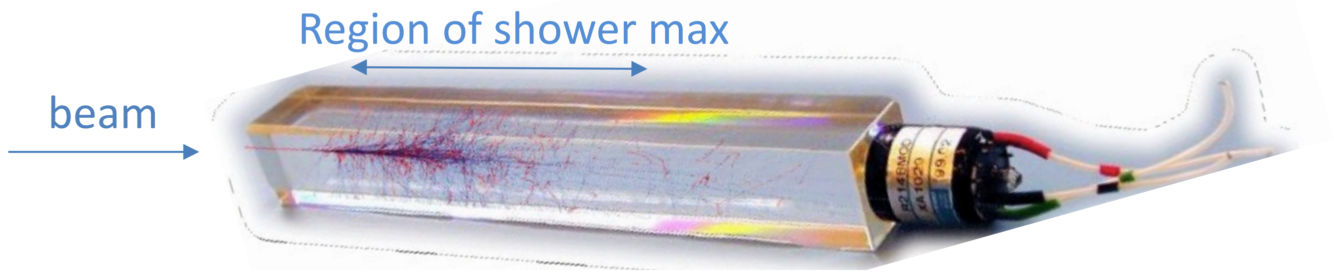

=> Light output non uniformity must be flat in this region

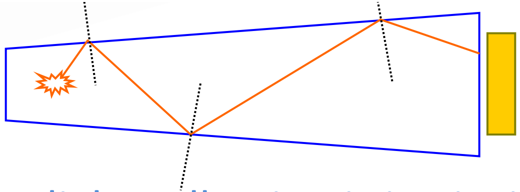

Due to the crystal tapering, the light collection is intrinsically non uniform along the crystal

Light collection Uniformity

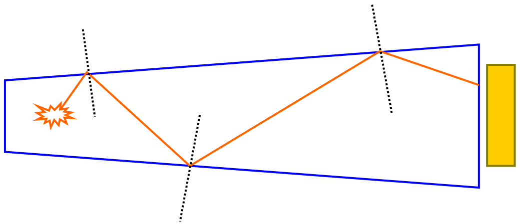

To restore uniformity, one method is to depolish one lateral face with a well defined roughness (Ra)

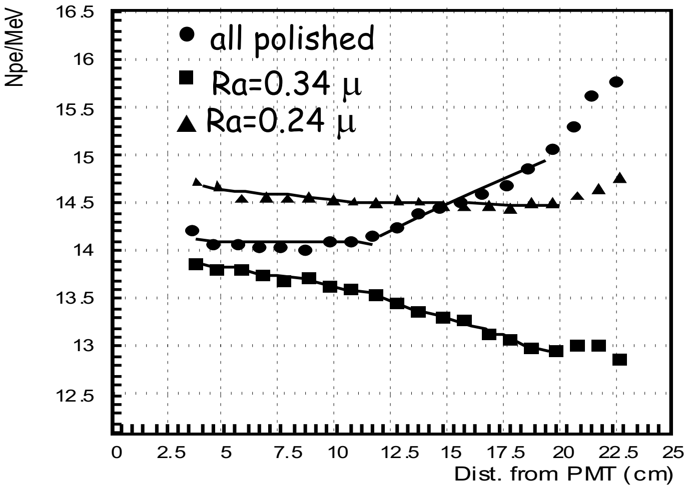

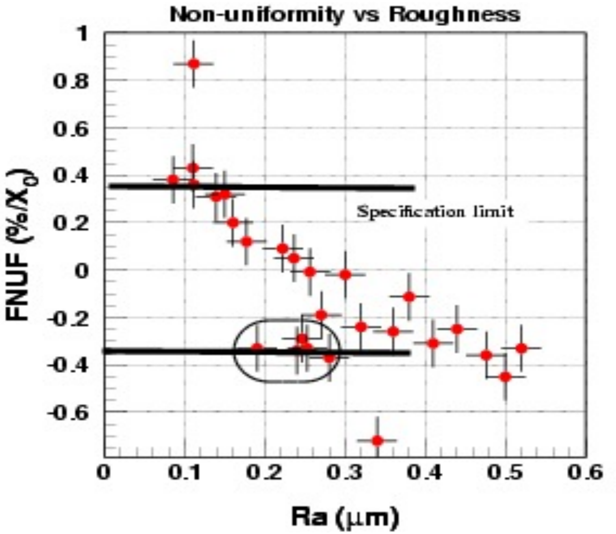

Crystal ball calorimeter

Crystal Ball @SLAC, 1979 for Charmonium spectroscopy

- 50cm diameter spherical ball of NaI(Tl) crystals
- 672 crystals 42cm long, PMT readout
- Very good resolution allowed precise spectroscopic study of charmonium states

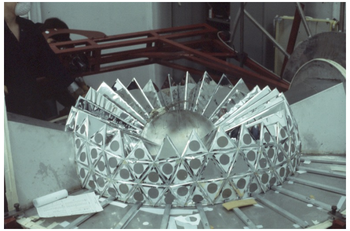

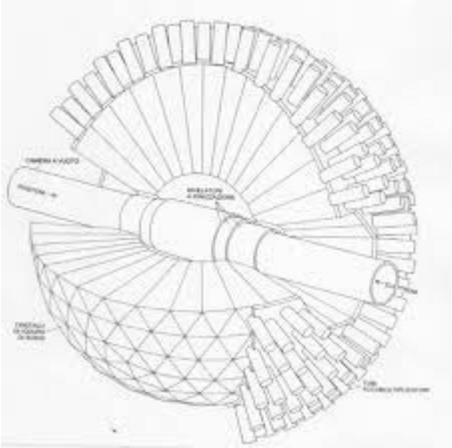

Charmonium decay

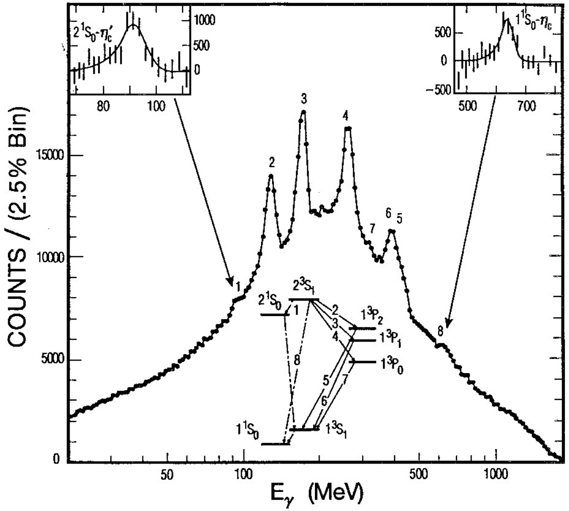

Babar detector at SLAC (PEP-2)

Detailed study of b-quarks, b-quark containing hadrons, and CP violation

- Cylindrical geometry
- 6580 CsI:Tl crystals, ≈34 cm long,
- Excellent energy, position resolution to reconstruct π0s.

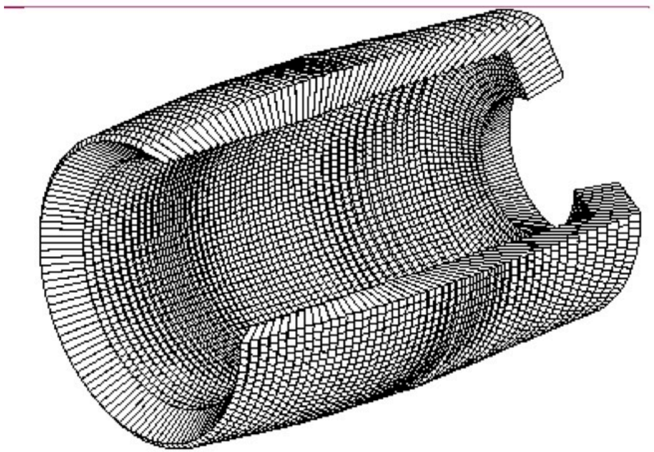

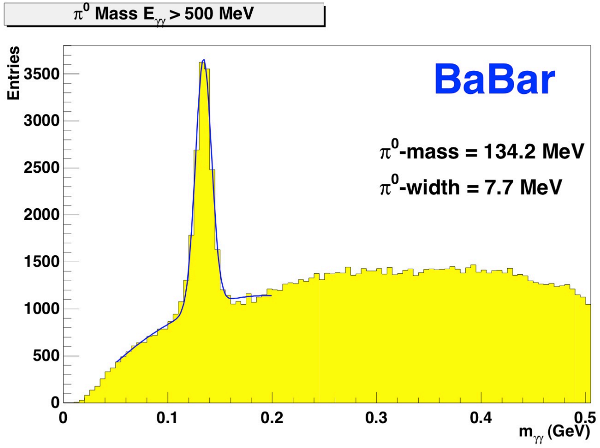

L3 electromagnetic calorimeter

- Cylindrical geometry
- 10752 BGO crystals (7680 in barrel & 2*1536 in endcaps: (2x2)*(3*3)* 24cm
- Excellent energy, position resolution from 100 MeV to 10 GeV

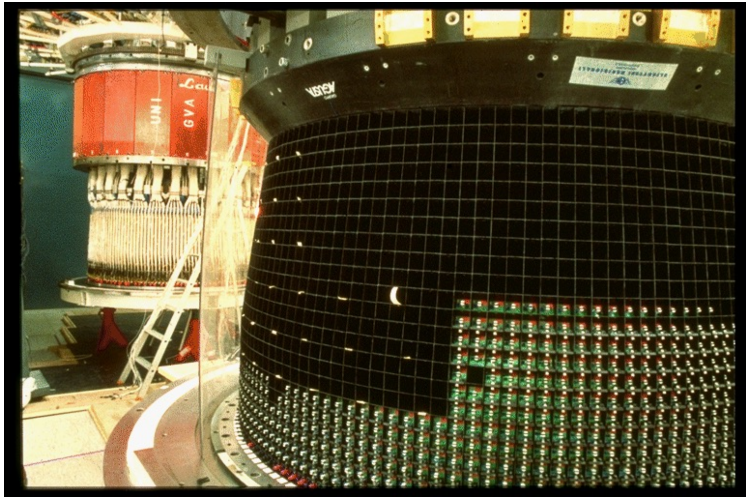

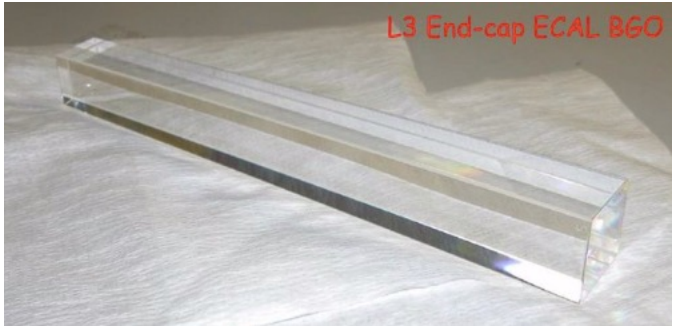

@CERN in LHC

2 experiments use scintillating crystals : Lead tungstate crystals : $PbWO_4$

ALICE :17920 crystals

CMS

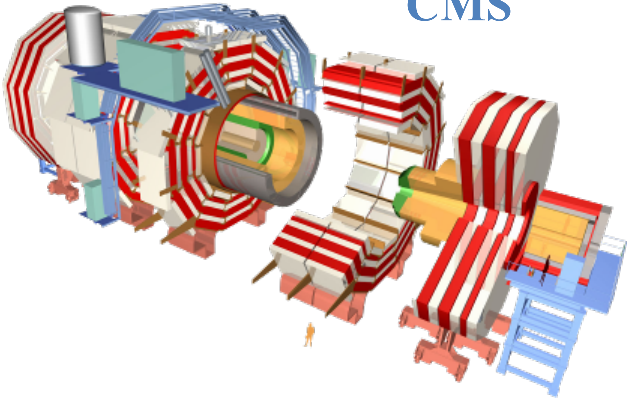

75848 crystals = 100 tons

To build such detector a big challenge 20 years of work

From R&D to Production

Optical properties improvement

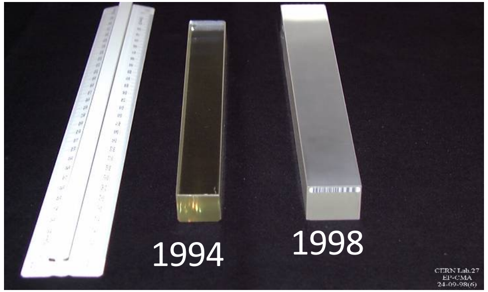

Transmission improvement

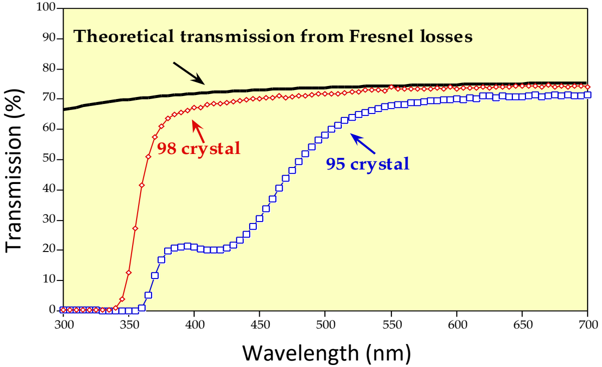

Radiation hardness improvement

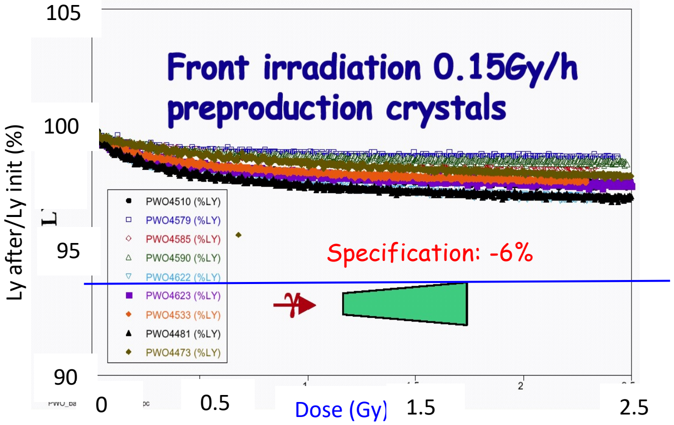

Delivery of the first 100 PWO Crystals Sept 98

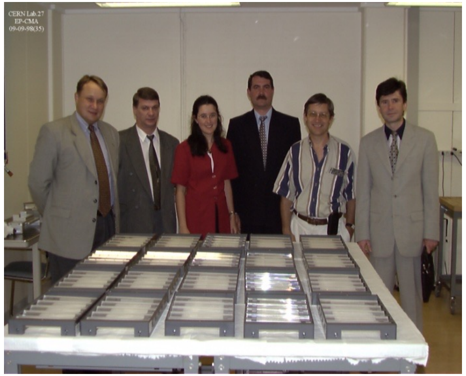

Crystal quality control

Capacity of 60 crystals/day on each machine

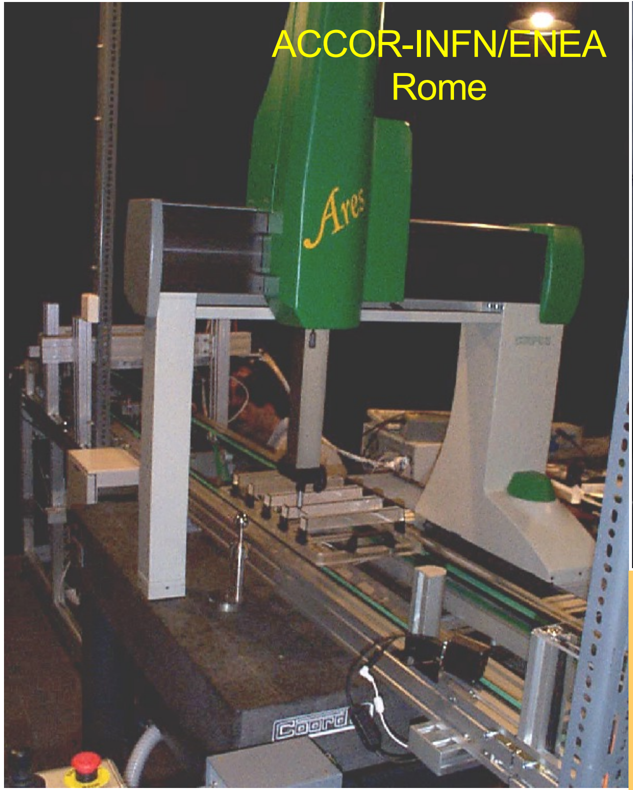

Automatic control of:

- Dimensions
- Transmission
- Light yield and uniformity

has been performed on each crystal installed in ECAL (75848!!)
All data stored in database

E. Auffray et al, NIMA 456 3 (2001) 325, E. Auffray et al, NIMA 523 3 (2004) 355
S. Baccaro et al., NIMAA459 (2001) 278

CMS ECAL assembly: 1998-2007

61200 crystals

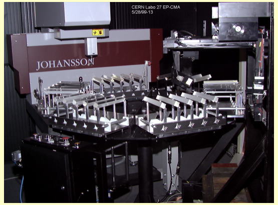

Crystal Characterisation

61200 sub-units

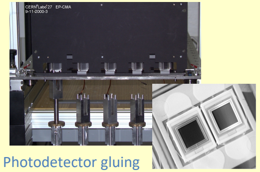

Photodetector gluing

6120 sub-modules

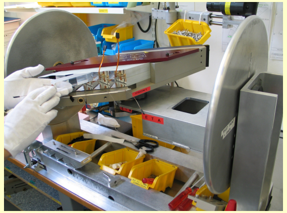

Submodule assembly

144 modules

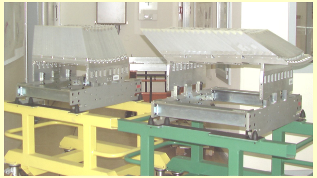

Module assembly

36 Super- modules

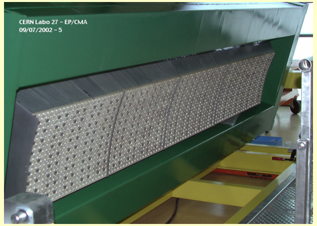

Supermodule asembly

36 Super- modules

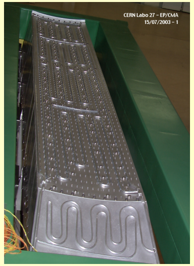

Thermal screen installation

36 Super- modules

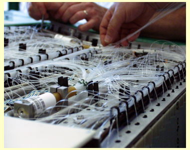

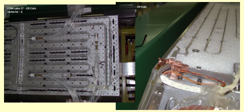

Monitoring system installation

36 Super- modules

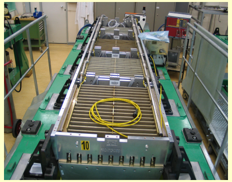

Cooling system Installation

36 Super- modules

Supermodule transport

ECAL in CMS at P5 Cessy, France

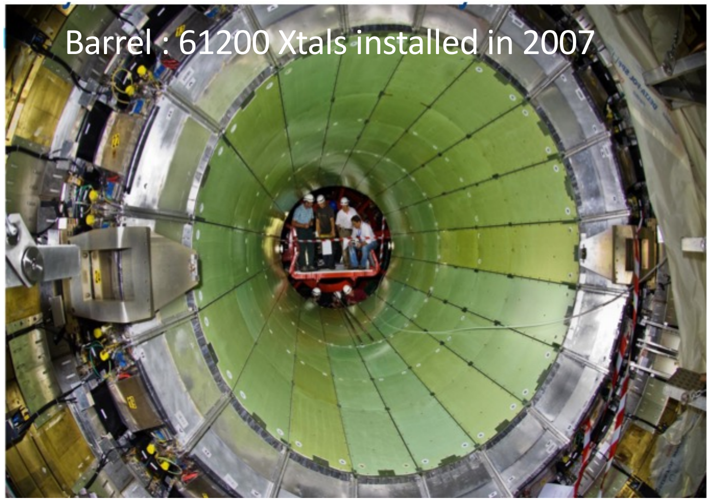

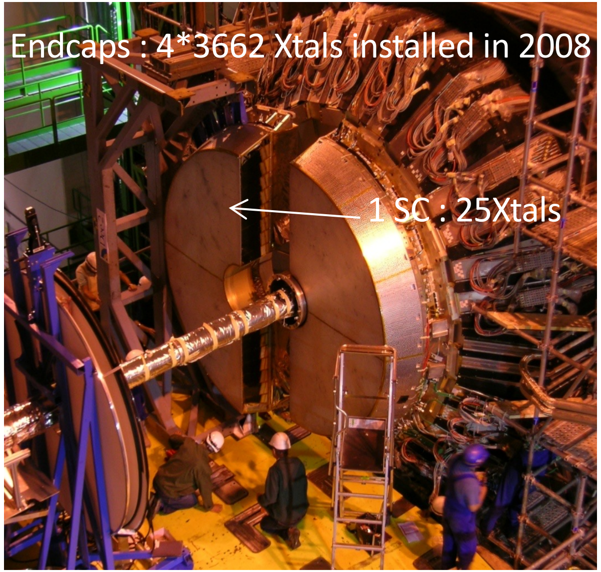

CMS ECAL: Higgs boson discovery

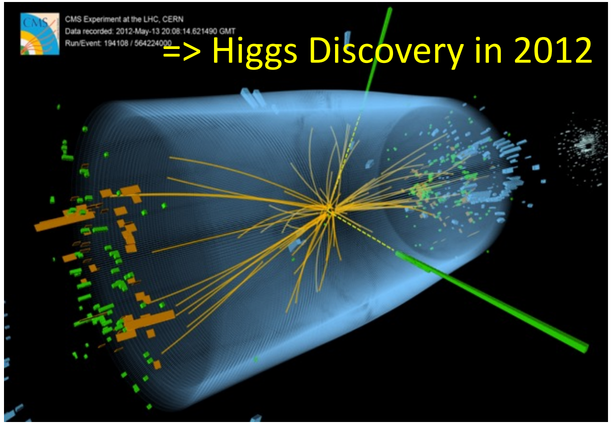

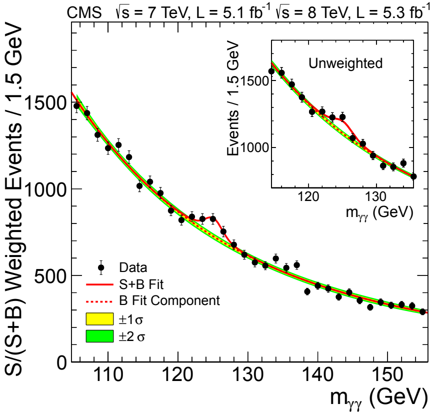

François Englert et Peter Higgs, Physic Nobel Price in 2013

Positron emission tomograph (PET) Principle

A positron emitting radiopharmaceutical is injected into the patient:

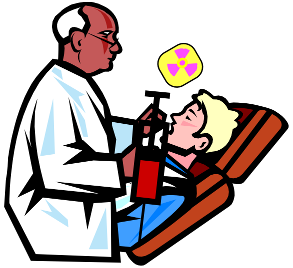

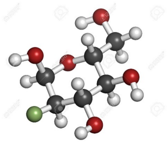

Fluorodeoxyglucose (18F-FDG)

The patient is placed in the imaging scanner

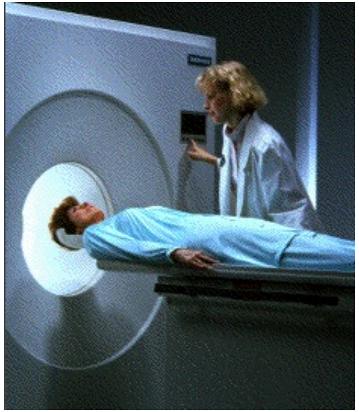

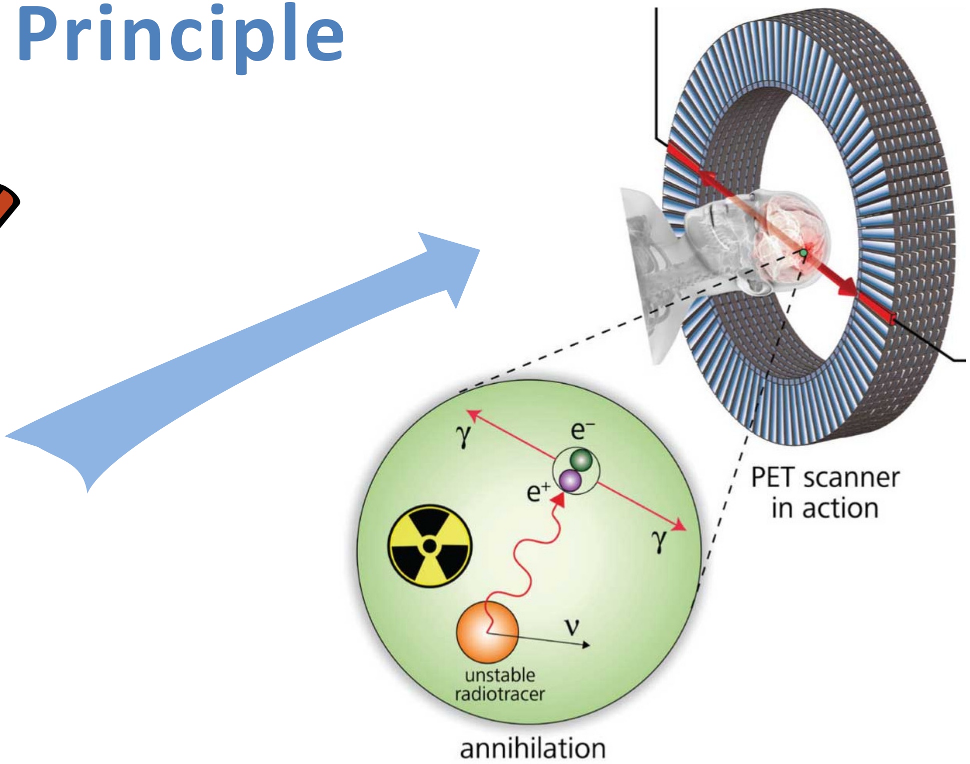

Annihilation of the emitted positrons with electrons in the tissue producing back-to- back photons detected by scintillating crystals

Advantage of PET?

Table I. – *A list of the most common Imaging techniques with their main performance related to molecular imaging.*

Imaging technique	Source of signal	Spatial resolution	Sensitivity (mol/l)	Quantitative/Morphological information
PET	γ-rays (511 keV)	1–4 mm	10^{-11}–10^{-12}	+++/+
SPECT	γ-rays (< 300 keV)	0.3–10 mm	10^{-10}–10^{-11}	++/+
Optical bioluminescence	Visible light	3–5 mm	10^{-15}–10^{-17} (theoretical)	+(++)/n.a.
Optical fluorescence	Visible light and NIR	2–3 mm	10^{-9}–10^{-12} (probable)	+(++)/n.a.
MRI	Radio waves	25–100 μm	10^{-3}–10^{-5}	++/+++
CT	X-rays (40–120 keV)	10–200 μm	n.a	n.a./+++

from *A. Del Guerra et al., 2016 Positron Emission Tomography: Its 65 years Riv. Nuovo Cimento 39 155*

PET medical fields

- Oncology
- Neurology
- Cardiology
- Drug development
- More…

Oncology

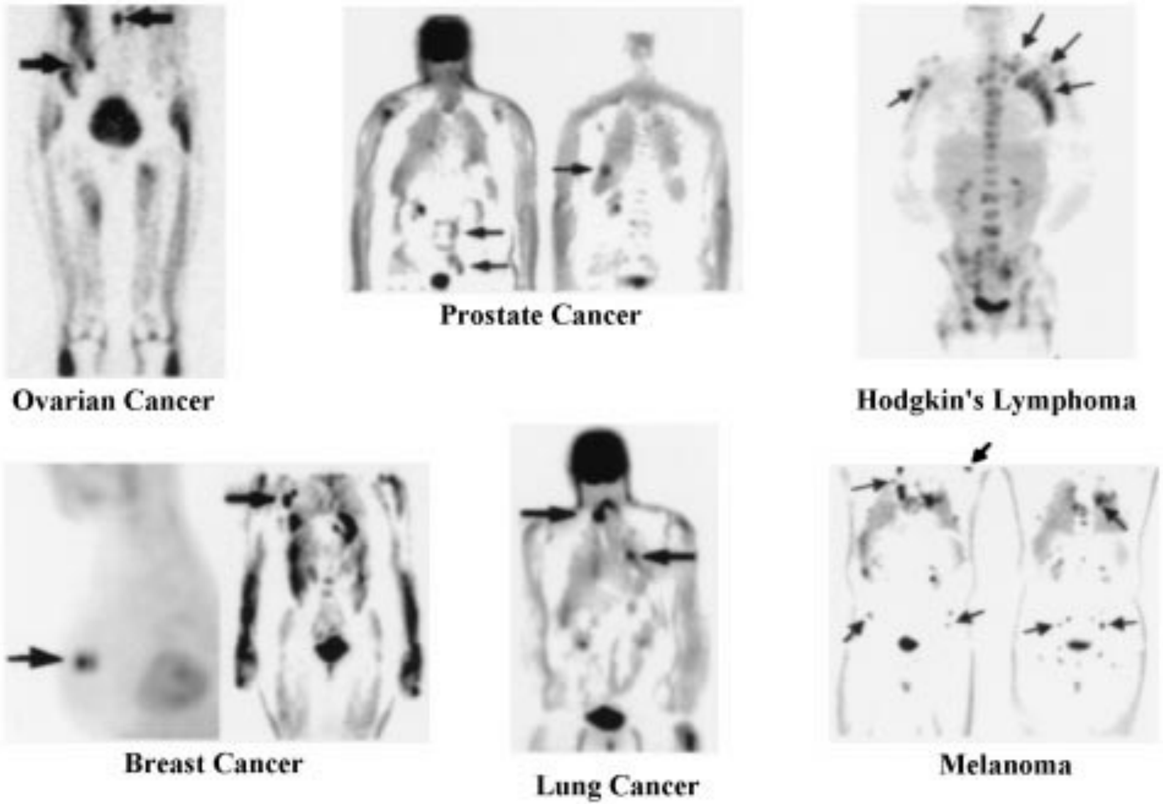

Fig5 from M. E. Phelps, PNAS, 97 (6) 2000, 9226-9233

Similar technics in calorimeter detectors for HEP and PET devices

Electromagnetic Calorimeter of CMS experiment

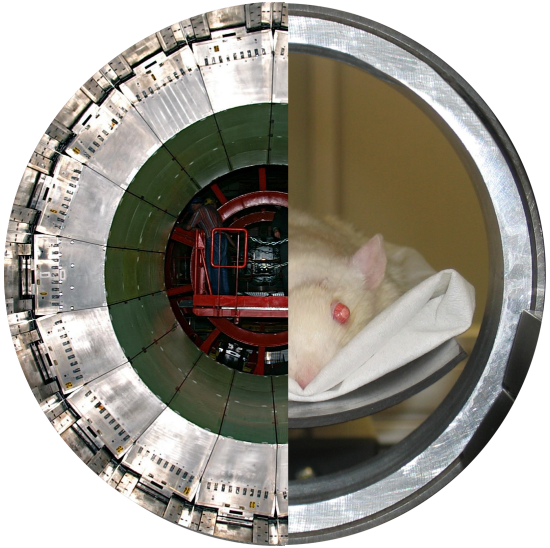

PET scanner

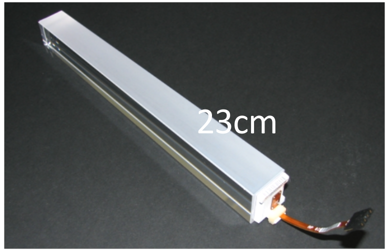

Crystals + photodetectors + electronic

At LHC
Energy of particles < TeV
For PET
0.000000511 TeV* (511keV)Photons

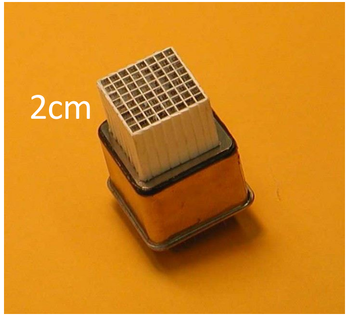

RECENT DEVELOPMENT IN SCINTILLATOR FIELD

New production methods

Czochralski method
Fibres cut from large ingot

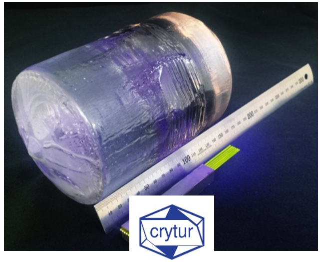

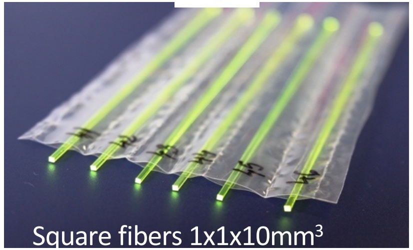
Square fibers 1x1x10mm^3

Micropulling down technique

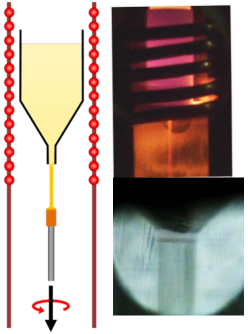

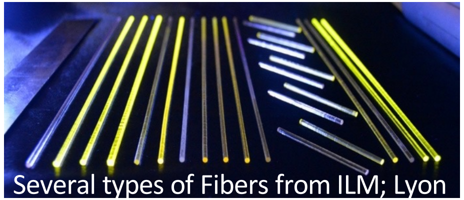
Several types of Fibers from ILM; Lyon

Intelum

3D printing

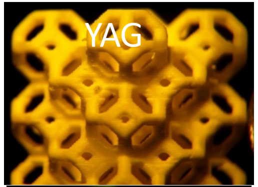

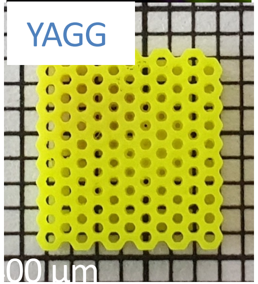

⇒ Feasibility study of crystal fibres production: in the ANR project INFHINI and Intelum project (European Rise grant 644260) with 16 Partners (many from CCC) from 12 different countries: 11 academia and 5 companies

Courtesy of G. Dossovitky, Kurchatov Institute

Development of crystal fibres allows for flexibility in the calorimeter design

From bulk crystal

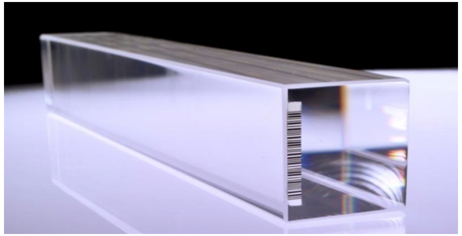

To bloc of fibres

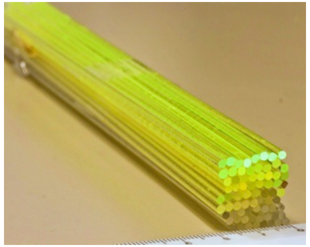

To SPACAL

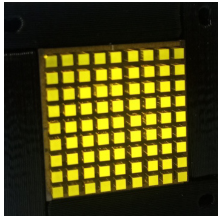

Homogeneous calorimeter

=> Requires large volume of fibres with high density

Sampling calorimeter

⇒ requires less fibres, possibility to use materials with lower density

Could be multifunctional: mixed type of fibres
Cerenkov + scintillation +neutrons sensitive
Could play on sampling fraction

Flexibility of SPACAL geometry

Can select the sampling fraction

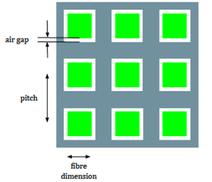

GAGG fibers/W absorber

Studied for a pitch fixed at 1.67 mm with variable fibre sizes

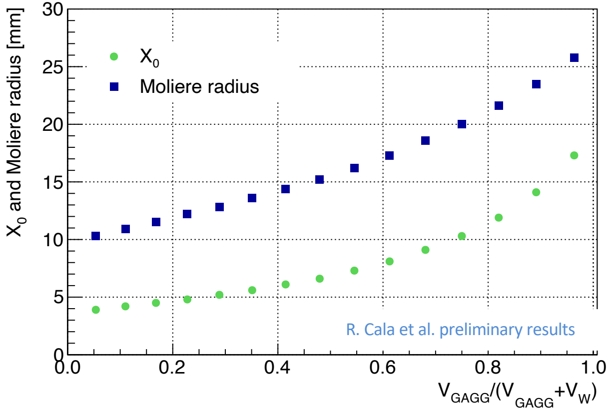

Modification of Moliere radius and X_0
=> optimisation of granularity

R. Cala et al. preliminary results

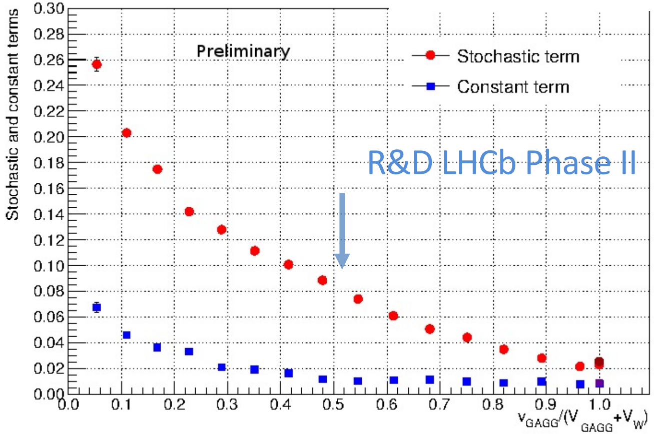

Optimisation of sampling fraction
⇒ optimisation of energy resolution

⇒ R&D on SPACAL with garnet and tungsten in framework of EP&RD and LHCb upgrade II

Motivation for the Upgrade II of the LHCb ECAL

Current LHCb ECAL:

- Optimised for π^0 and γ reconstruction in the few GeV to 100 GeV region at 2 x 10^{32} $cm^{-2}s^{-1}$
- Radiation hard up to 40 kGy
- Shashlik technology: 4x4 / 6x6 / 12x12 cm^2 cell size
- Energy resolution: $\sigma(E) / E \approx 10\% / \sqrt{E} \oplus 1\%$
- Large array (8 x 7 m^2) with 3312 modules and 6016 channels

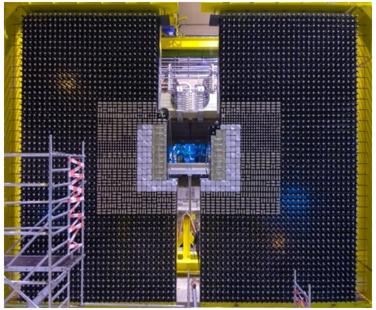

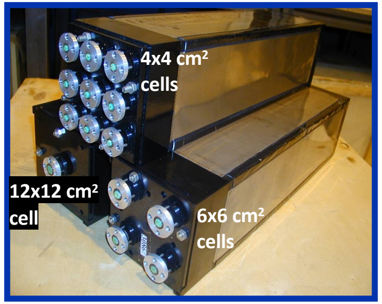

<u>Requirements for the Upgrade II:</u> operation at L = 1-2 x 10^{34} $cm^{-2}s^{-1}$

- Sustain radiation doses up to 1 MGy and $\leq 6 \cdot 10^{15} cm^{-2}$ for 1MeV neq/cm^2 at 300 fb^{-1}
- Keep at least current energy resolution
- Pile-up mitigation crucial
  - ✓ Timing capabilities with O(10) ps precision, preferably directly in the calorimeter modules
  - ✓ Increased granularity in the central region with denser absorber
- Respect outer dimensions of the current modules: 12x12 cm^2

SPACAL W/GAGG prototype test at DESY2020/2021

9-cells of 1.5x1.5cm^2 GAGG & YAG fibres in W-absorber

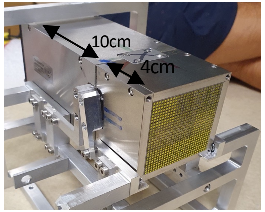

$\Rightarrow$ **Possible solution SPACAL for central part : W/Garnet (GAGG) or W/plastic fibres**

SPACAL-W/GAGG: energy resolution

Energy resolution measured at DESY in 2020 for electrons up to 5.8 GeV

SPACAL W/GAGG prototype test at DESY2020/2021
9-cells of 1.5x1.5cm^2 GAGG & YAG fibres

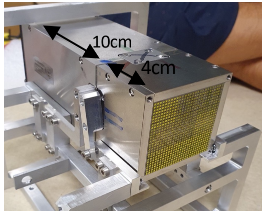

2 sections with double side readout (7+18 Xo)
Hamamatsu R12421 and PMMA light guides readout

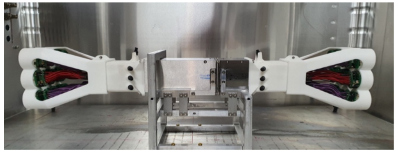

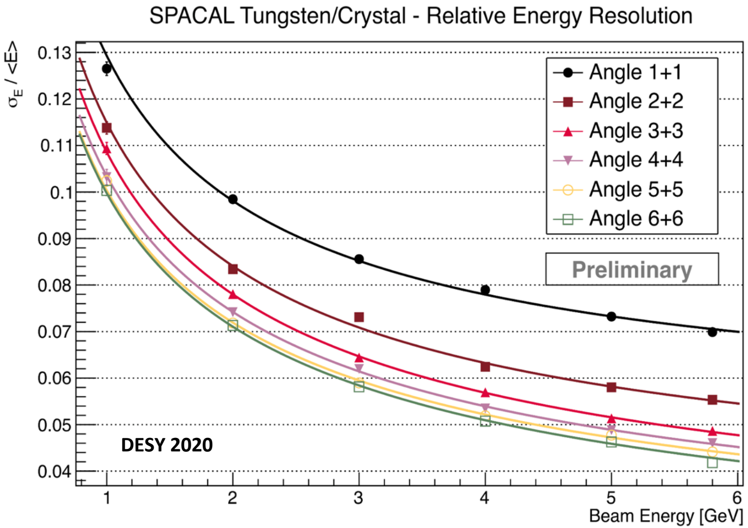

Measurements performed at several vertical and horizontal incidence angles
Energy resolution improving for increasing angles
Preliminary fit results to low energy data at 3°+3° give
sampling term of 10.6% and
constant term of 1.9% ± 0.5%

EP R&D

SPACAL-W: time resolution

with electrons up to 5GeV at an incidence angle of 3° vertically and 3° horizontally

W/GAGG

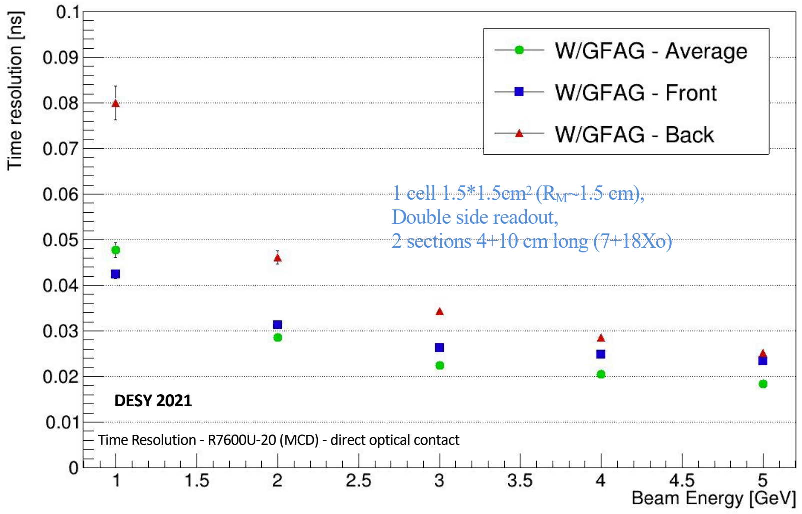

W/polystyrene

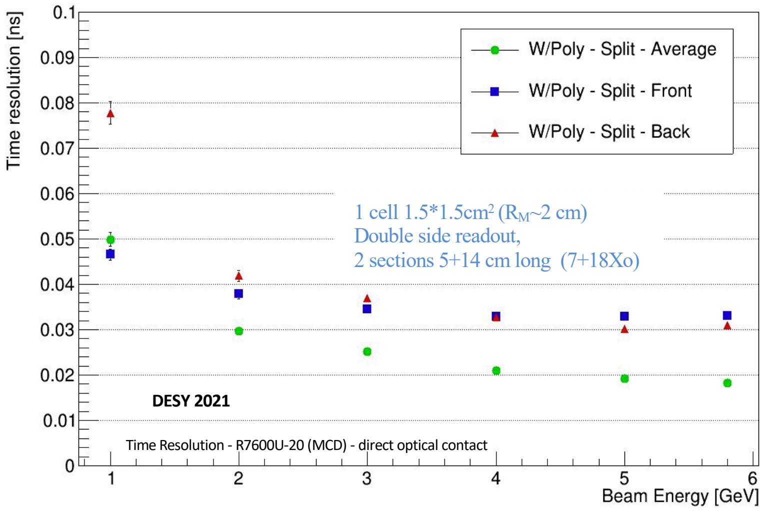

Time resolution <20ps @ 5 GeV for R7600U-20 and direct coupling

Why FAST timing is important in HEP?

Search for rare events implies high luminosity accelerators

→ Rate problems;

→ Pileup of >140 collision events per bunch crossing at *High Luminosity-LHC;*

→ Pileup mitigation via TOF requires TOF resolution < 50ps.

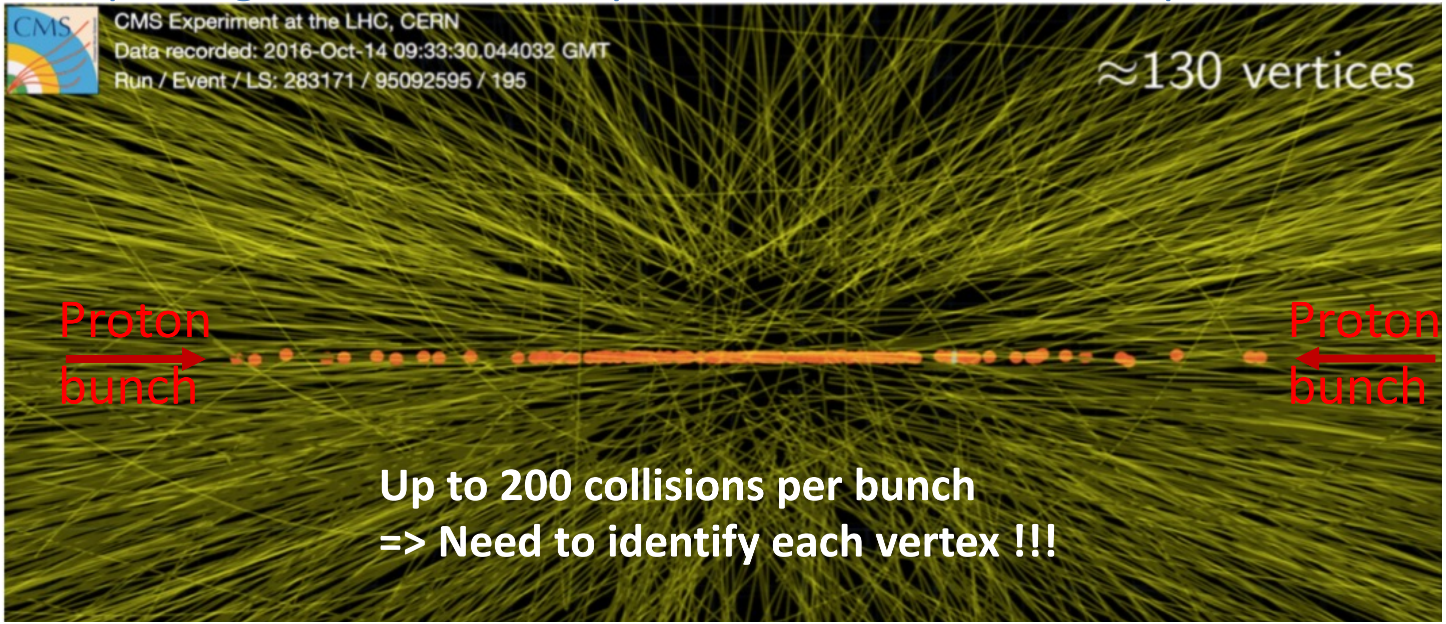

The advantage of timing information

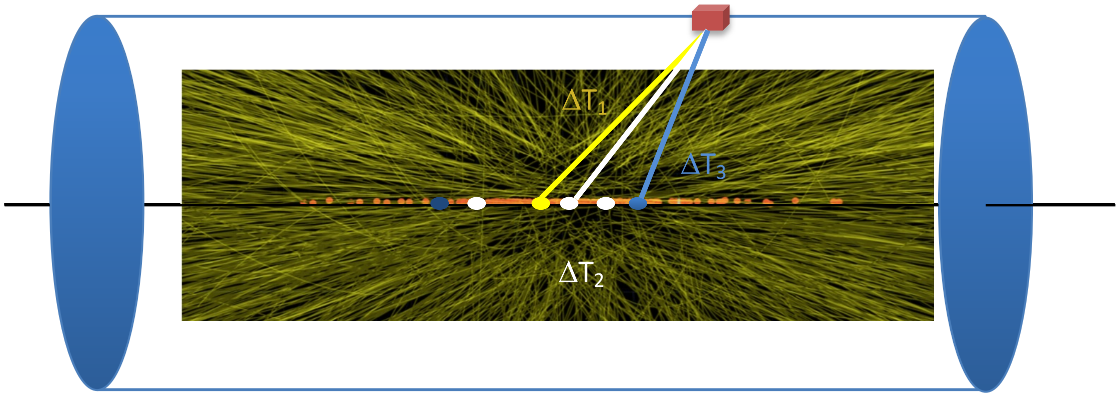

The information of timing will allow to identify the vertex

Exemple of CMS experiment at HL-LHC

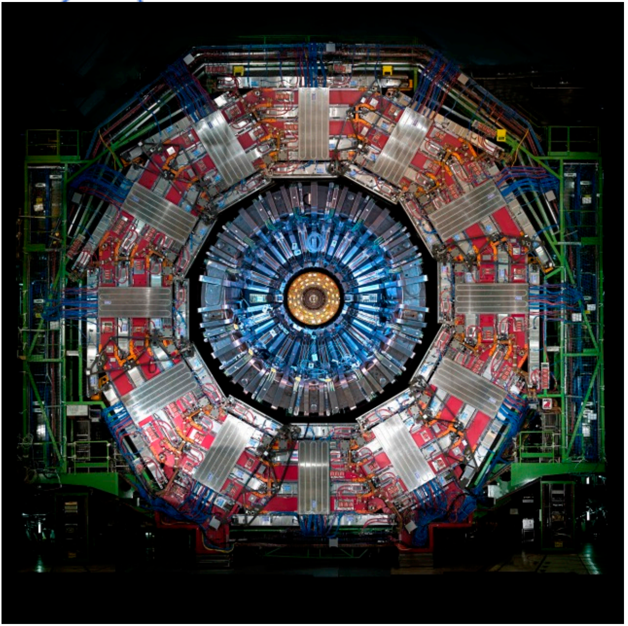

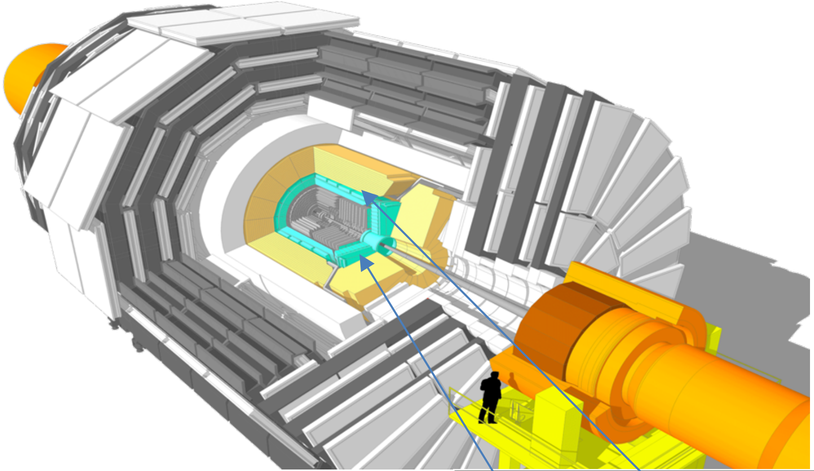

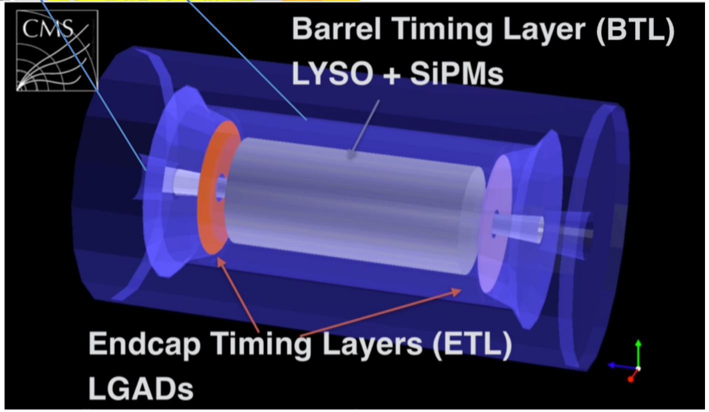

Between tracker and ECAL
Introduction of timing layer
With mip sensitivity with time resolution of 30-50ps

CMS Barel timing layer (BTL)

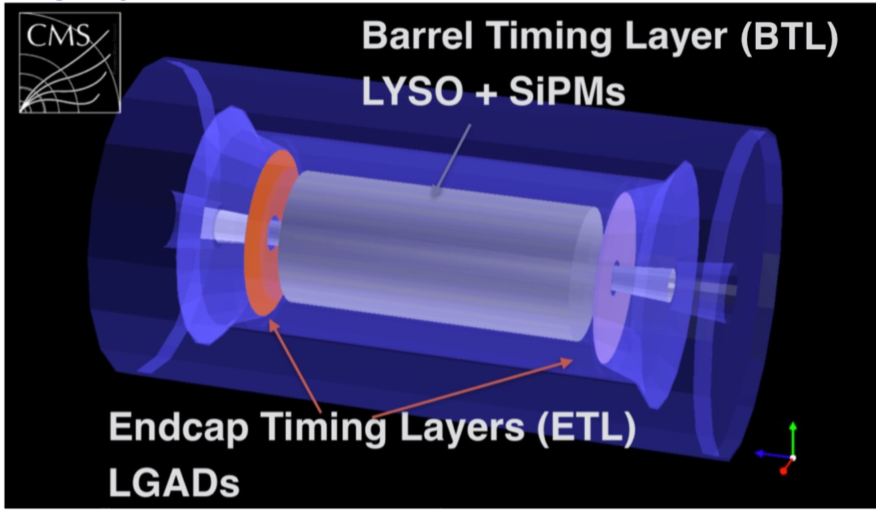

short fibres (3*3*57mmm³)

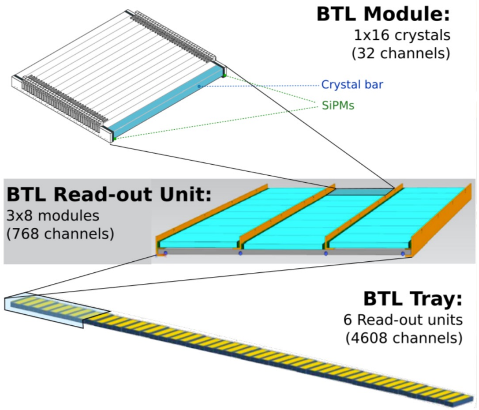

LYSO crystals with dual-end SiPM readout

Basic unit: 16x1 array of crystals (~ 3 x 3 x 57 mm^3)

Coverage: Iηl<1.45, surface ~38 m2; 332k channels

Nominal fluence: **1.9x10^{14} neq/cm^2** (3000 fb-1)

Target 30ps time resolution in barrel

State of the art time resolution with mips

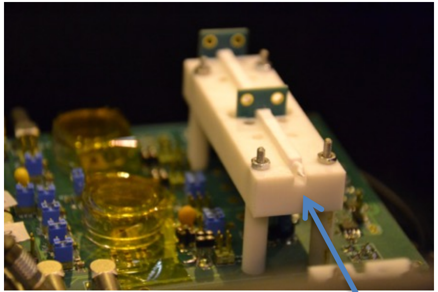

pions beam

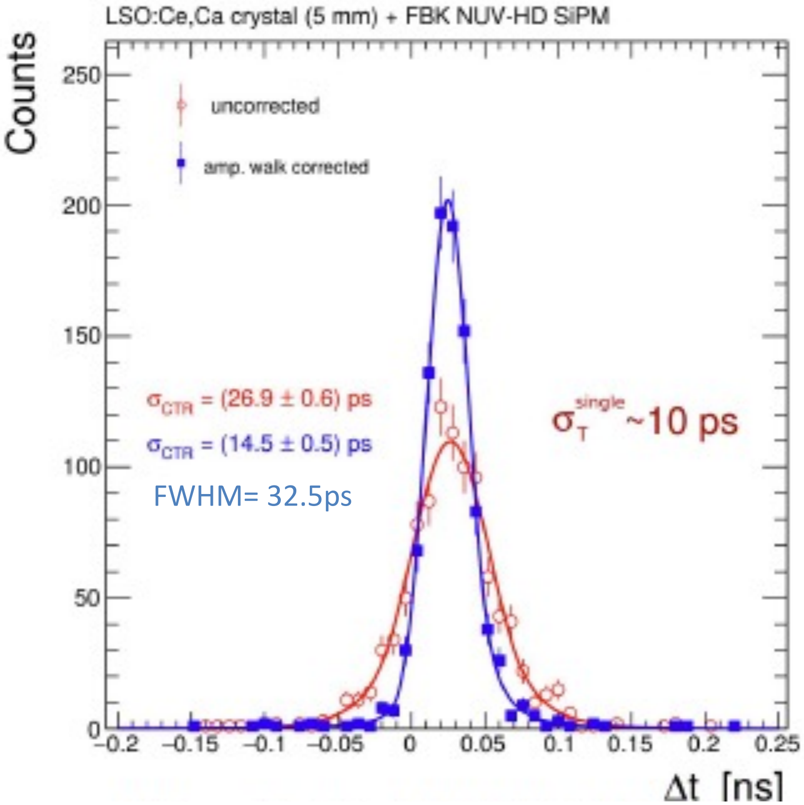

A. Benaglia, et al., NIM A (2016), 830, 30-35

CMS Barel timing layer (BTL)

BTL sensor performance in test beam

- Timestamp of a MIP traversing BTL: $t_{Ave} = (t_{left} + t_{right})/2$
- Achieved 30 ps time resolution per BTL sensor before irradiation
- Uniform time response and resolution across sensor area

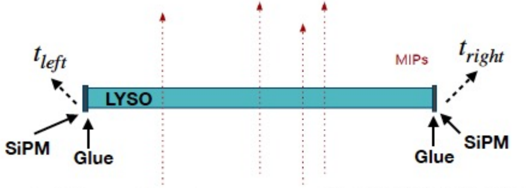

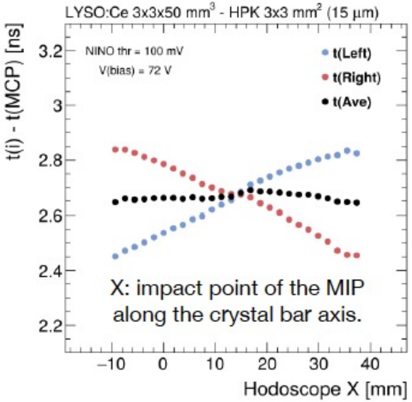

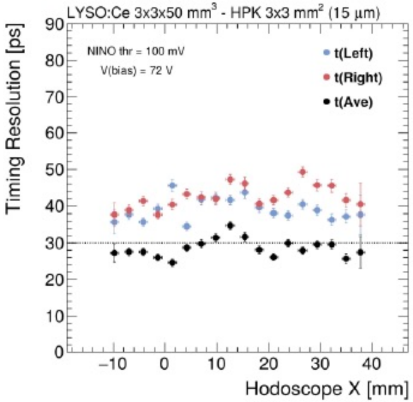

Nan Lu, ICHEP 2020 7 Precision Timing with CMS MTD Barrel Timing Layer

Merits of Time of Flight PET (TOF-PET)

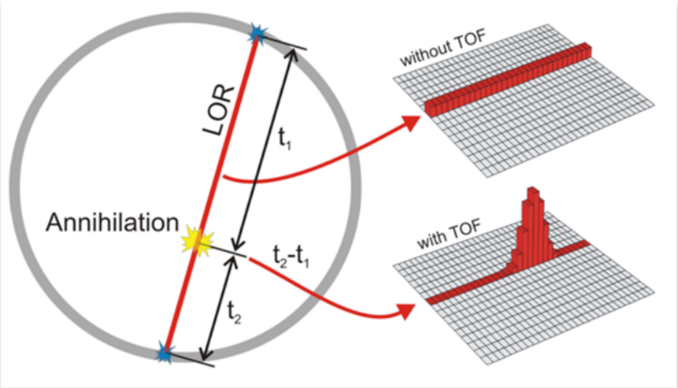

https://the10ps-challenge.org

➔Improve event localization along the line of response (LOR)

$$\Delta x = c\frac{\Delta t}{2}$$

➔Improve signal to noise ratio (SNR)

$$SNR_{TOF} \sim \sqrt{\frac{D}{\Delta x}} \cdot SNR_{CONV}$$

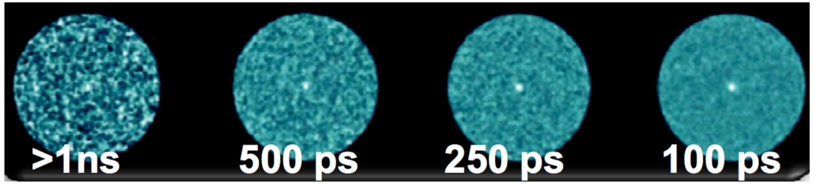

Current status commercial TOF-PET

TOF PET SIEMENS: BIOGRAPH VISION

3.2mm section crystals

CTR 215ps

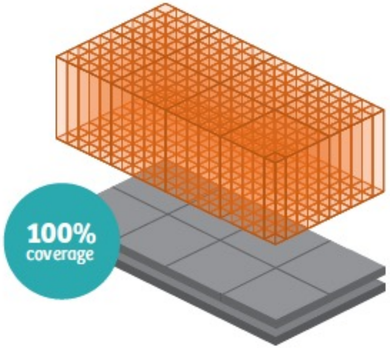

Webpage SIEMENS:
https://static.healthcare.siemens.com/siemens_hwem-hwem_ssxa_websites-context-root/wcm/idc/groups/public/@global/@imaging/@molecular/documents/download/mda4/mzmy/~edisp/biograph_vision_technical_flyer-05440720.pdf

State of the art time resolution with with PET size crystal at 511keV

FBK NUV-HD 4x4mm^2, **40x40µm^2 SPAD** + LSO:Ce:Ca

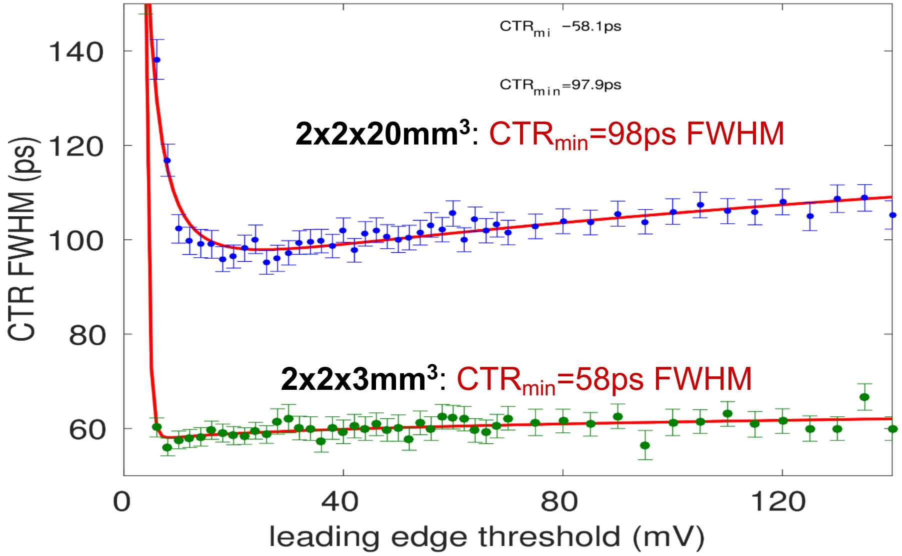

=> Limit of "standard" crystals around 100ps

S. Gundacker et al., Phys. Med. Biol. (2019) 64 055012

New TOF-PET frontier :10ps

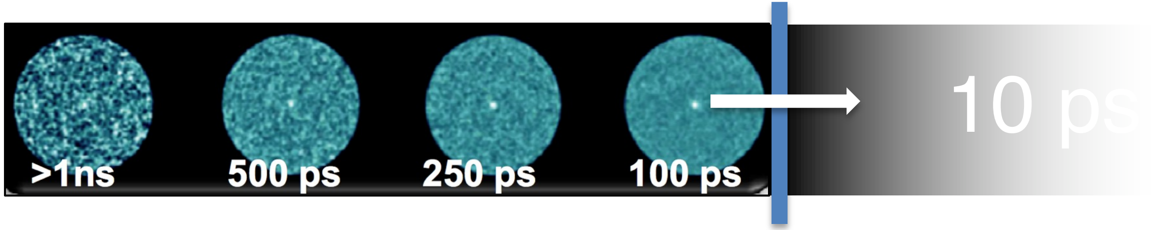

10ps: Spatial localization directly from TOF (1.5 mm)

Sharp improvement in SNR

Less dose to the patient

More accurate dynamic studies

No need for full angular coverage

Need to understand the full photodetection Chain

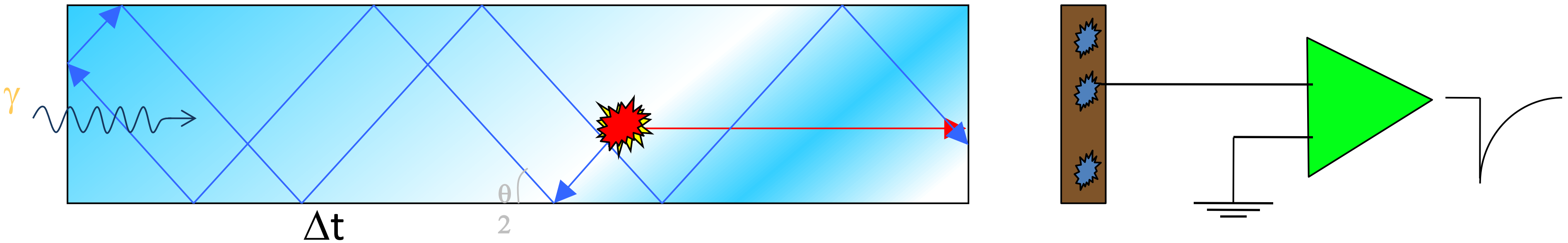

$t_{kth\ pe} = \Delta t + t_{k'\ ph} + t_{transit} + t_{SPTR} + t_{TDC}$

Conversion depth | Scintillation process | Transit time jitter | Single photon time spread | TDC conversion time

Scintillator
- Particule Interaction
- Light generation
- Light transport
- Light transfer
- Light collection

Photodetector
- Reduce SPTR and DCR
- Increase fill factor (PDE)
- Digital SiPM
- MCP for PET & HEP

Electronics
- TDC < 10ps bins
- Monolithic architecture
- High bandwidth
- Low noise
- Massive parallel data
- High number of channels

crystal length influence on time resolution

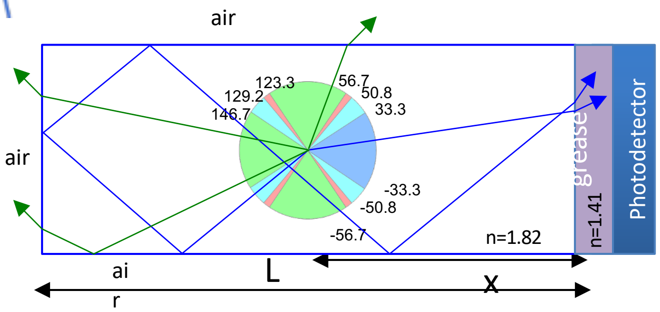

$$-50.8° \le \theta \le 50.8° \; : \; t_{prop} = \frac{n}{c} L_p = \frac{n}{c} * \frac{x}{\cos(\theta)}$$

$$129.2° \le \theta \le 146.7° \; or \; -129.2° \le \theta \le -146.7° \; :$$

$$t_{prop} = \frac{n}{c} L_p = \frac{n}{c} * \frac{(2L - x)}{\cos(\theta)}$$

50.8° critical angle for crystal (LSO) -grease interface

Propagation time @ different emission angles for emission position averaged over crystal length

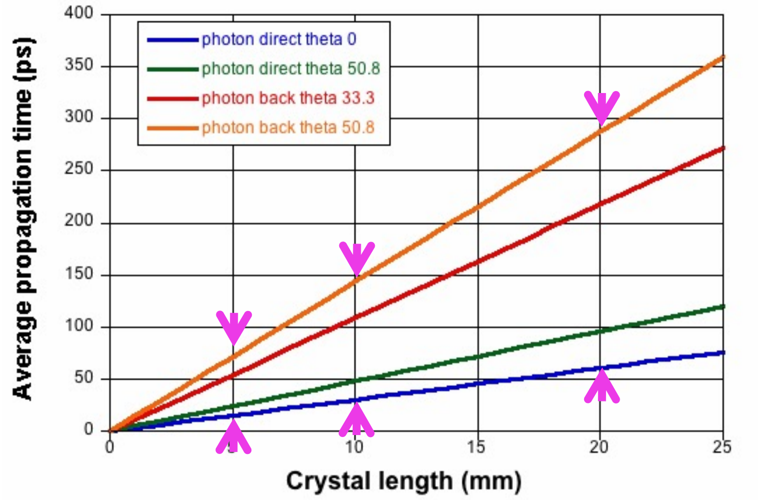

- Impact of light propagation on the coincidence time resolution increases with length;
- Maximum contribution averaged over length
  - For L= 5mm : Δt=56.8ps
  - For L=10mm : Δt=113.6ps
  - For L=20mm : Δt=227.2ps

E. Auffray, TNS Vol. 60, no. 5, 2013, 3161-3171

Crystal length influence on time resolution

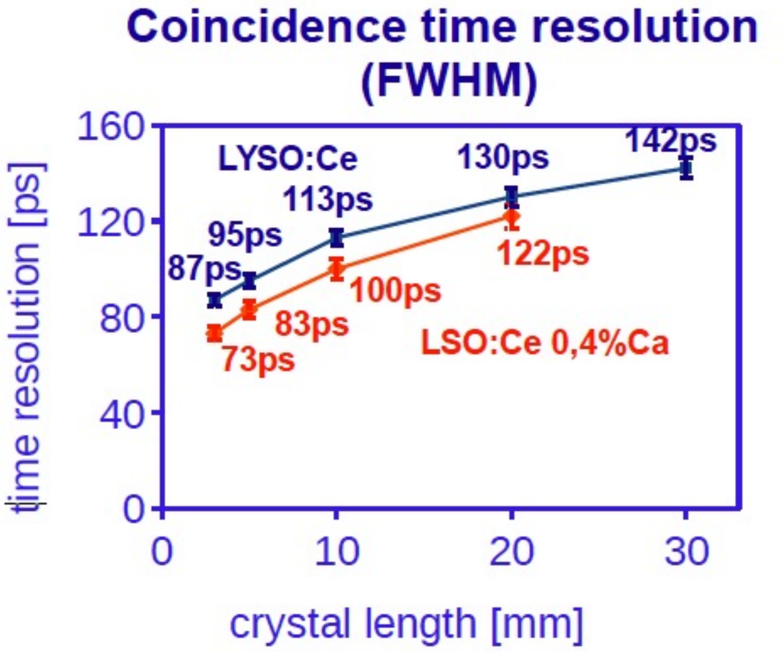

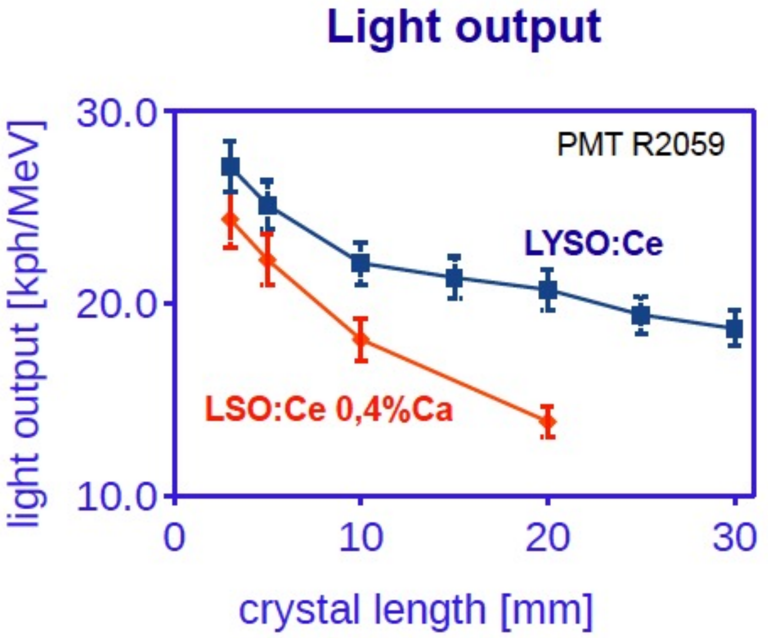

Measured with NUV-HD (25µm SPAD size, 4x4mm^2 device size, 2x2mm^2 crystal cross section T=15°C

S. Gundacker et al. JINST 2016 JINST 11 P08008

Influence of depth of interaction (DOI)

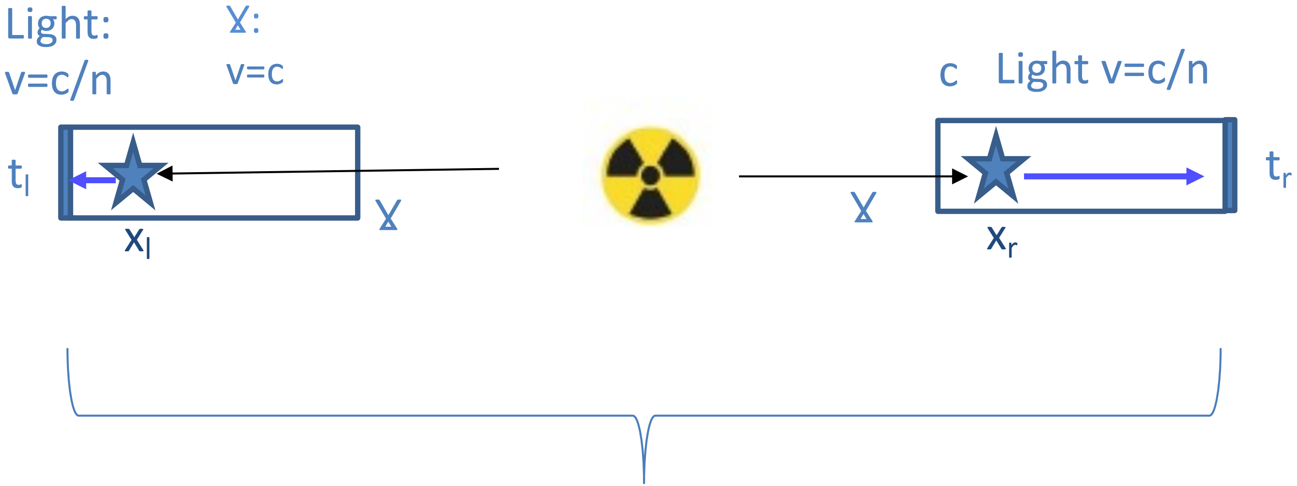

$$t_l - t_r = (x_l - x_r)((1-n)/c)$$

⇒ Unknown DOI introduced degradation of the CTR

⇒ Knowledge of DOI and correction of DOI improve the CTR

Improvement of light collection

Inorganic scintillating crystals usually have high index of refraction

Coupling medium:
Air, Glue
Photodetector

Crystal

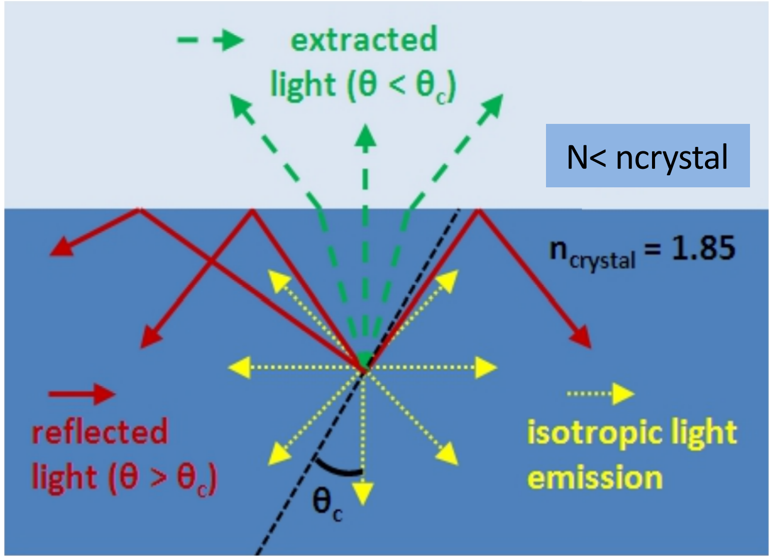

Up to 50% of the light may not exit the crystal

S. Gundacker et al 2016 JINST 11 P08008

Photonic crystals

Structuration of exit surface with nanopaterning

Crystal air

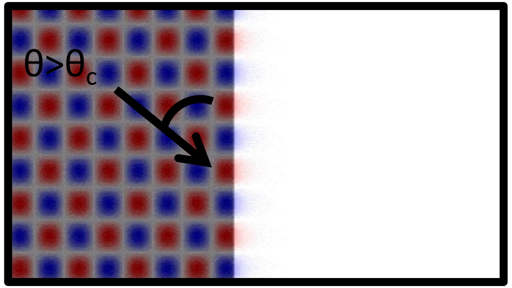

Total Reflection at the interface

Crystal- air interface with PhC grating:

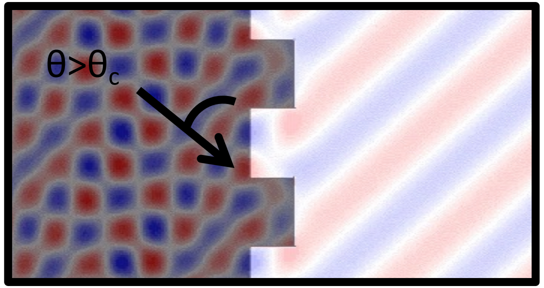

Extracted Mode

$\theta>\theta_c$

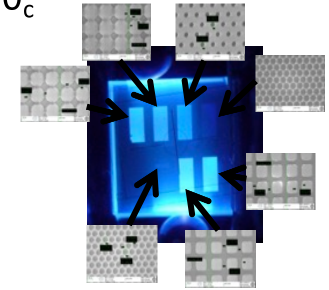

A gain of up to factor 2

A. Knapitsch et al. IEEE TNS, VOL. 63, NO. 2, April 2016
M. Salomini et al., Crystals 8 (2), 78
R. Pots et al, NIM A, 240 (2019) 254-261

Improvement of CTR with photonic crystals

CTR Measured on 1cm³ of LSO without & with paterning

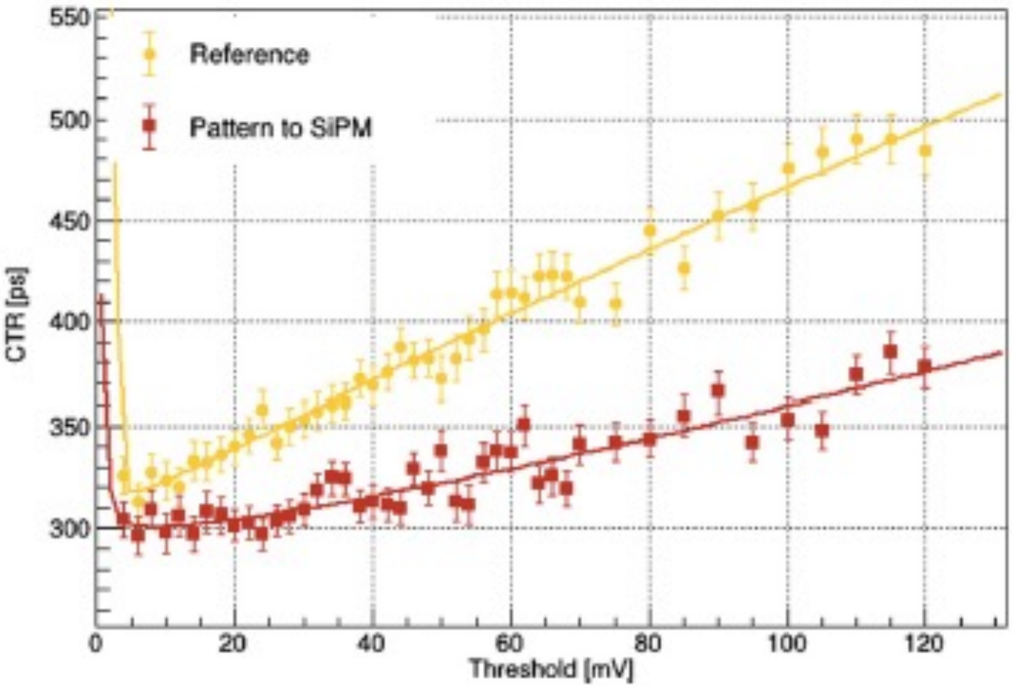

R. Pots et al, NIM A, 240 (2019) 254-261

Improve photodetector parameters

CTR variation with Single photon time resolution (SPTR)

Not only the crystal properties but also the photodetector properties are important:

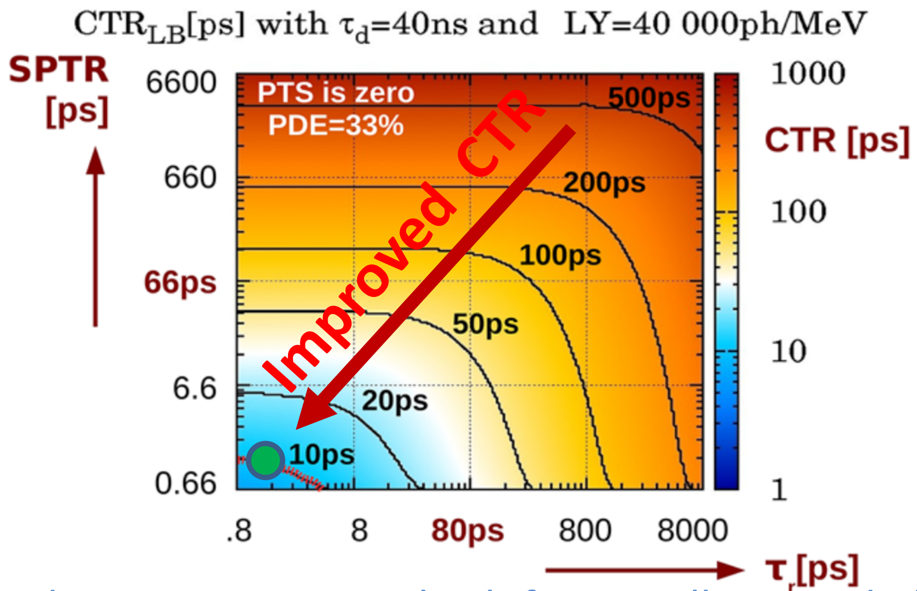

=> Need good timing properties both for scintillator and photodetector

S. Gundacker, PhD thesis

S. Gundacker et al, Phys. Med. Biol. 61 (2016) 2802-2837 & JINST 11P08008

SiPM SPTR investigation

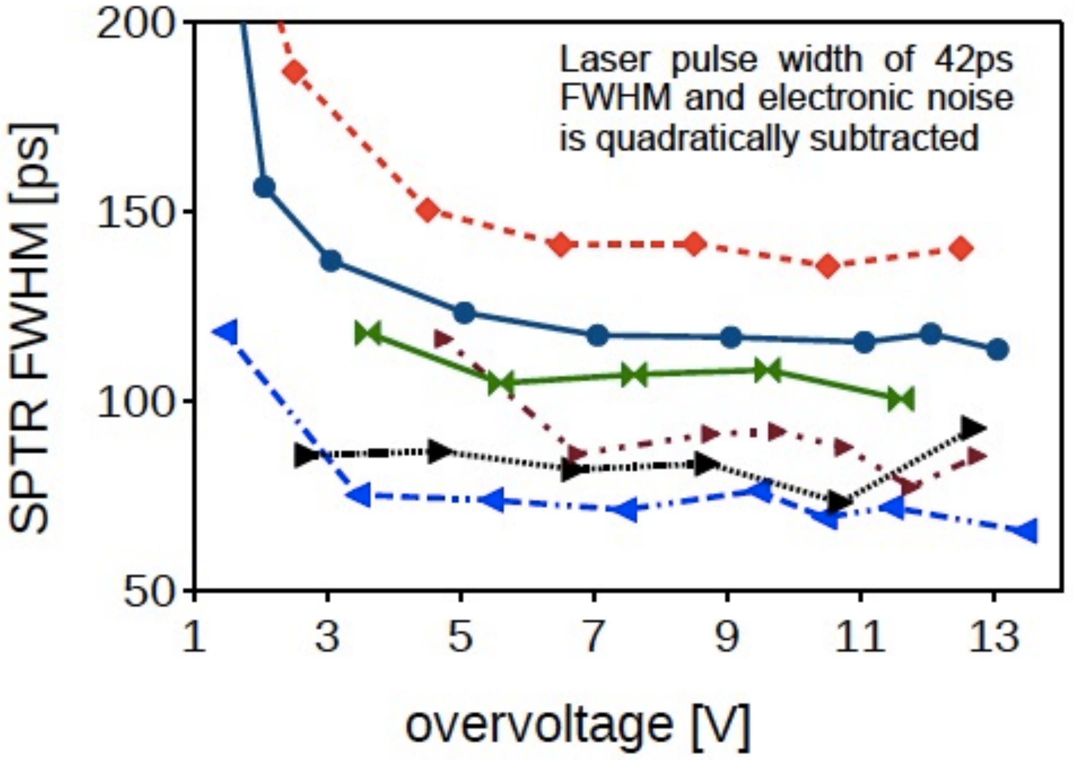

HPK S13360, 3x3mm², 50µm
HPK S14160, 3x3mm², 50µm
SensL FJ, 3x3mm², 35µm
Broadcom, 4x4mm², 30µm
Ketek WBA0, 3x3mm², 50µm
FBK NUV-HD, 4x4mm², 40µm

Large variation among various types of SIPMs

S. Gundacker et al. Phys. Med. Biol. 65 (2020) 025001

Influence of SPTR on CTR

CTR measured with2x2x3mm³ LSO:Ce codoped 0.4%Ca corrected for measured PDE as if 59%

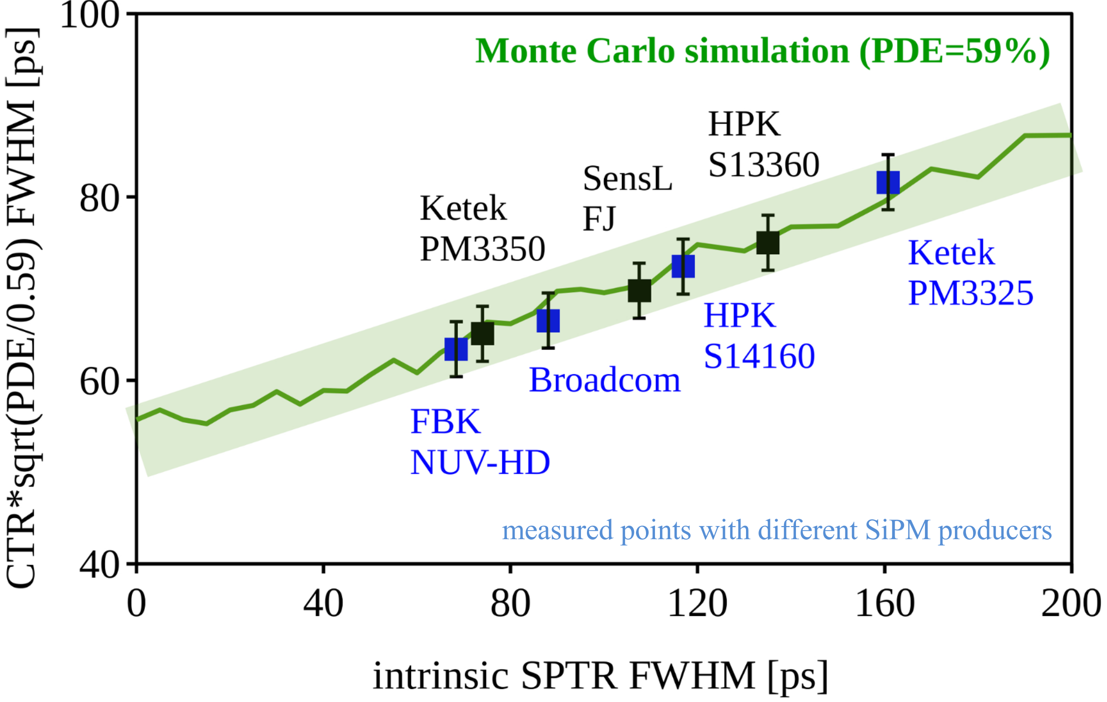

S. Gundacker et al. Phys. Med. Biol. 65 (2020) 025001

Influence of photon detection efficiency (PDE)

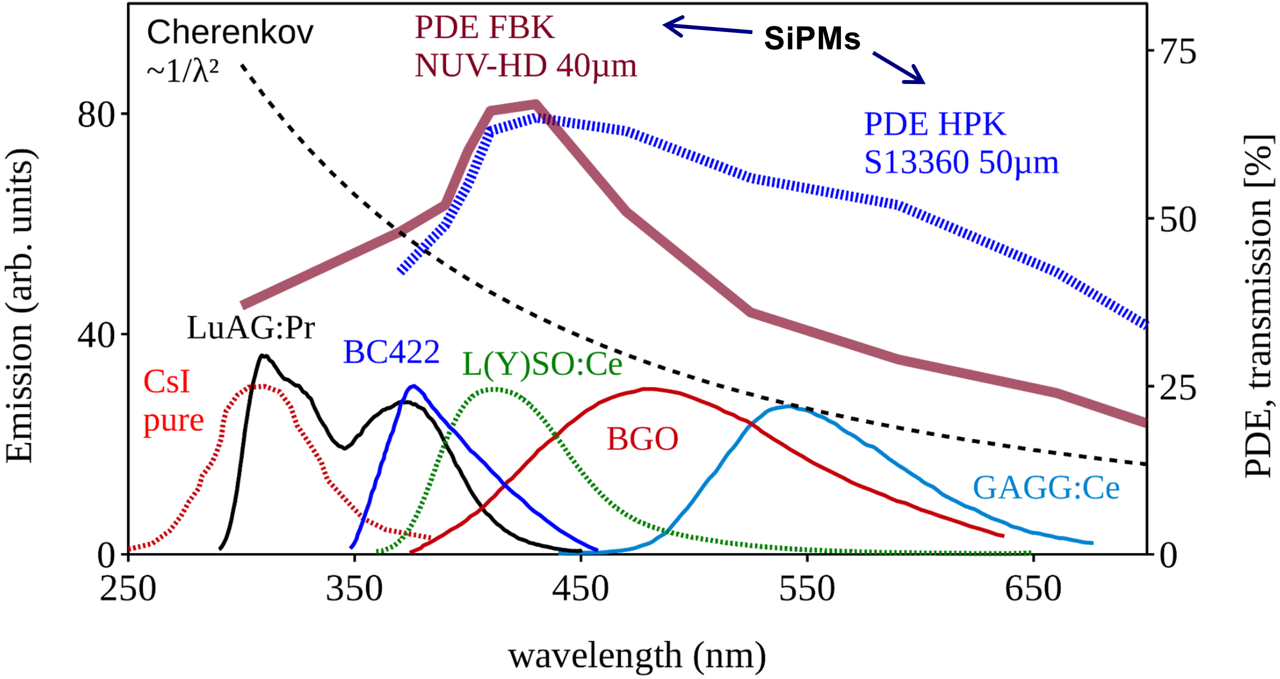

S. Gundacker et al. Phys. Med. Biol. 65 (2020) 025001

How to improve scintillation properties ?

Several emission process

- Excitonic emission (STE, excitations of anion complexes)
- Emission of activators (Ce, Pr, …)
- Crossluminescence
- Hot intraband luminescence (HIL)

Slow

↓

fast

Modification of properties of « standard » scintillator

- **Excitonic emission (STE, excitations of anion complexes)**
- **Emission of activators (Ce, Pr, …)**
- Cherenkov radiation
- Crossluminescence
- Hot intraband luminescence (HIL)
- Quantum confinement driven luminescence

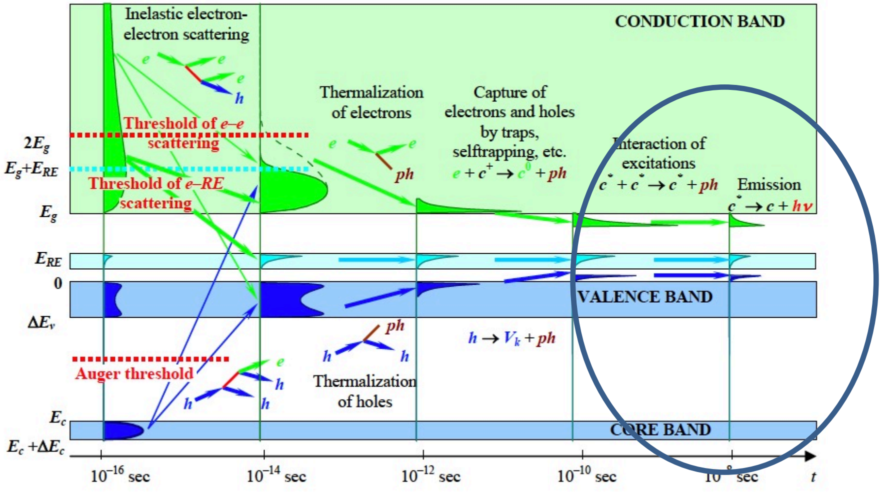

Example in garnet crystals

LuAG:Ce: decay time

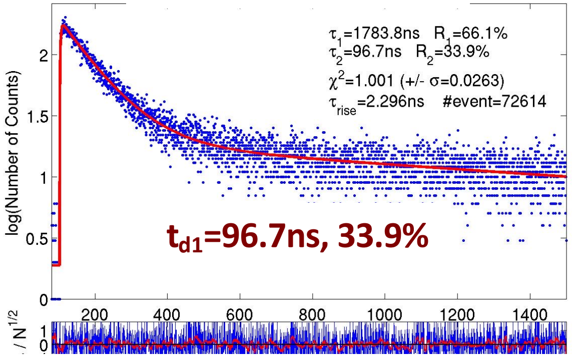

t_{d1}=96.7ns, 33.9%

LuAG:Ce, Mg: decay time

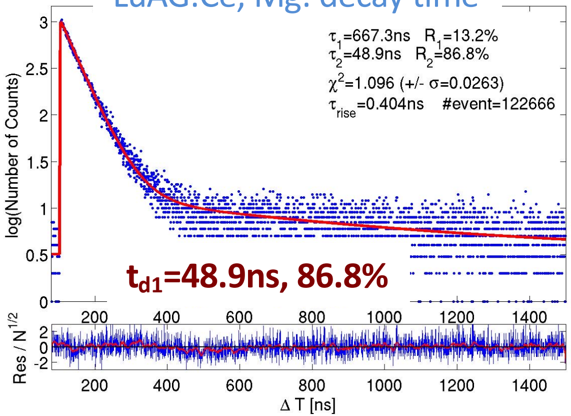

t_{d1}=48.9ns, 86.8%

Time resolution @ 511 KeV versus photon density of various GAGG samples from various producers

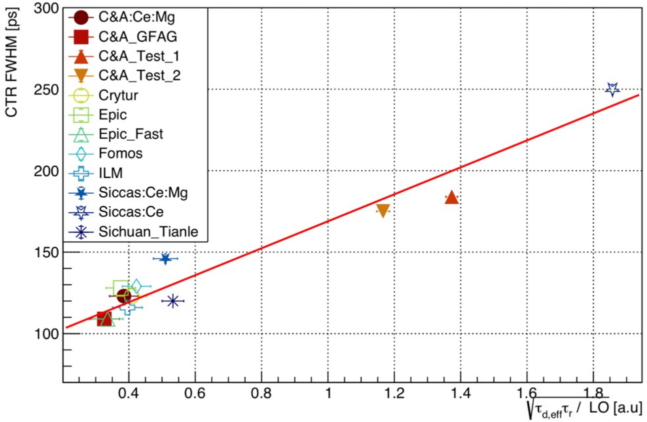

=> Properties can be tuned

S. Gundacker et al., *Phys*. Med. Biol. 61 (2016) 2802–2837
S. Gundacker et al, NIMA A 891 (2018) 42–52

M. Lucchini et al, NIM A Volume 816 (2016), pp 176–183,
L. Martinazzoli et al., NIM A, Volume 1000, (2021), 165231

Hot intra-band luminescence

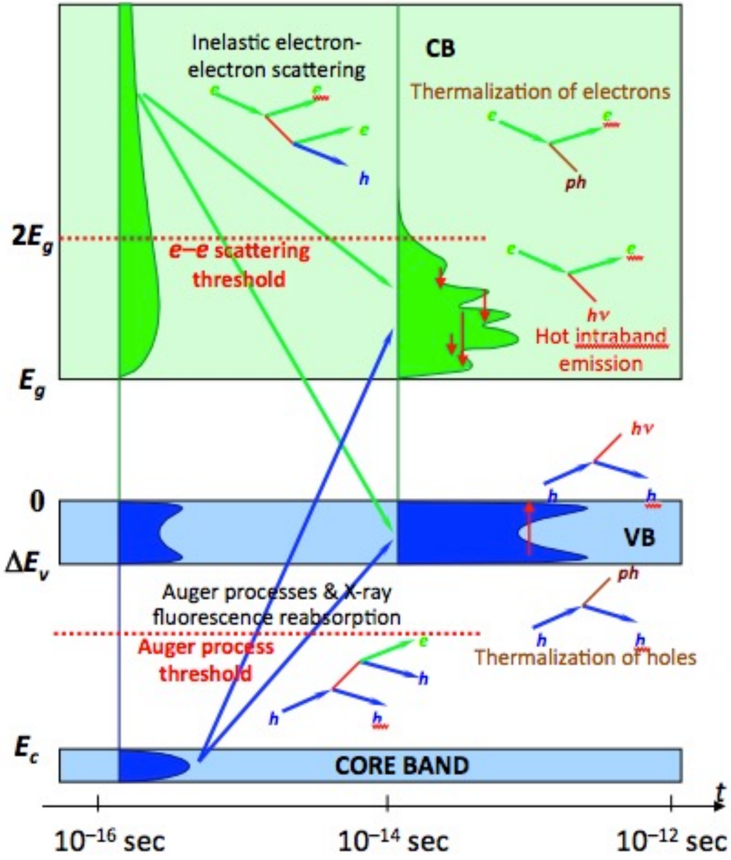

- Ultrafast emission ≤ 10^{-12}s
  - e-IBL: spectrum in visible range
  - H-IBL: NIR spectrum
- Independent of temperature
- Independent of defects
- Absolute Quantum Yield
  - $W_{h\nu}/W_{phonon} = 10^{-8}/(10^{-11}\text{-}10^{-12})$
  - ≈ 10^{-3} to 10^{-4} ph/eh pair

P. Lecoq, M. Korjik, A, Vassiliev, TNS, VOL. 61, NO. 1, 2014

Hot intra-band luminescence

Observed in several crystals but very low light yield: 30ph/MeV in CsI

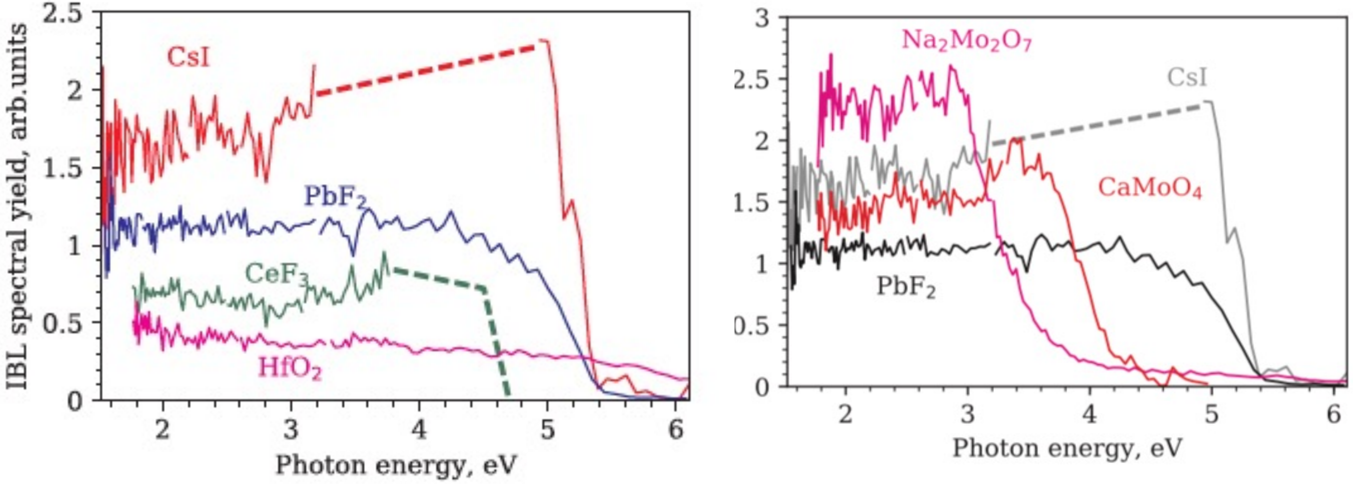

Measured with pulsed cathodoluminescence (PCL) in Tartu
electron beam with Emax~120 keV, pulseFWHM 200 ps, peak electron current ~15 A/cm2

S. Omelkov et.al., J. Lum., 198 (2018) 260-271

Crossluminescence

Radiative transition between the core- and valence bands.

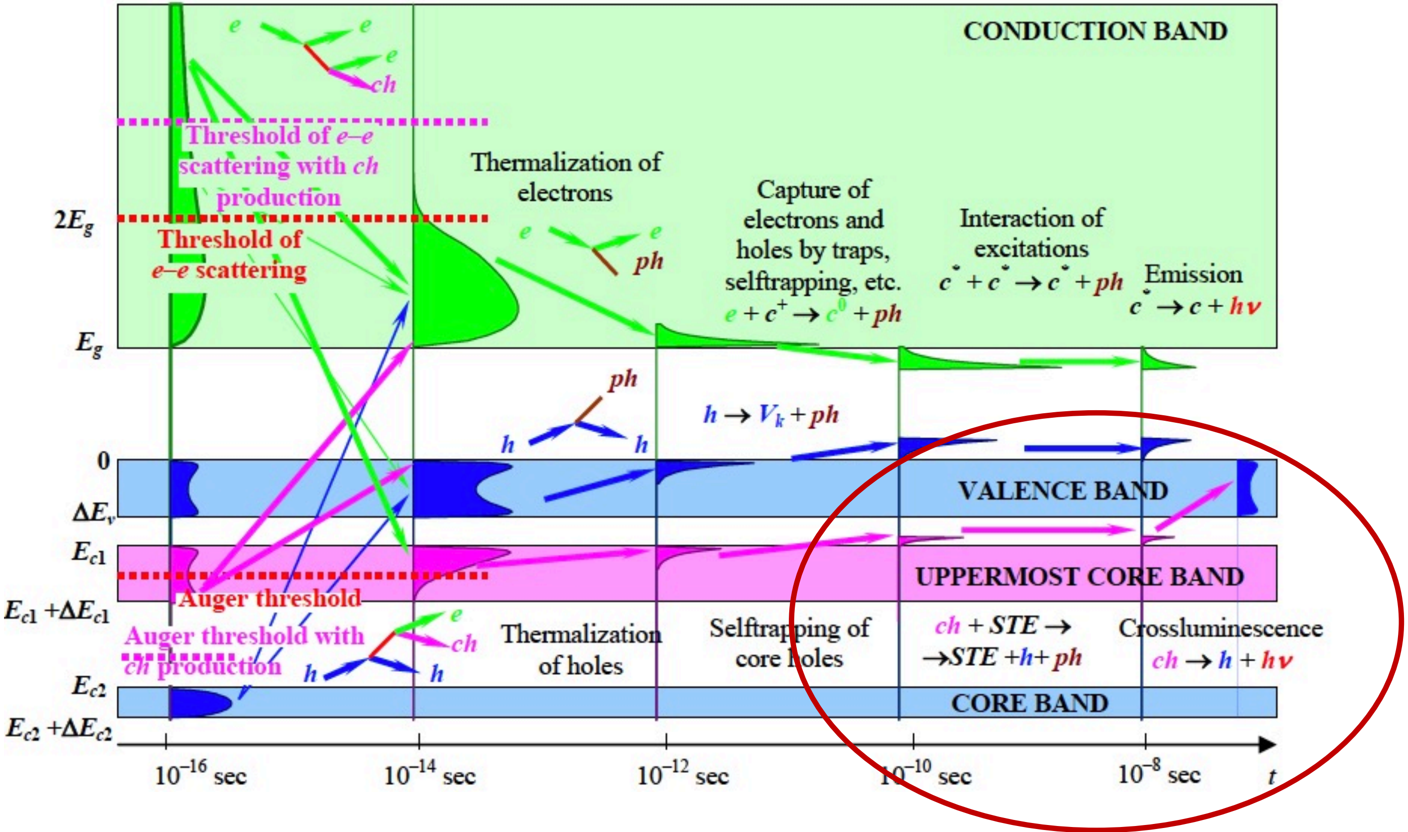

Crossluminescence

Many Materials available

C.W.E. Van Eijk Journal of Luminescence60&OI 1994! 9~694!

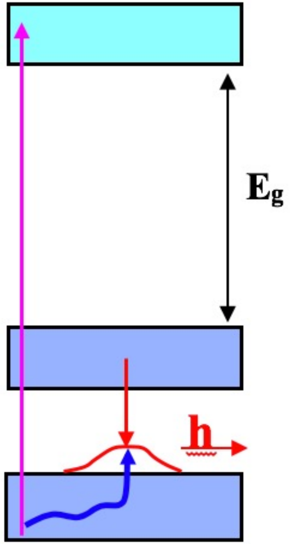

Compilation of CL data at 293 K

	$E(C-V)$ (eV)	$E(G)$ (eV)	Theoretical	Observed (eV)	λ (nm)	Light yield (photons/MeV)	τ (ns)	Density (g/cm^3)	References
KF	7.5–10.5	10.7	+	7.5–8.5	156	--		2.5	[13, 18]
KCl	10–13	8.4	—						
KBr	10–13	7.4	—						
KI	9.5–14	6.0	—	STE					
RbF	0–7.5	10.3	+	3–6	203, 234	1700	1.3	3.6	[11–14, 18]
RbCl	4–9	8.2	+	5.5–7.5	190	1		2.8	[12]
RbBr	6.7–9.5	7.4	?						
RbI	5–10	6.1	?	STE					
CsF	0–4.5	9.9	+	2.5–4	390	2000	2.9	4.1	[6, 11, 14]
CsCl	1–5	8.3	+	4–5.5	240, 270	900	0.9	4.0	[6, 14, 15, 17, 18]
CsBr	4–6	7.3	+	4.5–6.5	250	20	0.07	4.4	[6, 14, 15, 18]
CsI	0–7	6.2	?	—/STE					
CaF_2	12.5–17.3	12.6	—	—/STE					[1]
SrF_2	8.4–12.8	11.1	?	—/STE					[1]
BaF_2	4.4–7.8	10.5	+	5–7	195, 220	1400	0.8	4.9	[1, 3, 4, 9]
$K_xRb_{1-x}F$				5–6/8					[13, 18]
$KMgF_3$				6–9	140–190	1400	1.3	3.2	[7–10]
$KCaF_3$				6–9	140–190	1400	< 2	3.0	[10]
KYF_4					170	1000	1.9	3.6	[9, 16]
K_2YF_5				5.5–8.5	170	300	1.3	3.1	[8, 9]
$KLuF_4$				5.5–8.5	170–200	~ 200	1.3	5.2	[8, 9, 16]
KLu_2F_7				5.5–8.5	165	~ 200	< 2	7.5	[8]
K_2SiF_6				5–9	140–250				[21]
$CsCaCl_3$					250, 305	1400	~ 1	2.9	[10, 17, 19]
$CsSrCl_3$					260, 300		~ 1		[19, 21]
$LiBaF_3$					190, 230	1400	0.8	5.2	[10]
$BaMgF_4$					190, 220	1000		4.5	[21]
BaY_2F_8				4–7.5			0.9	5.0	[20]
K_2LiGaF_6				5–9	140–250				[21]
K_2NaAlF_6				5–9	140–250				[21]

BaF_2

Very fast emission < 2ns but emission < 400nm

Crossluminescence in BaF_2

Sub ns emission but in UV &additional slow component

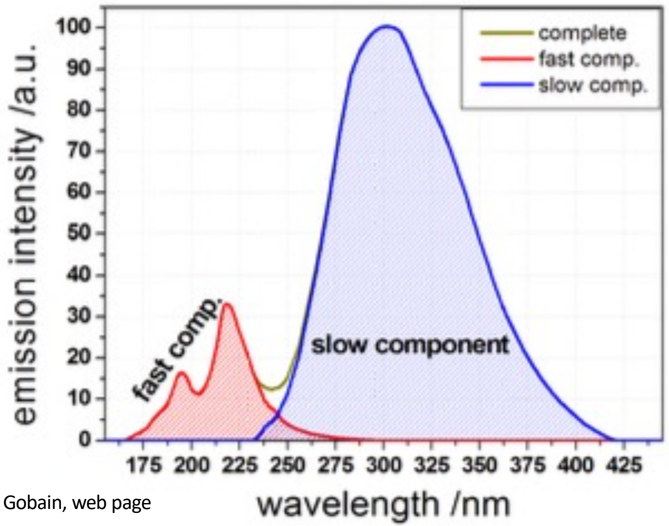

St Gobain, web page

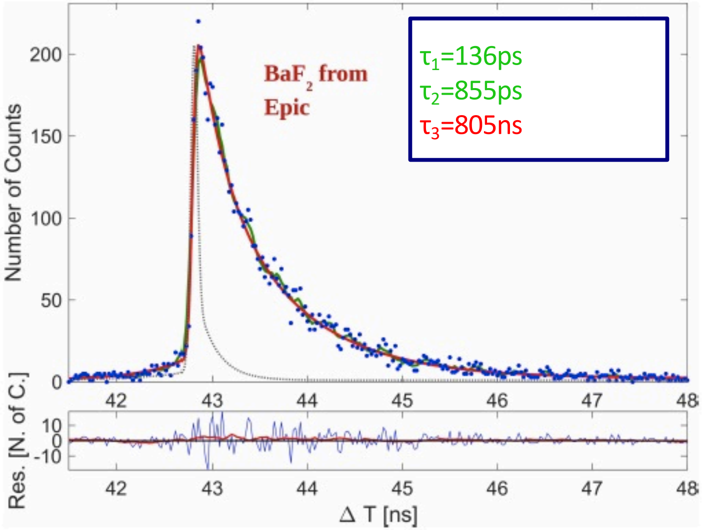

R. Pots et al., Front. Phys. 8:592875. doi:10.3389/fphy.2020.592875
S Gundacker et al 2021 Phys. Med. Biol. 66 114002

Reduce the slow component in BaF_2

Decay time spectra for various % Y doping

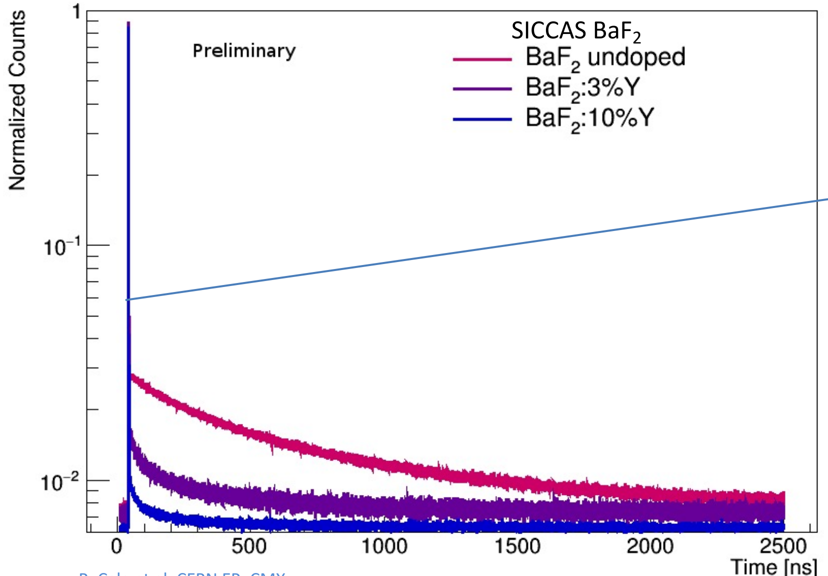

R. Cala et al, CERN EP_CMX

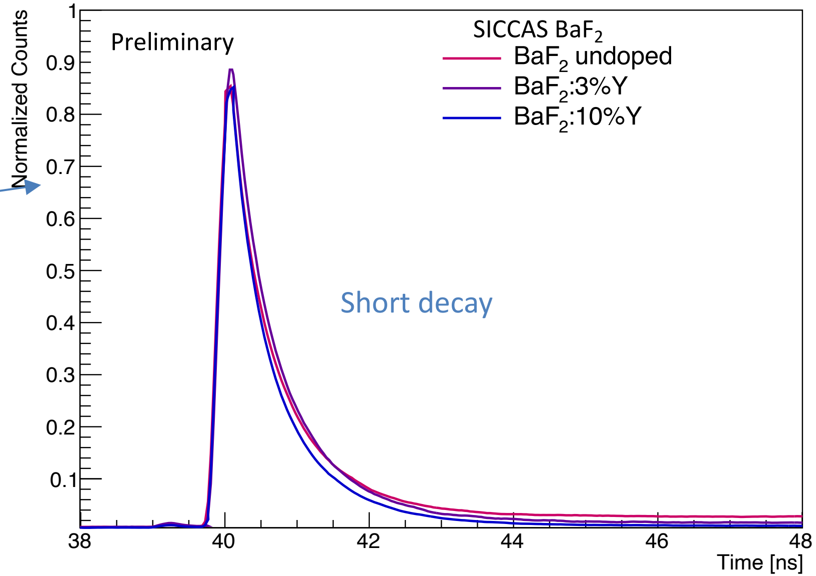

R. Cala et al, CERN EP_CMX

R&D to suppress the slow component by doping

⇒No change in short decay

⇒but slow component suppression

J. Chen, et al., IEEE Trans. Nucl. Sci., vol. 65, no. 8, pp. 2147-2151, 2018.
S. Gundacker et al., Phys. Med. Biol. 66 (2021) 114002

Improvement of UV photodetection

Development on going on VUV SiPMs (eg: for nEXO experiment (Xe liquid @175nm)*) both in Hamatmasu: HPK S13370-CN & FBK NUV HD to increase PDE (>20%)

Time resolution measured @CERN with BaF_2 (2x2x3mm^3) pixels @511keV

LSO:Ce,Ca 2x2x3mm^3
with optical coupling,PDE 59%

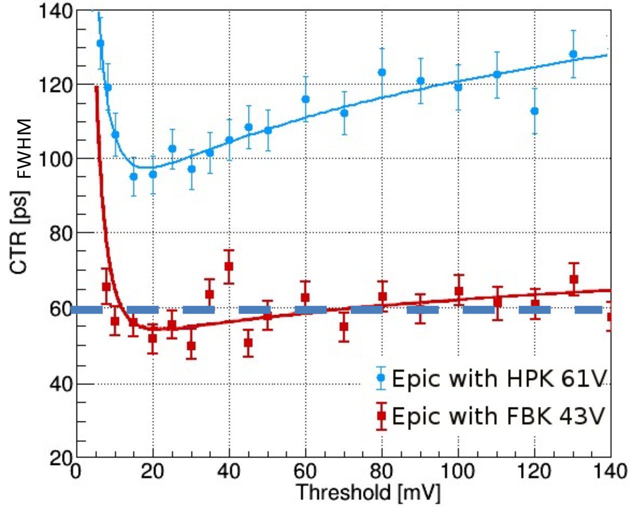

HPK S13370-CN

Better SPTR & PDE

FBK VUV HD

PDE: 15-20%
No optical coupling

Further improvement of PDE in UV and optical coupling may improve time resolution

* A. Jamil et al., in IEEE TNS, vol. 65, no. 11, pp. 2823-2833, 2018, doi: 10.1109/TNS.2018.2875668.

R. Pots et al, Front. Phys. | doi: 10.3389/fphy.2020.592875
S. Gundacker et al., Phys. Med. Biol. 66 (2021) 114002

Prospective for BaF_2

Typical crystal size 2x2x3mm[3]

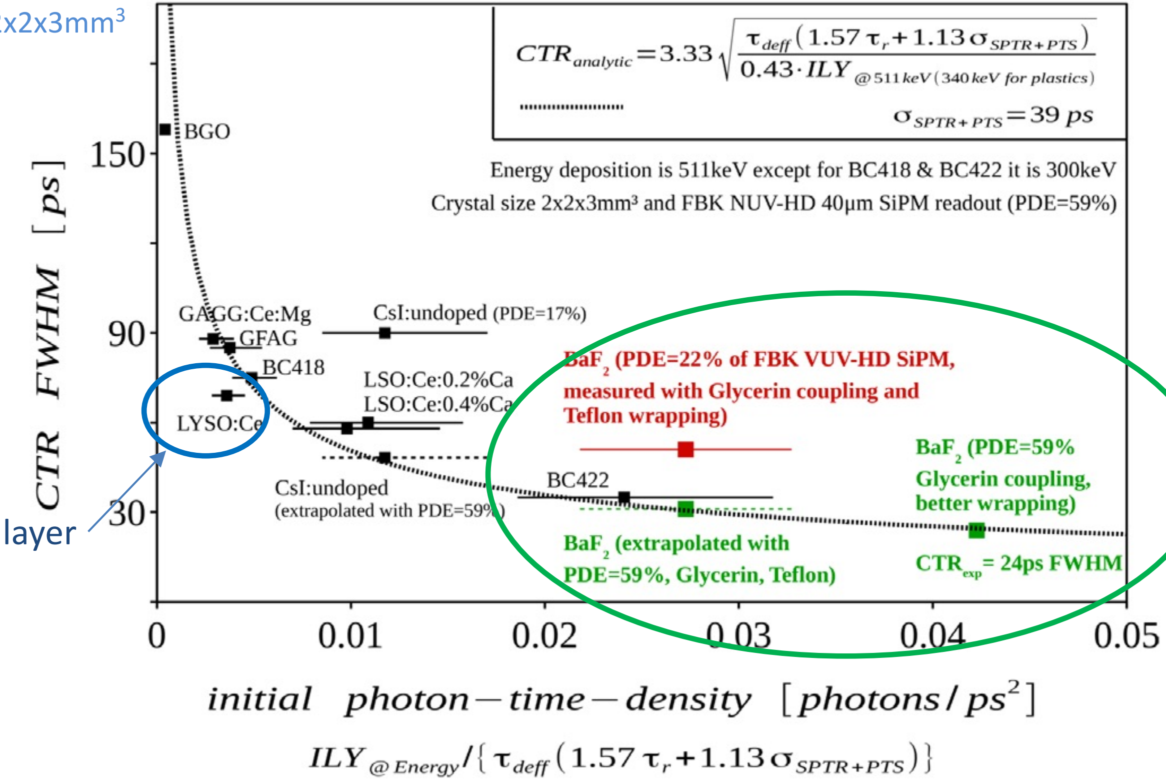

Analytic CTR expression
S. Vinogradov,
NIMA 912 (2018) 149-153

BaF_2 promising for fast timing

Used in CMS timing layer

S. Gundacker et al., Phys. Med. Biol. 66 (2021) 114002

Development of cross luminescence material more in UV visible region

Emission spectra

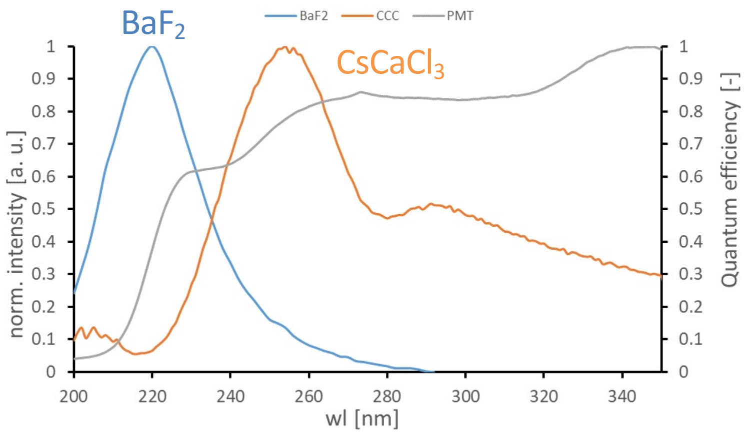

Courtesy V. Vanecek, M. Nikl, FZU Prague
Data for BaF$_2$ from M. Laval et al. , NIM Phys. Res., 206 (1983) 169–176

Decay spectra

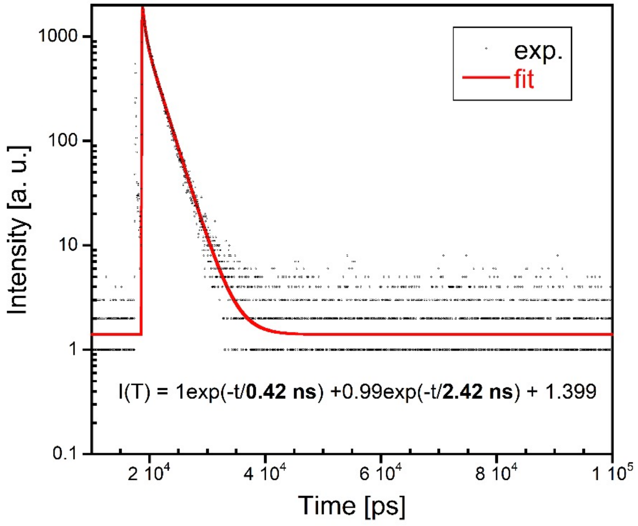

Courtesy V. Vanecek, M. Nikl, FZU Prague

Emission @ 260nm

2 fast decay times: 0.42ns, 2.42ns

Fyzikální ústav
Akademie věd
České republiky

How to go further towards 10ps?
=> Exploit faster light processes

Better time resolution with prompt photons

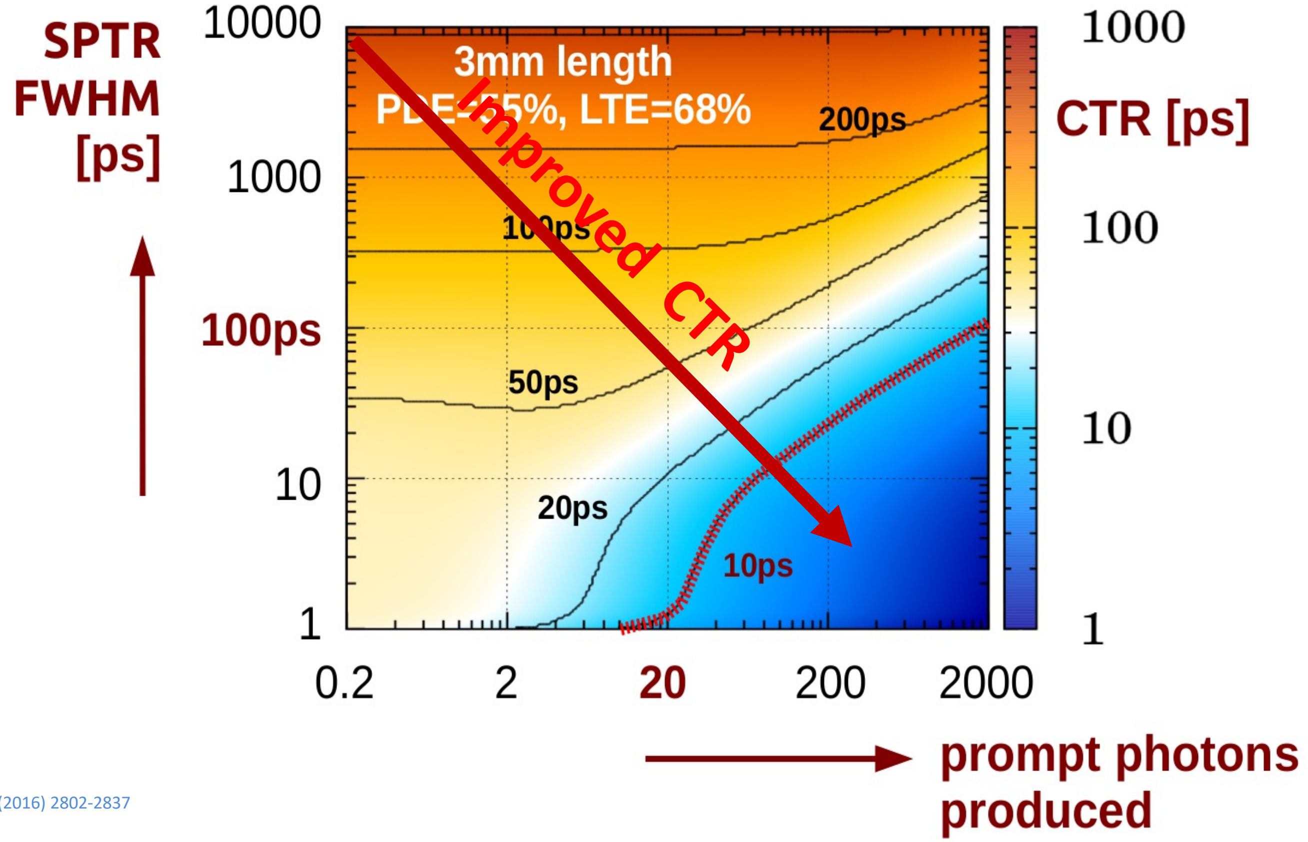

S. Gundacker, CERN-THESIS-2014-034
S. Gundacker et al, Phys. Med. Biol. 61 (2016) 2802-2837
S. Gundacker et al., JINST 11P08008

Cherenkov emission

Cherenkov radiation is produced when charged particles travel through a dielectric medium faster than the speed of light in that medium (shoke wave).

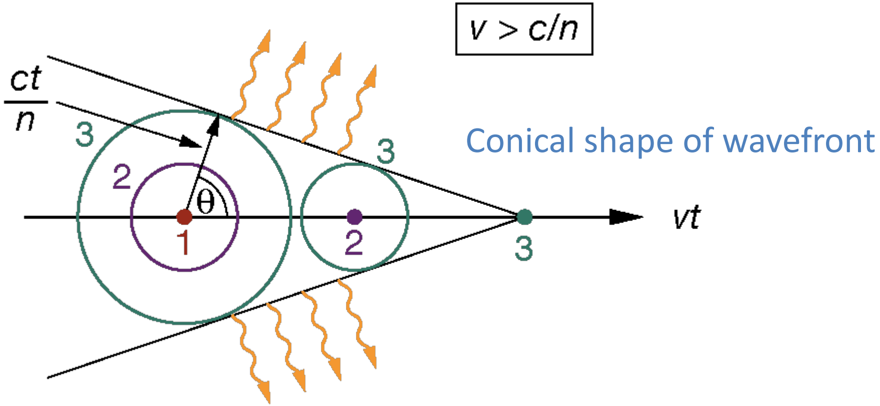

⇒ Emission is quasi instantaneously (< 10 ps) but few photons are emitted

$$\frac{dN}{dx} = 2\pi\alpha\left(\frac{1}{\lambda_1} - \frac{1}{\lambda_2}\right)\left(1 - \frac{1}{\beta^2 n^2}\right)$$

=> Emission in all wavelength ranges : $1/\boldsymbol{\lambda}^2$ but more in UV

=> Emission higher with increasing refractive index

Exploitation of Cerenkov to improve time resolution of BGO

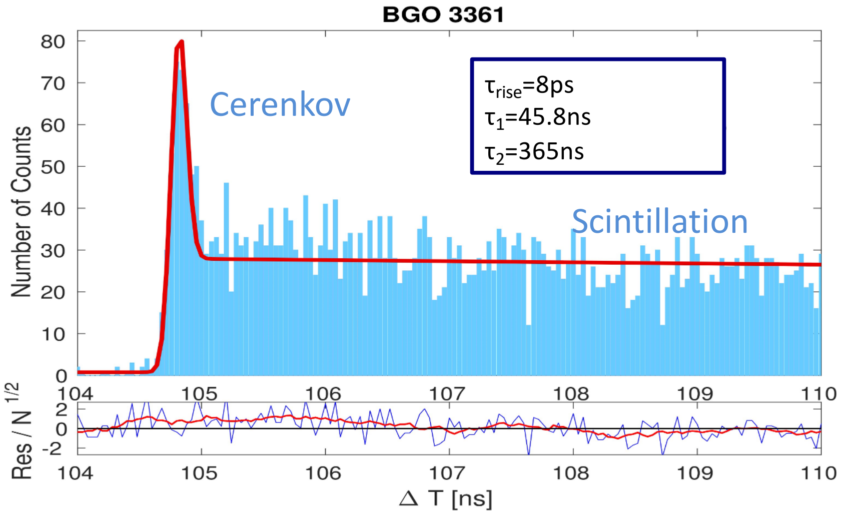

but only few photons:

17 photons in the 310-850nm range.

CTR histogram: **2x2x20** mm³ BGO crystals, fully polished, coupled to FBK NUV-HD

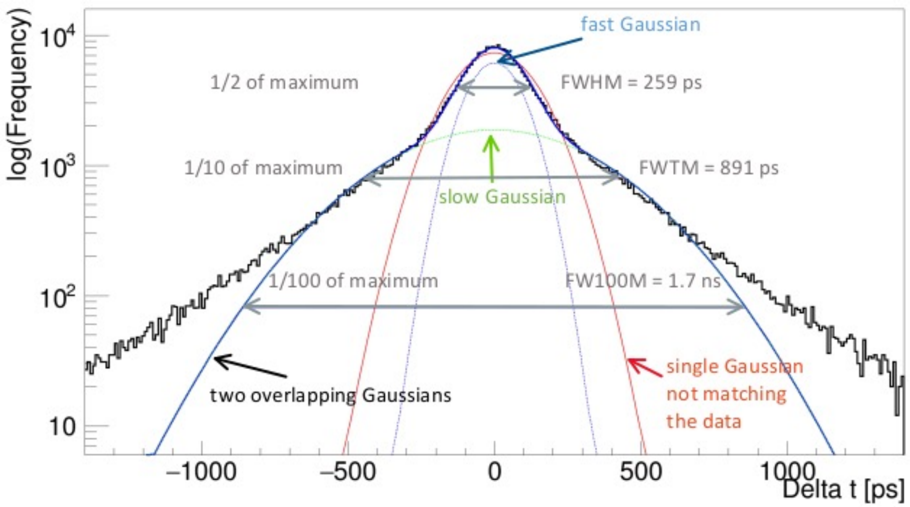

440-665 keV energy window -> CTR = 288 ps FWHM without time walk correction

440-665 keV energy window -> **CTR = 259 ps** FWHM with time walk correction

CTR: 259ps

S. Gundacker et al. (2019) Phys. Med. Biol. 64 055012
N. Kratochwil et al (2020), Phys. Med. Biol. 65 115004
N Kratochwil et al (2020) IEEE TRPMS 2020.3030483

Exploitation of Cerenkov to improve time resolution of BGO

Variation of rise time with amount of Cerenkov events

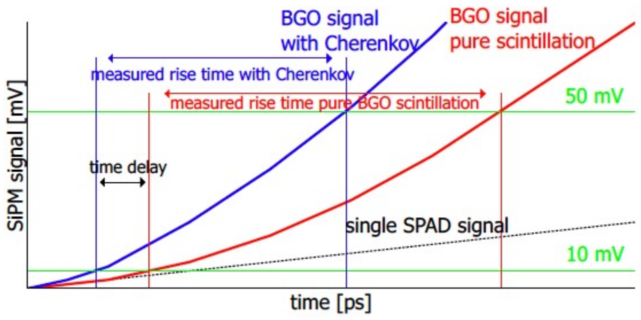

Classification of events with rise time

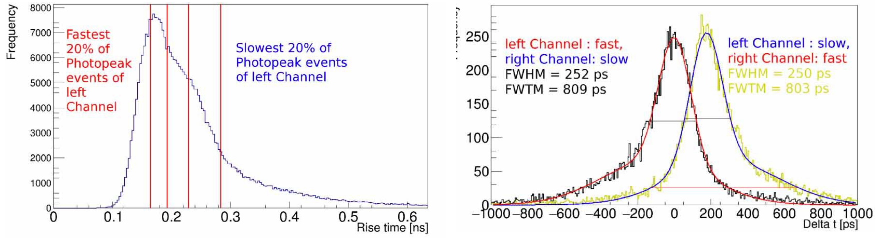

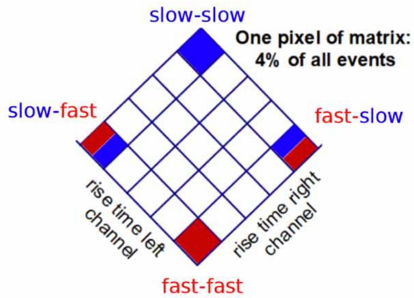

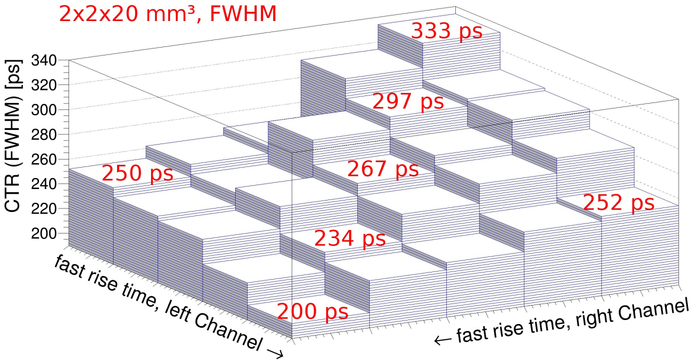

N. Kratochwil et al (2020), Phys. Med. Biol. 65 115004
N Kratochwil et al (2020) IEEE TRPMS 2020.3030483

For fastest events CTR of 200ps !

Impact on image reconstruction quality of the exploitation of Cerenkov in BGO

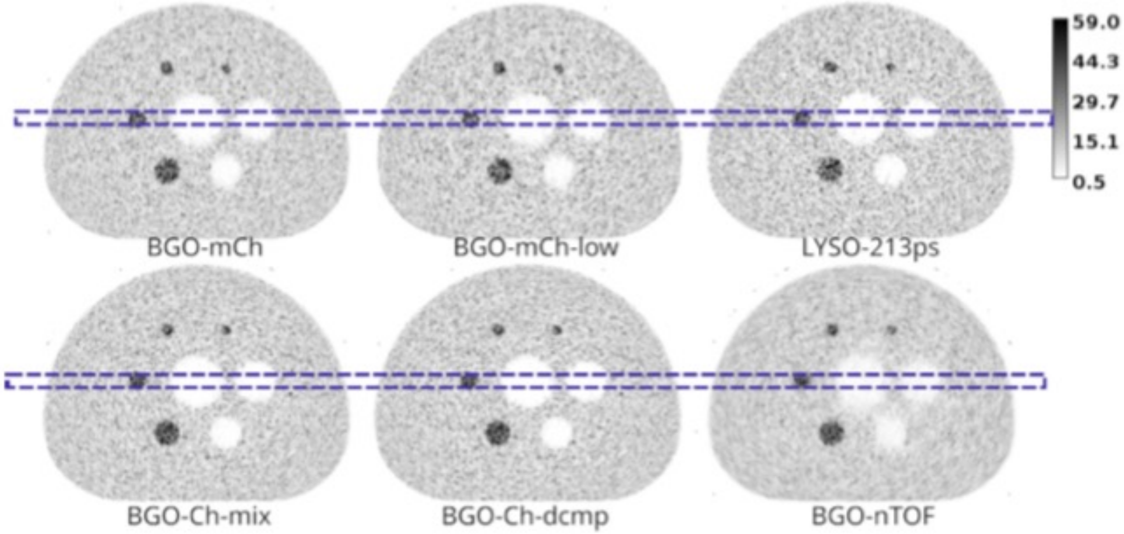

N. Efthimiou et al., IEEE TRPMS.2020.3048642

From bulk to nanomaterial: Quantum confinement

Same crystal lattice but nanometer-sized crystal particle

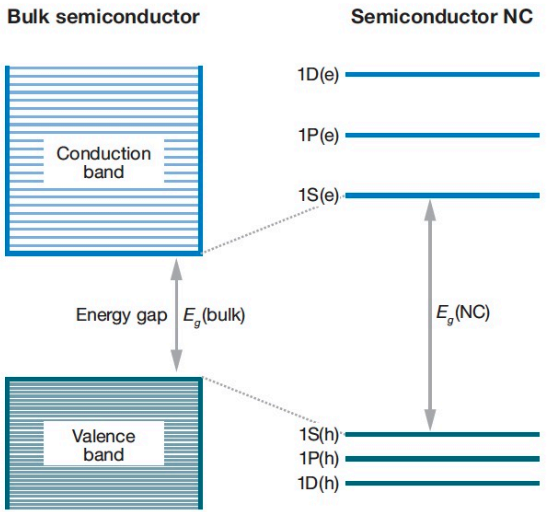

V. Klimov Annu Rev. Phys. Chem. 58 (2007) 535-573

Energy band gap (E_g) varies with quantum dot size
Decrease of size => increase of Eg

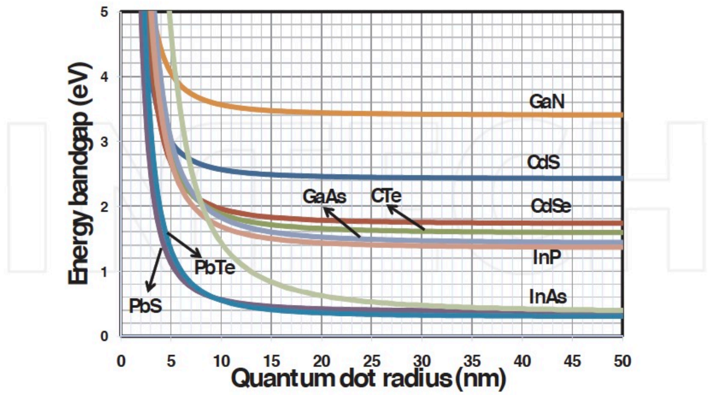

Figure 4. Variation of quantum dot energy bandgap vs. dot size for some common semiconductors. From [9].

With decreasing crystal size
From "continous band" to quantized energy levels

K. Jasim, Quantum Dots Solar Cells
http://dx.doi.org/10.5772/59159

Quantum confinement

from Benoit Dubertret and Hideki Ooba

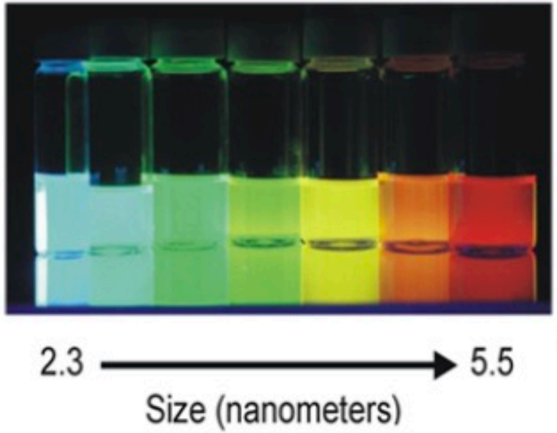

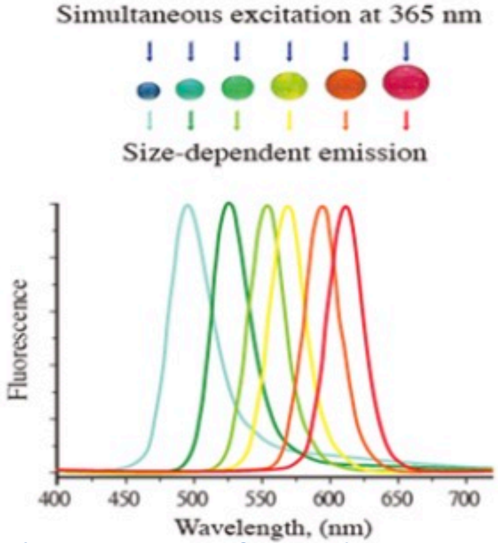

=> Tune the emission properties by changing size of nanodots

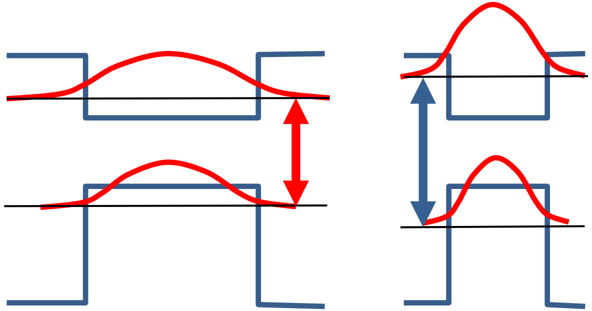

Exciton energy increases with decrease of nanostructure size – control of emission wavelength

Example of CdSe

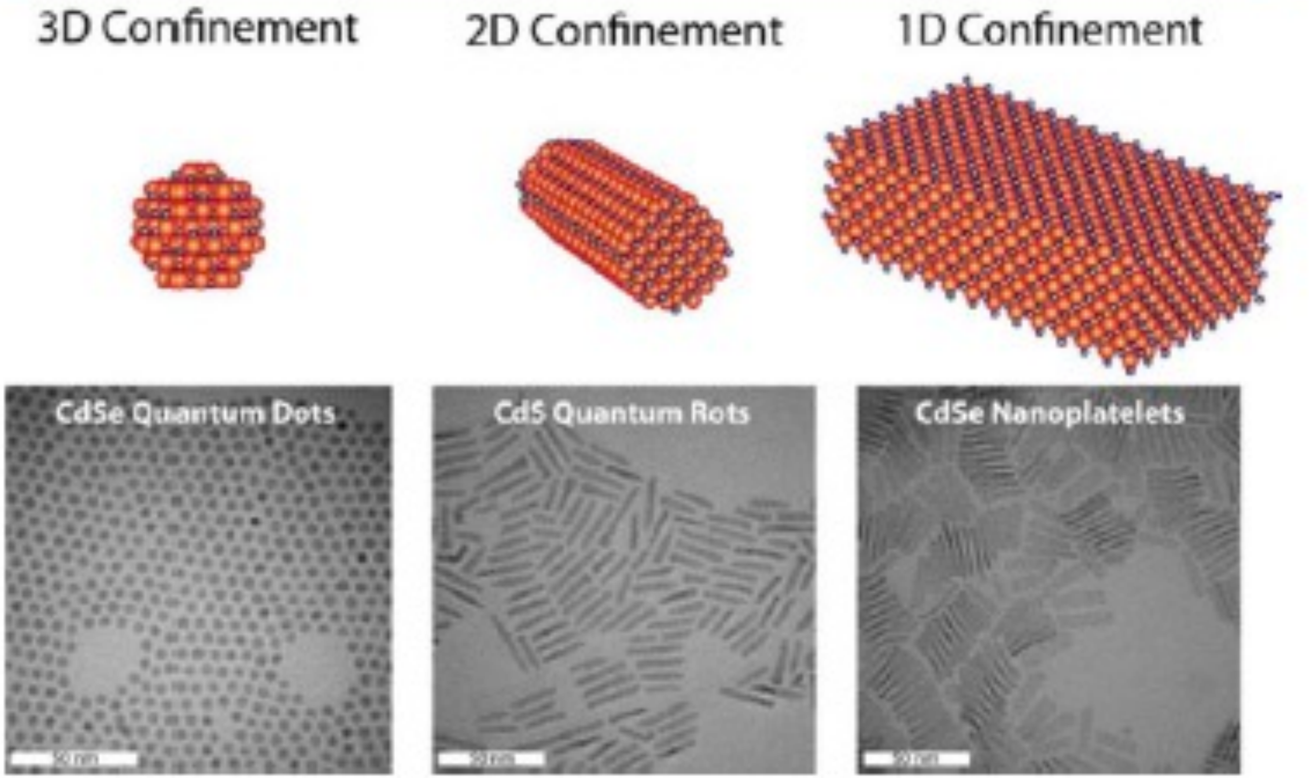

S. Bouet, et al. , Chem Mater 25(2013), 1262 (fig.1)

CdSe quantum well/quantum dot

CdSe nanoplatelet

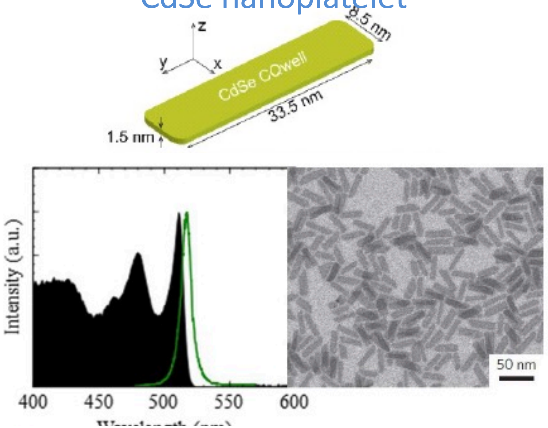

J.Q. Grim et al., Nature Nanotechnol. 9 (2014) 891.

CdSe/CdS Giant shell Quantum dot

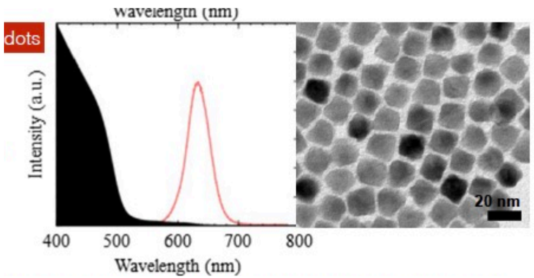

Christodoulou et al., *J. Mater. Chem.* **2014**, 2, 3439.

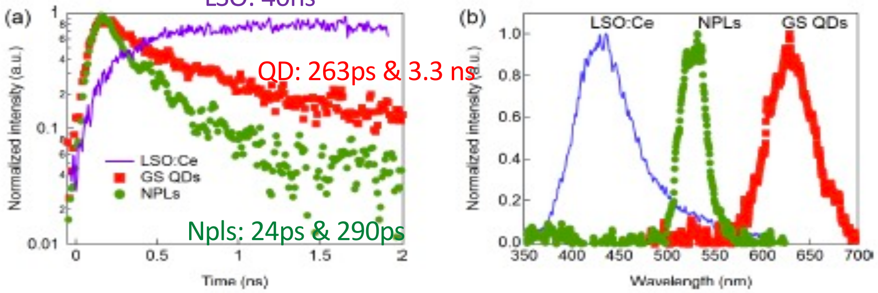

R. Martinez Turtos et al., 2016 JINST_11 (10) P10015

=> Much Faster than LYSO crystal

CdxZn1-xS/ZnS (CZS) QD Nanocomposite Synthesis

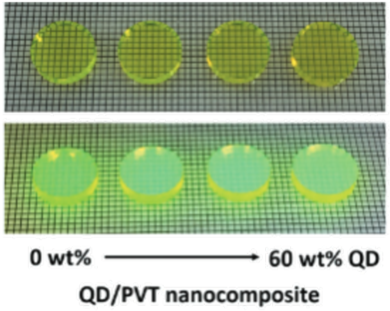

Cs^{137} photoelectric spectra

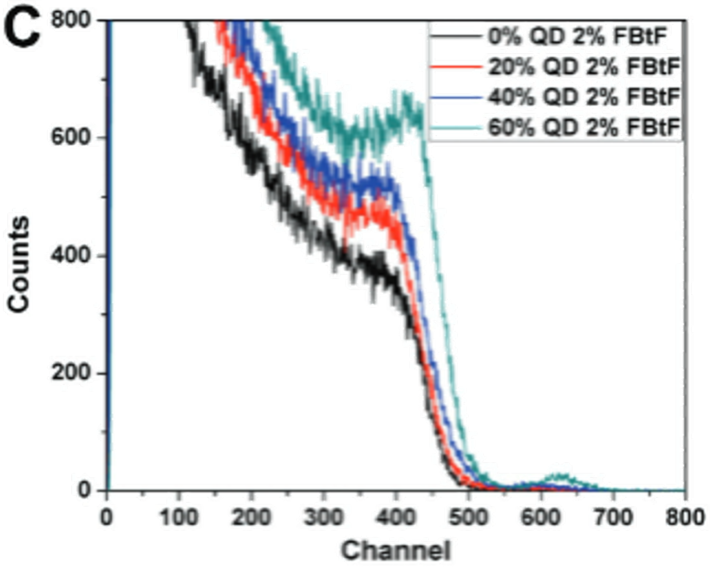

Decay time spectra

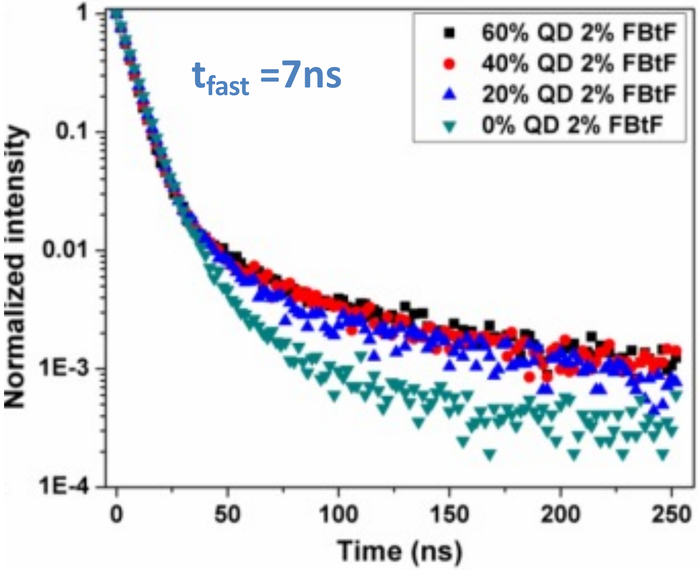

C. Liu *et al.* ACS Nano, 2017

ZnO:Ga Nanocomposite: photoluminescence properties

In SiO_2

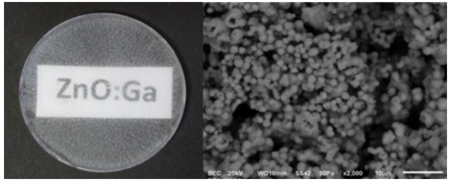

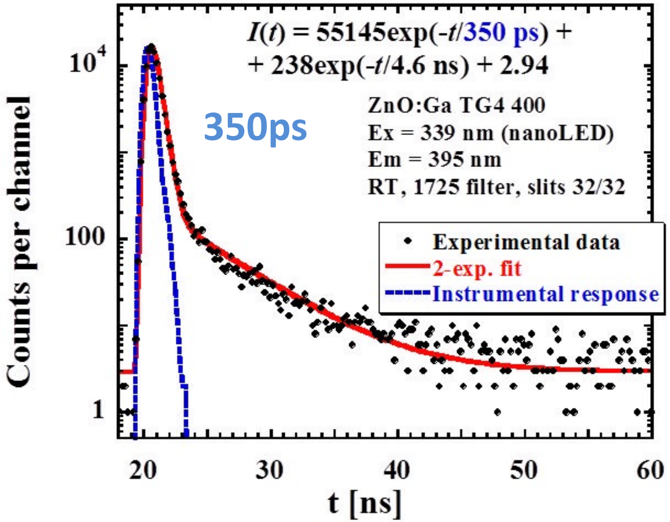

Procházková et al., Radiat Meas 90, 2016, 59-63

In Polystyrene

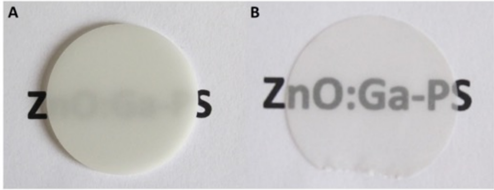

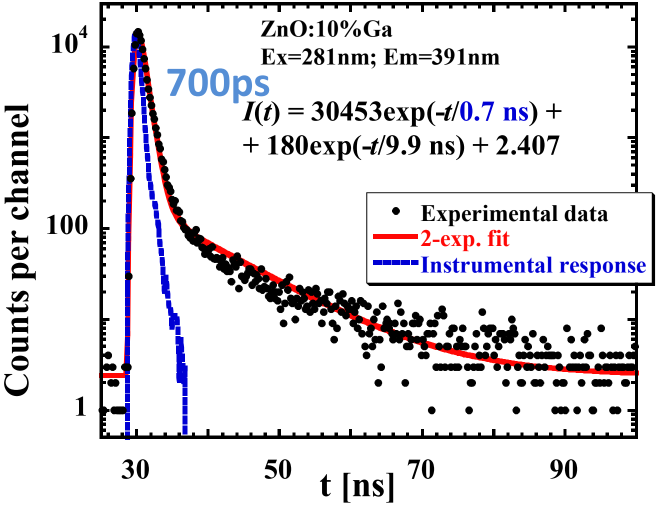

Buresova et al, *Opt. Express* **24**, 15289 (2016)

Perovskite thin film

$CsPbBr_3$ nanocrystals

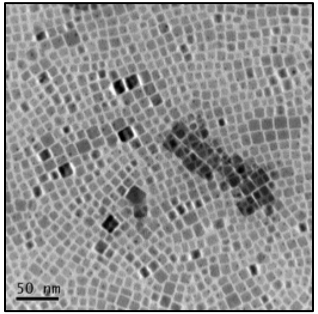

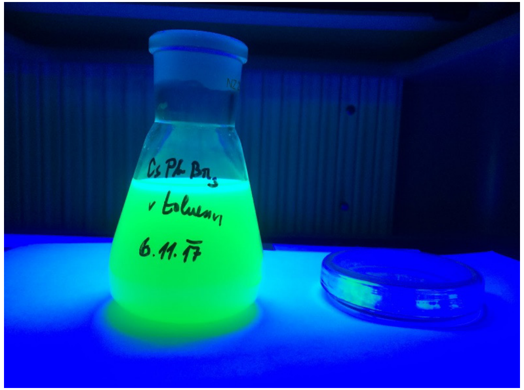

$CsPbBr_3$ thin films deposited on glass substrate

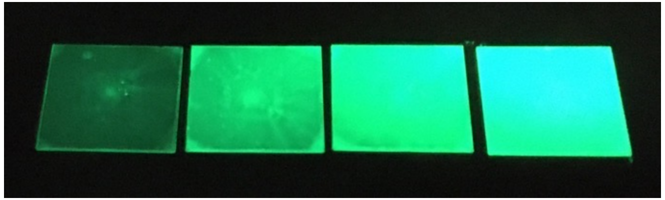

CsPbBr3 big square on glass
X-irradiated decay (40 kV); long time-window

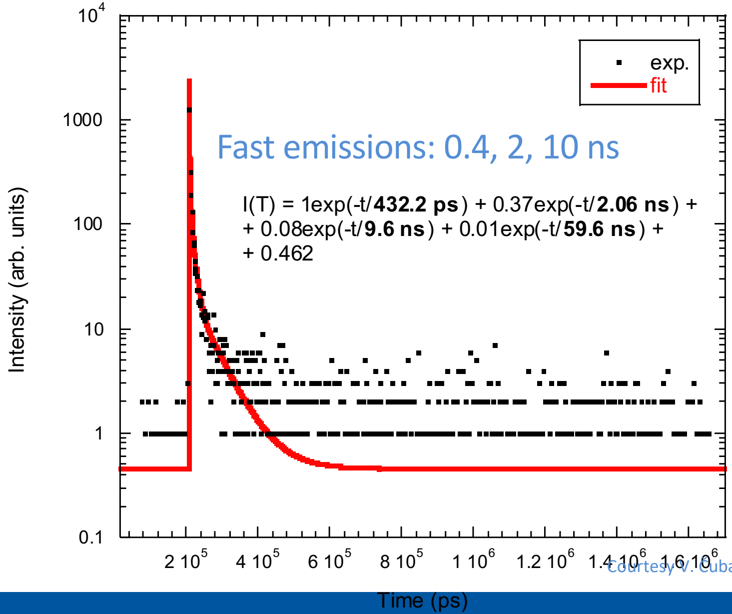

Courtesy V. Čuba, K. Děcká, A. Suchá CTU, Prague

Perovskite nanocomposite

$CsPbBr_3$ nanocrystals

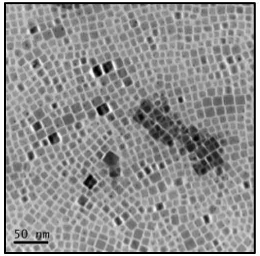

$CsPbBr_3$ nanocrystals imbedded in polystyrene

CsF decay time under Xray excitation

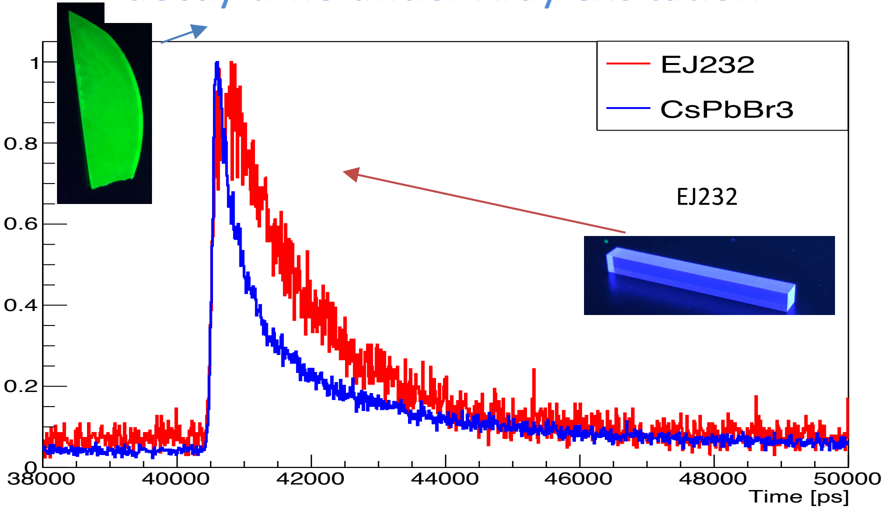

Nano-sized $CsPbBr_3$ embedded in polymer matrix

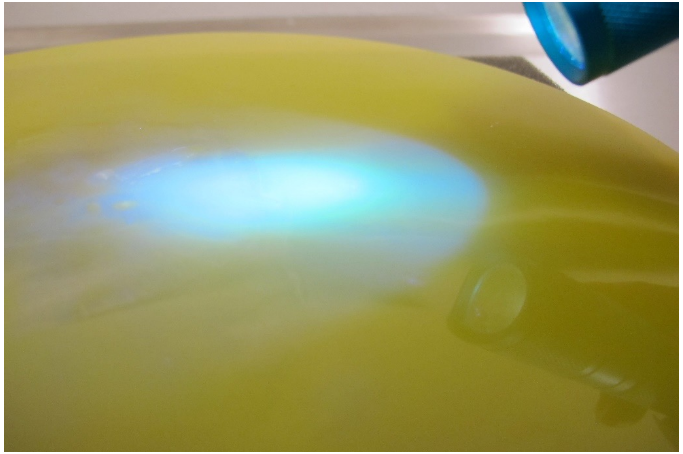

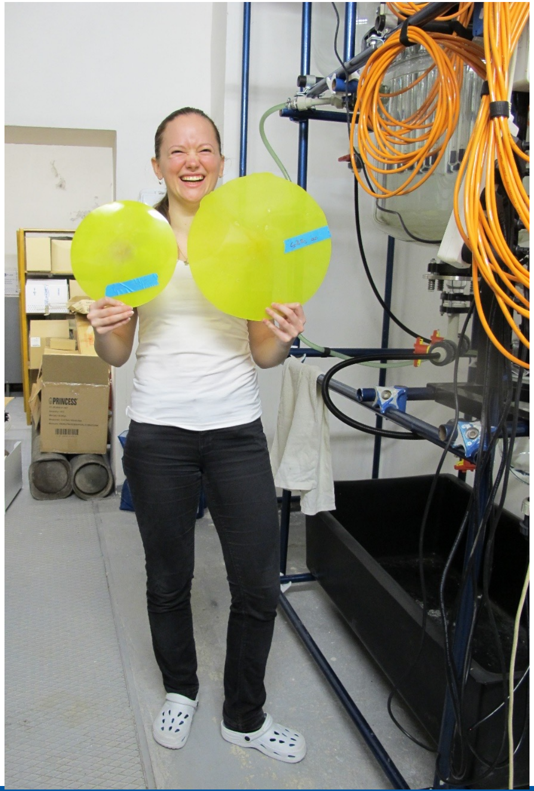

Courtesy V. Cuba, CTU, Prague

InGaN/GaN heterostructure: Multiple Quantum Wells (MQW)

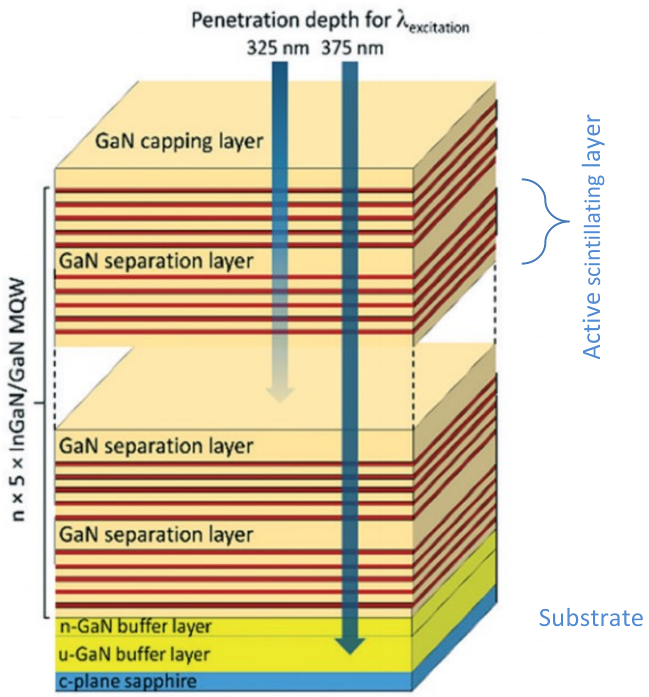

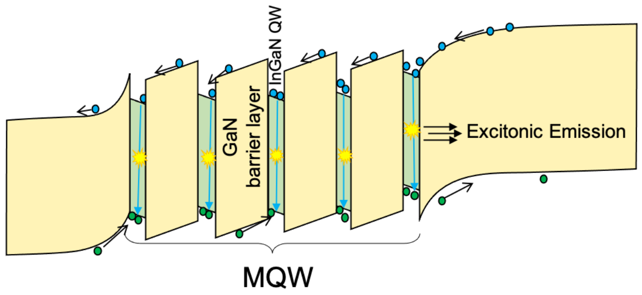

Electrons and holes are concentrated in narrow gap layers and radiatively recombine there being spatially confined by small thickness (few nm) of the layer.

MOVPE technology can prepare such nanostructures on 4-6 inch size Al_2O_3 substrates

T. Hubacek, CrystEngComm, 2019, 21, 356

InGaN/GaN heterostructure: Multiple Quantum Wells (MQW)

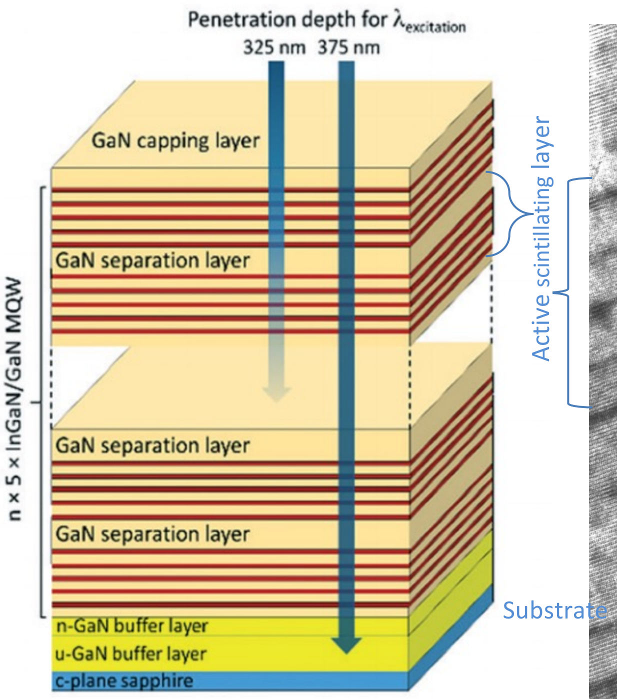

T. Hubacek, CrystEngComm, 2019, 21, 356

Picture from A. Hospodkova

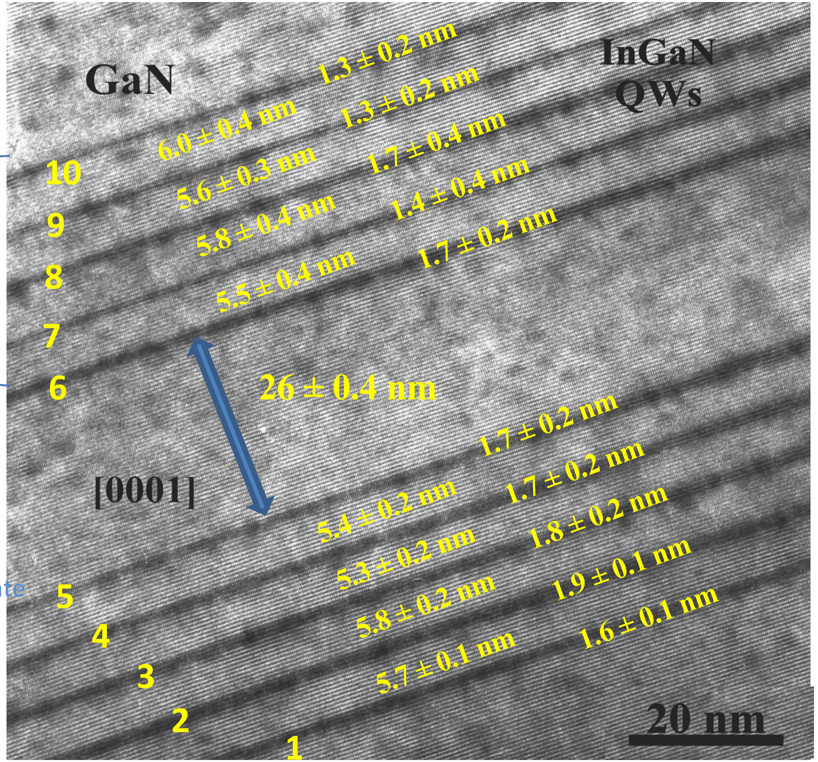

InGaN/GaN heterostructure: Multiple Quantum Wells (MQW)

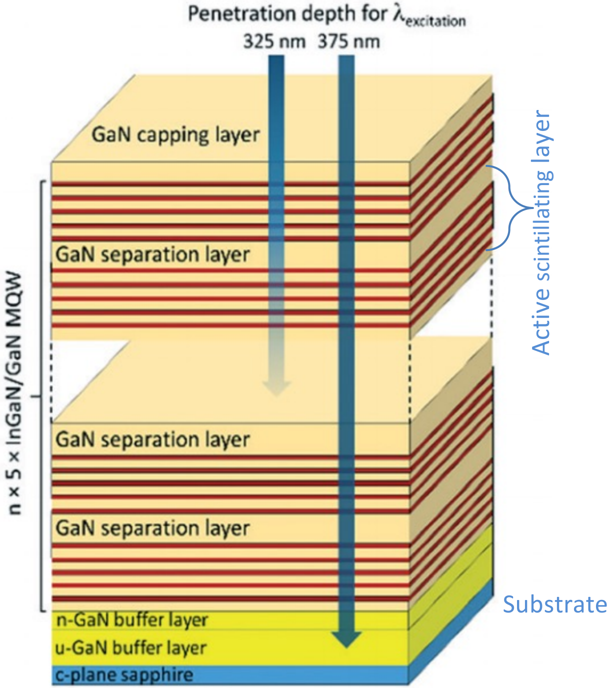

T. Hubacek, CrystEngComm, 2019, 21, 356

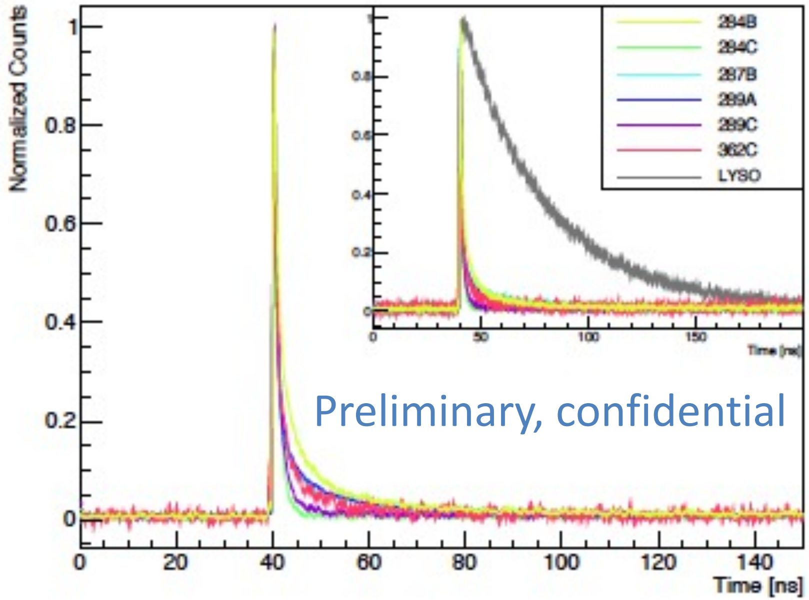

F.Pagano, CERN EP-CMX

Heterostructure concept

Combine scintillators with high light yield, high stopping power with prompt emission

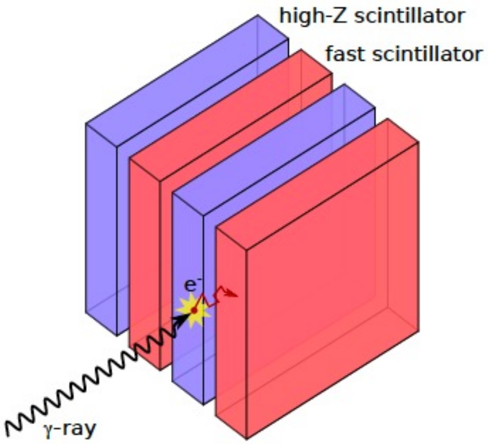

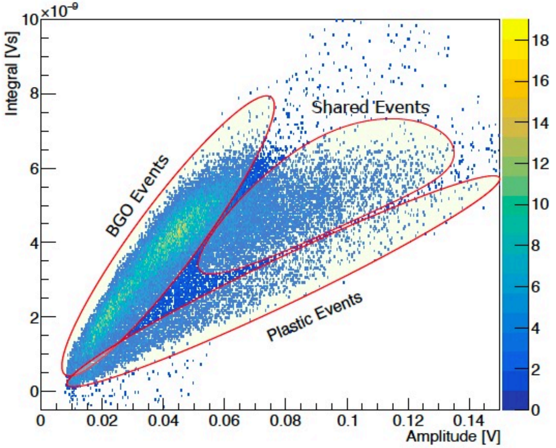

- The 511keV photon is mainly stopped by the heavy material
- In some cases, the recoil photoelectron deposits its energy both in the heavy and in the fast material

$\Rightarrow$ Shared 511keV events have a better timing

First attempt of Heterostructure

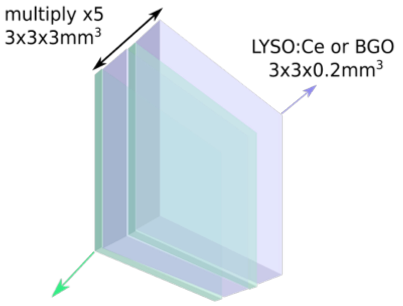

CdSe/CdS core crown nanoplatelets (CC NPLs) drop-casted film
Effective deposited mass equivalent to 20μm

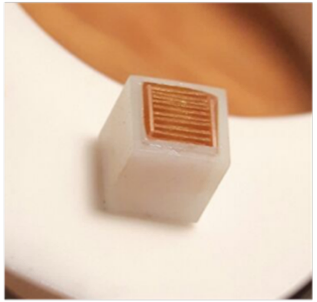

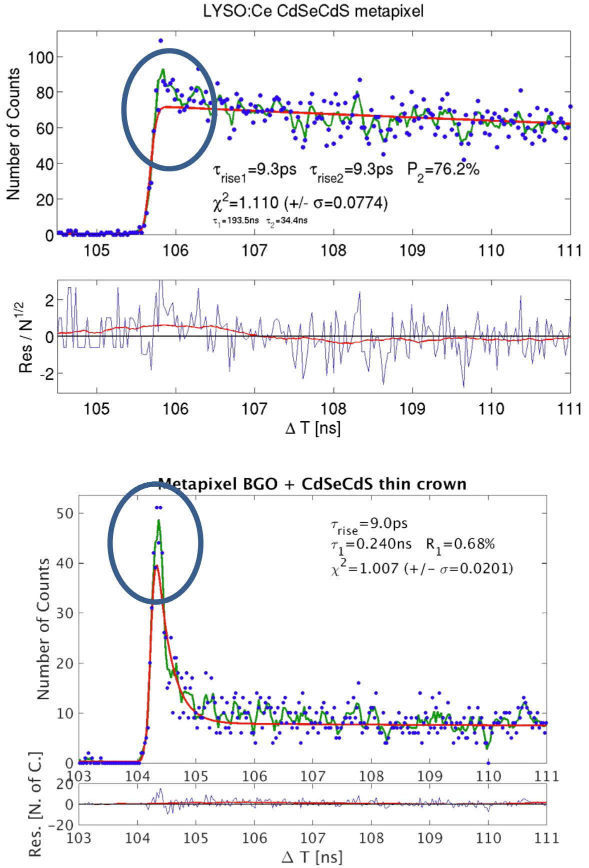

R. M. Turtos et al, Phys. Med. Biol. 64 (2019) 85018
R.M. Turtos, et al. npj 2D Materials and Applications vol. 3, article number: 37 (2019)

Heterostructure concept

Proof of concept with combining LSO or BGO with plastic scintillator on 3x3x3mm^3 pixels

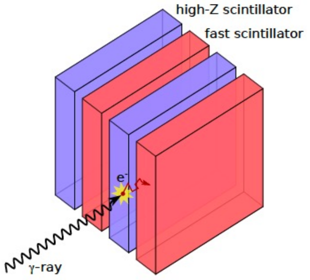

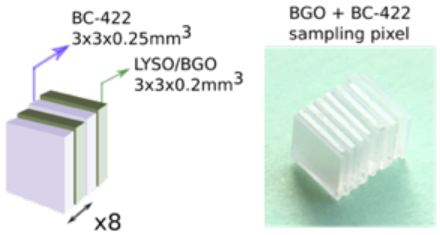

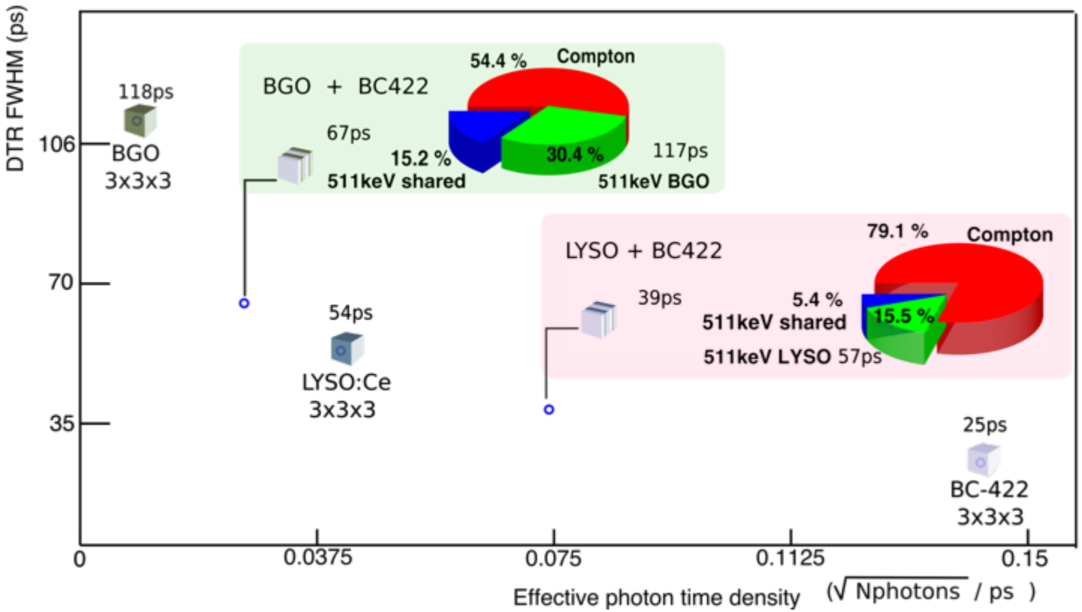

R. M. Turtos et al, Phys. Med. Biol. 64 (2019) 85018

The 10 ps challenge: a step toward reconstruction-less TOF-PET

https://the10ps-challenge.org

The 10 ps challenge:

- a spur on the development of fast timing
- an opportunity to get together
- an incentive to raise funding
- a way to shed light on nuclear instrumentation for medical imaging and beyond

One unique challenge launched for 5 to 10 years and operated by an international organisation with rules issued by the community based on the measurement of CTR combined to sensitivity

Several milestones and prizes:

– 3 years after the launch of the challenge:

the Flash Gordon prizes delivered to the 3 best certified achievements

– until the end of the challenge:

the Leonard McCoy prize for the first team meeting successfully the specifications of the challenge

Paul Lecoq *et al* 2020 *Phys. Med. Biol.* **65** 21RM01

Conclusion

- Scintillation detectors are widely used in many applications
- A wide variety of scintillators and photodetectors exist
- Choice of the scintillator and photodetector will depend on the application and performance requested
- Science of scintillators continuously evolves:
  - New materials
  - New production methods
  - Progress of understanding of scintillation
  - Development of new instrumentation for characterization with better time resolution

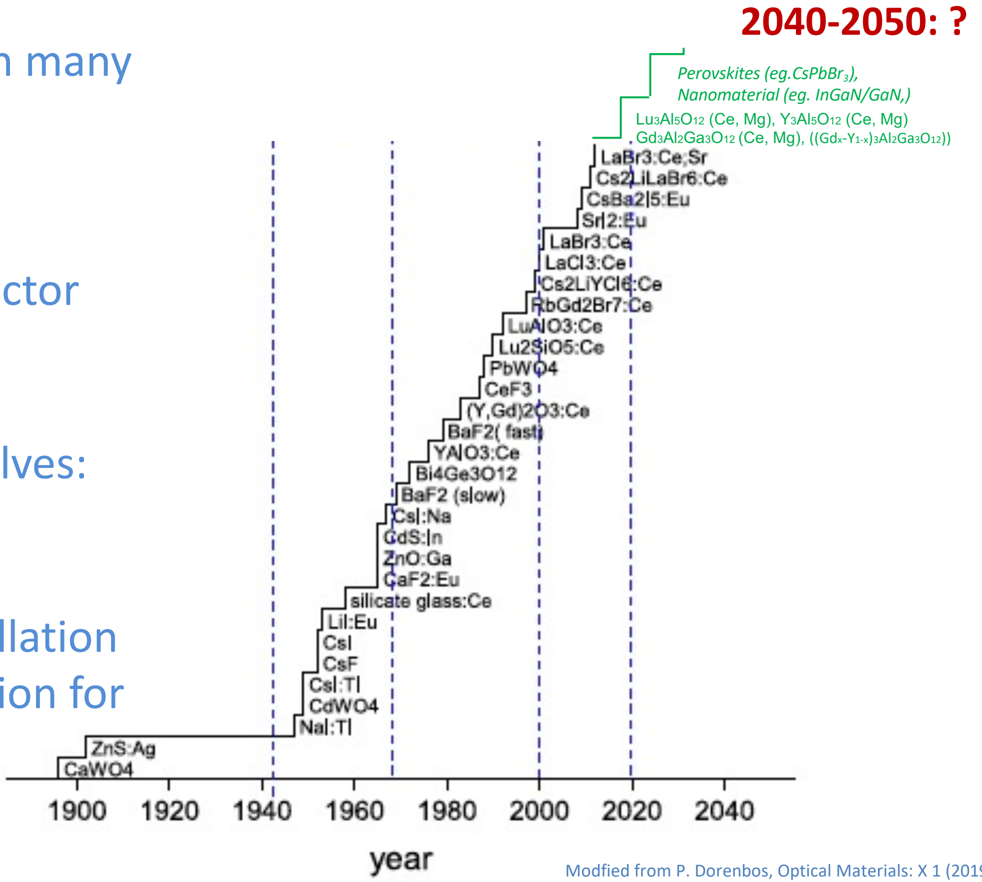

Modfied from P. Dorenbos, Optical Materials: X 1 (2019) 100021, https://doi.org/10.1016/j.omx.2019.100021

Conclusion

- Scintillation detectors are widely used in many applications
- A wide variety of scintillators and photodetectors exist
- Choice of the scintillator and photodet will depend on the application and performance requested
- Science of scintillators continuousl
  - New materials
  - New production me
  - Progress of un ng of scin
  - Developm w instrumenta character on with better time resolution

=>Scintillation detector: an excited field of research !

2040-2050: ?

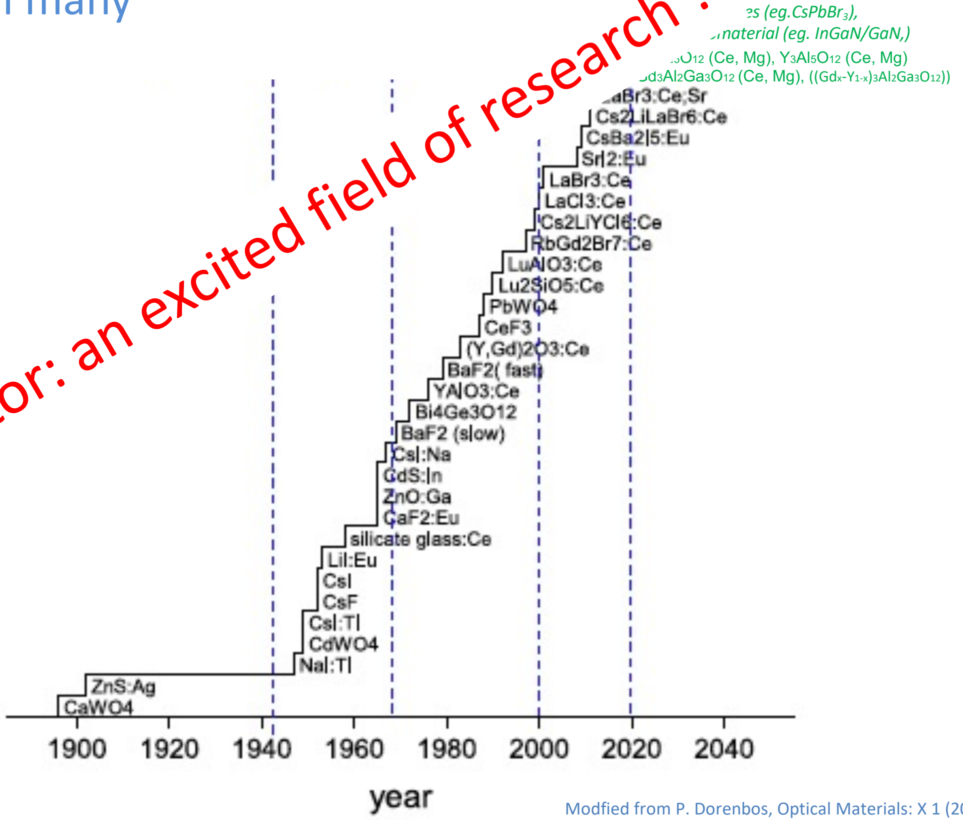

Modfied from P. Dorenbos, Optical Materials: X 1 (2019) 100021, https://doi.org/10.1016/j.omx.2019.100021

Some references

Books

J. B. Birks, The theory and practice of scintillation counting, 1964, Pergamon Press

D. Curie, Luminescence in Crystals (Methuen, London, 1963)

C. Gruppen, I. Buvat, Handbook of particle Detection and Imaging, 2012, 2018, Springer ISBN 978-3-642-13270-420

H.Kolonaski, N. Wernes, Particle Detectors fundamentals and applications, 2020, Oxford university ISBN978-0-19-885836-2

G. Knoll, Radiation Detection and Measurement, 2000, Willey

P. Lecoq et al, Inorganic Scintillators for Detector Systems Physical Principles, Springer, 2006/2017, ISBN 978-3-319-45521-1

W. R. Leo, Technique for Nuclear and particle Physics experiments, Springer-Verlag 1987, 1994, ISBN 0-387-57280-5

S. Tavernier, Experimental Techniques in Nuclear and Particle Physics, ED. Springer, 2010, ISBN 978-3-642-00828

P. Rodnyi, Physical Processes in Inorganic Scintillators, 1997, New York CRC Press

R. Wigmans, Calorimetry Energy Measurements in Particle Physics, Oxford university press ISBN 0-19-850296-6

P.A. Zyla et al. (Particle Data Group), Prog. Theor. Exp. Phys. 2020, 083C01 (2020)
https://pdg.lbl.gov/2020/download/Prog.Theor.Exp.Phys.2020.083C01.pdf

Conferences:

Scintillators: SCINT conferences: Conference on scintillators and their applications every 2 years: http://scint.univ-lyon1.fr/

Photodetectors: NDIP conferences: Conference on new developments in photodetection every 3 years: https://www.ndip.fr

Reference papers:

SCINT conference series proceedings:

C. Dujardin *et al.*, *IEEE Transactions on Nuclear Science*, vol. 65, no. 8, pp. 1977-1997, Aug. 2018, doi: 10.1109/TNS.2018.2840160.

P. Lecoq *et al* 2020 *Phys. Med. Biol.* **65** 21RM01

P. Kirzan, S. Korpar, Annu. Rev. Nucl. Part. Sci. 2013. 63:329–49

F. Acerbi, S. Gundacker, NIM A 926 (2019) 16–35

S. Gundacker, A. Heering, PMB 2020 Aug 21;65(17):17TR01. doi: 10.1088/1361-6560/ab7b2d.

Acknowledgment

The CERN Crystal clear team at CERN EP-CMX group,
and all the Crystal clear members
Supported projects:
European Union’s Horizon 2020 research and innovation programme under **ERC TICAL** (grant agreement 338953), the Marie Skłodowska-Curie **Intelum** project (grant agreement 644260), TWIN project **ASCIMAT** (Grant agreement no. 690599),
COST Action TD1401 (FAST),